

## **Copyright Warning & Restrictions**

The copyright law of the United States (Title 17, United States Code) governs the making of photocopies or other reproductions of copyrighted material.

Under certain conditions specified in the law, libraries and archives are authorized to furnish a photocopy or other reproduction. One of these specified conditions is that the photocopy or reproduction is not to be “used for any purpose other than private study, scholarship, or research.” If a user makes a request for, or later uses, a photocopy or reproduction for purposes in excess of “fair use” that user may be liable for copyright infringement,

This institution reserves the right to refuse to accept a copying order if, in its judgment, fulfillment of the order would involve violation of copyright law.

**Please Note: The author retains the copyright while the New Jersey Institute of Technology reserves the right to distribute this thesis or dissertation**

Printing note: If you do not wish to print this page, then select “Pages from: first page # to: last page #” on the print dialog screen

The Van Houten library has removed some of the personal information and all signatures from the approval page and biographical sketches of theses and dissertations in order to protect the identity of NJIT graduates and faculty.

## **ABSTRACT**

### **APPLICATIONS OF A MICROTRAP FOR ON-LINE MONITORING OF VOLATILE ORGANICS**

**by  
Chaohua Feng**

Microtrap is made by packing a narrow metal tubing with adsorbents. The advantage of a microtrap is that it can be heated and cooled in the order of seconds. It has been used previously as a concentration cum injection device for on-line gas chromatography and also monitoring non-methane organic carbon in air emissions. In this research breakthrough and desorption characteristics of the microtrap were studied. A two-stage microtrap system was developed to reduce breakthrough while making sharp injection for GC separation. Microtrap was also used as a concentrator cum injector in on-line mass spectrometry. Finally, a microtrap based, continuous non-methane organic carbon analyzer was field tested at an industrial site.

Breakthrough characteristics of the microtrap were studied as a function of analyte concentration. The logarithm of breakthrough volume decreased linearly with the logarithm of adsorbate concentration at low concentration. At high concentration, breakthrough volume remained constant. The adsorption isotherms illustrated that retention of methanol and acetone on Carbopack B was by monolayer adsorption while those of benzene and acetone on Carbopack C were by multilayer adsorption. Microtrap temperature was measured using an infrared thermocouple. Desorption efficiency at a given temperature depended upon the

analyte as well as the adsorbent. The desorption peak width decreased with increasing desorption temperature and sample flow rate.

A two-stage microtrap system was developed by connecting two microtraps in series. The first microtrap, packed with relatively more adsorbent, prevented breakthrough of small molecules, and served as the retention trap. The second, smaller diameter trap provided rapid desorption and served as the injection trap. Two-stage microtrap increased the breakthrough time for large volume sampling without decreasing chromatographic resolution.

Microtrap was used as an interface for mass spectrometry. The objective was to provide preconcentration and elimination of background molecules such as CO<sub>2</sub> and H<sub>2</sub>O. Different configurations combining the microtrap with a gas sampling valve were studied. On-line microtrap with backflush desorption was found to be most effective in direct sampling mass spectrometry. Due to the elimination of background gases, the detection limit was as low as the parts per trillion level. Emission from a catalytic incinerator was monitored using this technique.

A previously developed continuous non-methane organic carbon (C-NMOC) analyzer was field tested at a coating facility in North Carolina. The C-NMOC analyzer demonstrated high accuracy and high precision in the field study. The advantages of real-time monitoring, such as immediate response for transient events were also demonstrated. Continuous monitoring was possible in the presence of high concentrations of moisture and carbon dioxide.

**APPLICATIONS OF A MICROTRAP FOR ON-LINE  
MONITORING OF VOLATILE ORGANICS**

by  
**Chaohua Feng**

**A Dissertation  
Submitted to the Faculty of  
New Jersey Institute of Technology  
in Partial Fulfillment of the Requirements for the Degree of  
Doctor of Philosophy**

**Department of Chemical Engineering, Chemistry and Environmental Science**

**May 1999**

Copyright © 1999 by Chaohua Feng

ALL RIGHTS RESERVED

**APPROVAL PAGE**

**APPLICATIONS OF A MICROTRAP FOR ON-LINE  
MONITORING OF VOLATILE ORGANICS**

**Chaohua Feng**

---

Dr. Somenath Mitra, Dissertation Advisor Date  
Associate Professor of Chemistry, NJIT

---

Dr. Barbara Kebbekus, Committee Member Date  
Professor of Chemistry, NJIT

---

Dr. Richard Trattner, Committee Member Date  
Professor of Chemistry, NJIT

---

Dr. Henry Shaw, Committee Member Date  
Professor of Chemical Engineering, NJIT

---

Dr. Nicholas Snow, Committee Member Date  
Assistant Professor of Chemistry, Seton Hall University

## BIOGRAPHICAL SKETCH

**Author:** Chaohua Feng  
**Degree:** Doctor of Philosophy  
**Date:** May 1999

### Undergraduate and Graduate Education:

- Doctor of Philosophy in Environmental Science, New Jersey Institute of Technology, Newark, NJ, 1999
- Master of Science in Environmental Risk Assessment, Chiang Mai University, Chiang Mai, Thailand, 1994
- Bachelor of Engineering in Environmental Monitoring, Beijing Polytechnic University, Beijing, P. R. China, 1987

**Major:** Environmental Science

### Presentation and Publications:

1. C. Feng, S. Mitra, "Two-stage microtrap as an injection device for continuous on-line gas chromatographic monitoring", *J. Chromatogr. A*, vol. 805, pp. 169-176, 1998.
2. C. Feng, S. Mitra, "Microtrap interface for direct sampling mass spectrometry", *UNI-TECH Conference*, April 1998.
3. C. Feng, "Some organochlorine pesticide residues in fishes, shrimps and meats in Chiang Mai markets", *J. Sci. Fac. CMU*. Vol. 24 (2), pp. 123-134, 1997.
4. C. Feng, "Macrozoobenthos community", *Some selected environmental monitoring techniques and their applicability in the field, Environmental Risk Assessment Program, 1994*.
5. C. Feng, "China National Standard Hygienic Analytical Method (GB7917.1-87) and Explanation for Mercury (Hg), Arsenic (As), Hormones in Cosmetics," *Manual of hygienic monitoring of cosmetics. Tianjing University Publication, 1994*.



To my beloved family

## **ACKNOWLEDGMENT**

I would like to express my deepest appreciation to Dr. Somenath Mitra, who served as my research advisor, for his guidance, encouragement and support throughout this research. Special thanks are given to Dr. Barbara Kebbekus, Dr. Richard Trattner, Dr. Henry Shaw and Dr. Nicholas Snow for actively participating in my committee. Special thanks are also given to Mr. Clint Brockway for his constant support for this research.

I also would like to thank Lizhong Zhang, Naihong Zhu, Paul Yu and Xiumei Guo for their assistance and suggestions. I am grateful to my wife and my parents for their support and encouragement over the entire course of the research.

## TABLE OF CONTENTS

Chapter	Page
1 INTRODUCTION.....	1
1.1 Analysis of Volatile Organic Compounds in Air Sample.....	1
1.2 On-line, Continuous Analysis of VOCs.....	2
1.3 Instrumentation for Continuous Monitoring.....	4
1.3.1 FTIR.....	6
1.3.2 Gas Chromatography.....	7
1.3.3 Mass Spectrometer.....	9
1.4 Adsorption.....	15
1.4.1 Adsorbent and Adsorbate.....	15
1.4.2 Characteristics for Adsorption and Desorption.....	18
2 RESEARCH OBJECTIVES.....	27
3 BREAKTHROUGH AND DESORPTION CHARACTERISTICS OF A MICROTRAP.....	29
3.1 Introduction.....	29
3.2 Experimental.....	32
3.3 Results and Discussions.....	35
3.3.1 Breakthrough as a Function of Adsorbate Concentration.....	35
3.3.2 Desorption as a Function of Temperature.....	39
4 TWO-STAGE MICROTRAP AS INJECTION DEVICE FOR ON-LINE VOCs MONITORING BY GC.....	54
4.1 Introduction.....	54
4.2 Experimental.....	57

**TABLE OF CONTENTS**  
**(Continued)**

<b>Chapter</b>	<b>Page</b>
4.3 Results and Discussions .....	59
4.3.1 Breakthrough Characteristics of Retention and Injection Microtrap .....	59
4.3.2 Quantitative Desorption from the Microtrap .....	60
4.3.3 Performance of Two-stage Microtrap .....	63
4.4 Conclusion .....	68
5 MICROTRAP INTERFACE FOR ON-LINE MASS SPECTROMETRY .....	69
5.1 Introduction .....	69
5.2 Experimental .....	72
5.3 Results and Discussions .....	76
5.4 Conclusion .....	90
6 FIELD VALIDATION OF CONTINUOUS NON METHANE ORGANIC CARBON ANALYZER FOR AIR EMISSION MONITORING .....	91
6.1 Introduction .....	91
6.2 Experimental Approach .....	96
6.3 Results and Discussion .....	100
6.4 Conclusion .....	113
REFERENCES .....	114

## LIST OF TABLES

Table	Page
1.1 Classification of adsorbents and adsorbates and their subsequent .....	19
3.1 Desorption efficiency ( % ) of methanol as a function of temperature.....	44
3.2 Desorption efficiency ( % ) of propane as a function of temperature .....	44
3.3 Desorption efficiency ( % ) of toluene as a function of temperature.....	44
4.1 Peak width at half height in chromatograms generated using different size microtraps.....	65
4.2 Breakthrough times of different size microtraps.....	66
5.1 Detection limits for the different substances.....	87
6.1 QC data: checking the catalyst activity and system blank .....	102
6.2 NMOC monitoring results on testing day one.....	107
6.3 Spike recovery results on the first day of testing.....	108
6.4 Audit results .....	109
6.5 NMOC monitoring results on testing day two .....	111

## LIST OF FIGURES

Figure	Page
3.1 Schematic diagram of the experimental system .....	33
3.2 Breakthrough volumes (ml/g) as a function of concentrations of methanol, acetone on Carbopack B.....	36
3.3 Breakthrough volumes (ml/g) as a function of concentrations of acetone, benzene on Carbopack C .....	38
3.4 Adsorption isotherm for benzene on Carbopack C.....	40
3.5 Adsorption isotherm for acetone on Carbopack C .....	41
3.6 Adsorption isotherms for acetone and methanol on Carbopack B .....	42
3.7 Maximum temperature reached at different microtrap voltages and applying pulse of different durations.....	45
3.8 Temperature profiles of a microtrap heated with a 60 V power supply.....	47
3.9 Desorption profiles of toluene from Carbopack C .....	48
3.10 Effect of increasing microtrap voltage on analyte desorption profile.....	50
3.11 The desorption peak changing with sample flow rate .....	51
3.12 Toluene desorption peaks from Carbopack C at different sample flow rates, microtrap was desorbed at 60 V for 4 seconds.....	52
4.1 Schematic diagram of the experimental system. ....	58
4.2 Acetone breakthrough on 1.1 mm i.d. stainless steel microtrap measured by three different methods .....	61
4.3 The plot of peak height as a function of pulse time for different size microtraps .....	62
4.4 Chromatograms generated by using different sizes of microtraps as injection device .....	64

**LIST OF FIGURES**  
**(Continued)**

<b>Figure</b>	<b>Page</b>
4.5 Chromatograms generated by using two-stage microtrap as injection device .....	67
5.1 Schematic diagram of the experimental system .....	73
5.2 Schematic diagram of the experimental system for catalytic incinerator emission monitoring .....	75
5.3 The chromatogram generated by direct sampling .....	77
5.4 The chromatogram generated by SVMT.....	79
5.5 The chromatogram generated by OLMT-BF without helium purge. ....	81
5.6 The chromatogram generated by OLMT-BF with helium purge .....	83
5.7 The chromatogram generated by OLMT-BF with helium purge for multiple compounds .....	84
5.8 Calibration curves for toluene and TCE. ....	86
5.9 Calibration curves for hexane and benzene.....	86
5.10 Calibration curves for benzene and toluene measured by ion trap mass spectrometry.....	87
5.11 The chromatogram generated by Varian Saturn ion trap mass spectrometer with selected ion monitoring as m/z:78 and 91 .....	88
5.12 The concentration profile of test compounds changing with incinerator temperature .....	89
6.1 Schematic diagram of the field analytical system .....	95
6.2 Schematic diagram of the sampling system. ....	97
6.3 Schematic diagram of the C-NMOC analyzer.....	99
6.4 Typical calibration curve for NMOC monitoring.....	103
6.5 Typical chromatogram generated by the C-NMOC analyzer. ....	105

**LIST OF FIGURES**  
**(Continued)**

<b>Figure</b>	<b>Page</b>
6.6 NMOC concentration profile on testing day one.....	106
6.7 NMOC concentration profile on testing day two .....	110



## CHAPTER 1

### INTRODUCTION

#### 1.1 Analysis of Volatile Organic Compounds in Air Sample

Volatile organic compounds (VOCs) are defined by the United States Environmental Protection Agency (US EPA) as organics with vapor pressure greater than 0.01 kPA at 25 °C. The lists of VOCs include a variety of straight chains, aromatic hydrocarbons, as well as organic compounds containing different functional groups. They have received much scrutiny from the regulatory community because many of these compounds are toxic, carcinogenic and mutagenic. They are also major air pollutants. Hydrocarbons participate in the photochemical reactions that lead to smog formation at both urban and rural scale. Organic acids contribute to acid rain. Some VOCs also play an important role in global warming and destruction of the ozone layer [1-3].

The conventional approach to the measurement of VOCs requires sampling air using a sorbent trap or into a whole air sampler (for example canisters). This is followed by laboratory analysis using GC or GC/MS. Described in the Compendium Methods for the Determination of Toxic Organic Compounds in Ambient Air [4] are US EPA methods for monitoring volatile and semi-volatile organic compounds. Each of the first three methods calls for a different sampling technique, followed by thermal desorption to a capillary GC column for analysis. In method TO-1, compounds are trapped on a porous polymer adsorbent, transferred to a cold trap, and desorbed to the column. In Method TO-2, they are

trapped on a carbon molecular sieve adsorbent, transferred to a cold trap, and then desorbed to the column. In Method TO-3, they are trapped on a cold trap and desorbed to the column. Cryotrapping used in these methods is an attractive method, but in many cases the formation of ice plugs rapidly sets a limit to the amount of sample that can be concentrated when moisture is present in the sample. In this respect, the widely used adsorbents such as active charcoal, and carbon molecular sieve are more favorable. In method TO-14, a whole air sampler such as a canister is used for sampling. The canisters are then brought back to the lab for analysis.

All these EPA Methods are quite effective in routine environmental analysis. While these methods provide sensitive and reliable measurements, they are cumbersome and unsuitable for on-line or field analysis, where immediate results may have important health and safety benefits.

### **1.2 On-line and On-site Measurement of VOCs**

Evolving environmental regulations and the rising costs of compliance testing are pushing environmental scientist to explore the application of new, more cost-effective technology. Recently there has been much effort in the development of analytical techniques for continuous, on-line measurement of VOCs in air emission and in ambient air. The first consideration for these developments is the speed of analysis. Typically laboratory analysis has a turn around time of several days and the data can not be used for taking corrective actions in a process. The turn-around time is of the order of a few minutes or even a few seconds for most on-line

methods. In other words, on-line monitoring is valuable in monitoring emission transients and also in implementing process control.

Another consideration is cost. To assess and remediate contaminated sites worldwide with existing technologies is estimated to cost \$500 billion to more than a trillion dollars. Site characterization can represent as much as 40 % of total cleanup costs [5]. Of the average 10 years that it takes to clean up a Superfund site, seven are spent studying, characterizing, negotiating, and developing a remediation plan. The strict reliance on off-site laboratory analysis of collected samples contributes to this lengthy process. Typically, samples are collected in the field and sent to a laboratory for analysis. The results of the first phase of sampling and analysis are usually inadequate for the development of a remediation plan. On an average 70 % of the samples collected are nondetects, containing no contaminants. Therefore, additional trips must be made to collect samples for analysis in order to obtain an adequate information about the site. This iterative approach is costly in part because of unnecessary, expensive analysis of samples that are “clean”. Couple the number of sites that need to be assessed with the cost to perform each assessment, and one would question whether all the sites can be characterized with the time and money available. Considering all these factors, with prudent use of field analysis, the cost of environmental testing can be reduced significantly [6].

The other consideration for using on-line monitoring technique, is accuracy. Analyte concentrations can degrade during the period between sample collection and its chemical analysis. These concentration changes are complex and

are related to such factors as analyte volatilization, analyte kinetics, biodegradation, container leakage, preservation conditions, extraction efficiency, and analytical accuracy. During transport and storage of sample, the sample can degrade and contamination can occur. For example, many organic compounds, especially the polar compounds, are known to be unstable in canisters. Research showed that total organic concentration reduced about 7.9 % after 23 hours and 16 % after 19 days, indicating that unidentified analytes were being lost during prolonged storage [7]. Regulatory agencies have specified holding times for class of compounds (volatile organics, semi-volatile organics, and explosives) to standardize analytical laboratory procedures. For example, Code of Federal Regulations (40 CFR 136) requires that VOC samples stored at 4 °C must be analyzed within 7 days of collection. This requirement is very stringent for most analytical laboratories. Up to 80 % of the error in VOC analysis may be attributed to the delay between sample collection and chemical analysis [8].

From this standpoint, even if the precision of an on-line method is not as good as that of a lab method, it still provides more accurate results than a conventional lab method because transportation and storage are eliminated.

### **1.3 Instrumentation for Continuous Monitoring**

Continuous monitoring systems integrate three main subsystems: a sampling interface, an analyzer and a control and data analysis system. One method of classifying the system is by the type of sampling system. In general, the systems can be classified into extractive, in situ, and remote. In an extractive system, the

sample is physically transported from the source, conditioned and then introduced into the analyzer. In order for an instrument to measure gas concentrations, the gas sample must be free of particulate matter. Moisture usually must be removed. This requires the use of valves, pumps, and other components necessary for gas transport and conditioning. In the case of in-situ systems, the interface is simpler, composed of flanges designed to align or support the monitor and blower systems used to minimize interference from particulate matter.

The continuous monitor can also be categorized by the frequency of the sampling interface. For process monitoring applications, continuous, on-line monitoring is required to capture data regarding transient process events. Continuous, on-line monitors differ in the kind of information that they report. Some of them are non-selective and respond to gross process characteristics such as total non-methane organic carbon (NMOC) or total chlorine content. Others fall into the category of speciation monitors that provide individual concentrations of process components. The need for speciation is often determined by environmental regulations where the relative toxicity or the potential of a particular compound for production of smog may dictate an individual quantitative measurement.

Continuous, on-line monitors also need to have good engineering design to assure simple operation and maintenance. A number of analytical techniques are available that can be applied to continuous, on-line monitoring but they must also be amenable to automated operation and data analysis. Other important distinctions are the same as with any analytical instrument such as selectivity, detection limits, size and cost. The most common techniques used for continuous,

on-line measurement of VOCs include direct FID, Fourier transform infrared spectroscopy (FTIR), gas chromatography (GC) and mass spectrometry (MS).

### 1.3.1 FTIR

Infrared spectroscopy (IR) has been used to provide useful qualitative and quantitative information about chemical processes. Fourier transform (FT) instruments allow rapid data acquisition for high sensitivity and signal averaging [9]. FTIR techniques have been applied to on-line analysis and in chemical process control where only a few reactants and products are present at relatively high concentrations. Equipped with sandwich detector which normally has gas cell with 10 – 20 meter path length, FTIR has been demonstrated to be useful for monitoring gas and vapor emissions in specific industrial hygiene applications [10-14]. However water vapor which exists in air samples interferes with the analysis [15] because the water vapor has strong absorption in middle IR. When multiple components are present in the sample, the peaks generated by C-H-containing organic compounds may overlap. Even through different components presented in the sample can still be quantified using a completely overlapped peak in the presence of interference, it is difficult to use this technique to analyze unknown complex mixtures. The detection limit of FTIR is usually too high for trace level pollution monitoring. In general, FTIR is not a suitable method for most air monitoring applications that require the identification of individual compounds in a complex mixture, especially when a large quantity of moisture are present.

### 1.3.2 Gas Chromatography

Gas chromatography offers a large selection of excellent columns and detectors for a variety of different types of separations. GC has been used for process stream analysis since the 1950s [16]. Unlike spectroscopic techniques in which a sample stream can continuously pass through the detection cell, a sample injection in the form of a pulse is needed for GC separation. The most common sample introduction device in continuous gas chromatography is gas sampling valve. Valves can automatically make injections from a sample stream intermittently into a GC column [17-19].

However, sample valves have certain limitations. Being mechanical devices, they tend to wear during extended periods of operation. Another problem with sample valves is that they withdraw a small fraction of sample stream for injection into the GC. The sample size that is injected into the GC is between a few microliters to a couple of milliliters. Injection of a larger sample quantity causes excessive band broadening and degrades chromatographic resolution. A small injection volume results in small sample quantity and poor sensitivity. In many applications, especially in environmental monitoring, low concentrations are encountered and sample valves are found to be inadequate [20].

The other approach for continuous, on-line GC analysis employs a thermal desorption modulator placed before the analytical column [21-24]. Modulators are in principle quite similar to cryogenic traps used in chromatography. The conventional purge-and-trap devices are designed to preconcentrate analytes from a sample or to sharpen an injection, whereas modulators are used to continuously

modulate the concentration of analytes in a flowing stream. Chromatography using modulators does not need any injection device because the equivalent of an injection is generated internally within the flow stream. Potential advantages of using modulators are faster operation, smaller bandwidth, lower detection limit, and improved reliability [25]. Moreover, it is a continuous analysis technique as compared to conventional valves that offer intermittent analysis. Some of the problems associated with using low-capacity modulators are low modulation efficiency, low sensitivity, inability to modulate volatile components, and derivative peak shape. The increase in capacity factor of the modulator results in a change in the chromatographic peak shape and the modulation efficiency increases.

Recently sorbent traps have been widely used as injection devices for continuous, on-line gas chromatography [20, 26-30]. A trap made by packing narrow metal tubing with adsorbents is placed in front of the GC column. When sample stream passes through the trap, organic compounds of interest can be adsorbed by the adsorbent. At the end of sampling, the trap is thermally desorbed to produce a concentration pulse as injection to GC column. The sorbent trap is not only an injection device that can make the analysis continuous, on-line, but also a preconcentrator that enriches the sample during sampling. Membrane combined with microtrap has also been developed for continuous, on-line VOCs monitoring in air or water [27, 31, 32]. Simultaneous extraction and stripping of VOCs by membrane combined with microtrap injection have shown some advantages such as elimination of moisture in humid samples.



### 1.3.3 Mass Spectrometer

Mass spectrometry (MS) plays a prominent role in environmental monitoring because of its high chemical specificity, and sensitivity. Molecular weights and structural information are both available through the appropriate choice of ionization methodology. It is particularly attractive for on-line analysis because of fast response time and high mass resolution. GC/MS has been used for field monitoring of VOCs at hazardous waste sites [33 – 38]. Efforts are currently under way to improve the speed of the chromatography without sacrificing resolution, and new high-temperature columns extend the lifetime of the column, and to expand the range of compounds currently studied by GC/MS. In addition, the packed columns have largely been replaced by capillary columns. GC retains the advantages of simplicity, lower weight, and much lower cost. Only recently, as mass spectrometers became more amenable to field analysis, has GC/MS commonly been employed in the field [39].

Compared to conventional GC/MS methods that provide separation of all components in a sample, direct sampling mass spectrometry methods simply introduce all components simultaneously into the mass spectrometer. In a complex mixture, the mass spectrum of all the components overlaps, resulting in complex spectra. This makes identification of individual components difficult. The advantage here is that GC separation takes a long time where as mass spectrum is obtained instantly. Consequently, this method is most effective in situations where the immediate availability of results is critical. One of the problems facing on-line, direct sampling mass spectrometry in air monitoring applications is the inlet

systems which extract analytes directly without sample preparation, and act as a protective barrier between atmospheric pressure, in which sampling is performed, and the high vacuum inside the instrument. This function is critical in preventing excessive amounts of permanent gases such as oxygen, H<sub>2</sub>O and CO<sub>2</sub> from entering the ionization chamber.

Four major types of inlets have been reported for direct sampling mass spectrometry. Capillary restrictors, membrane inlets, sorbent trap inlets, atmospheric pressure ionization (API) and atmospheric sampling glow discharge ionization (ASGDI). Capillary restrictors, a good choice for sampling polar and nonpolar compounds, consist of a narrow-bore (50 –150 μm) deactivated fused-silica capillary that extends from the atmosphere into the ion source. Transport time of a sample through the capillary restrictor is about 100 ms, providing nearly instantaneous response. Capillary inlets may require heating to prevent absorption of some analytes. The primary disadvantages of capillary restrictors are that air and water vapor enter the mass spectrometer during sample analysis and the limitation of the flow rate. The capillary limits the gas flow into the instrument to 0.1 to 1.0 ml/min, which is compatible with instruments equipped with conventional EI or CI sources. Capillary restrictors are inadequate for trace analysis at such flow rates.

Membrane inlet employs flow injection analysis procedures for sample handling to provide an on-line capability, detects organic compounds in aqueous solution or in air, and offers relatively rapid response time (in the range of 0.5 - 5 min). Thus, there is the capability for continuous, on-line operation. It provides selectivity towards the organics. The analytes are extracted from sample and

directly introduced to mass spectrometer while blocking the flow of background species. In addition, internal or external standard solutions can provide quantitation. Membrane introduction mass spectrometry (MIMS) requires minimal operator intervention. Various polymeric materials have been employed as membranes. The most commonly used are hydrophobic, nonporous polymers such as the silicones. These membranes have excellent permeability for VOCs present in water or air and low permeabilities for the sample matrix. Microporous membranes have also seen some use in MIMS. In spite of the lack of selectivity of such membranes, their fast response times allow specialized applications where solvent removal is not essential, for example, in the determination of polar organic compounds in hydrocarbon matrices, where the hydrocarbon was used as the chemical ionization reagent gas in the subsequent mass spectrometric analysis [40]. Hollow fiber membranes have been used to introduce VOCs from aqueous and air samples directly into the ionization chamber of the mass spectrometer [41]. Recently Silvon demonstrated the pneumatically assisted transport of the membrane permeate to the ionization region of the mass spectrometer [42]. Cooks further advanced this design by incorporating a jet separator to remove excess water from the membrane permeate to provide two stages of enrichments in analyte [43]. Other recent advances and applications described in a set of associated papers on this issue, include detection of VOCs in water at the parts-per-quadrillion level [44]; on-line monitoring of biological metabolites at low levels [45]; and on-site monitoring of complex mixtures of hazardous organic

contaminants at chemical waste sites [46]; on-line monitoring of VOCs in air, water, soil by two-stages membrane introduction mass spectrometry [47].

The limitations of membranes are the slow response, low permeation efficiency, and selectivity between polar and non-polar compounds. Membranes discriminate among compounds on the basis of their solubilities in the membrane material. The performance of membrane is also temperature-dependent. When using membrane inlets for air monitoring, because they are not in direct contact with a liquid, they can often operate at higher temperatures, thereby lowering response and recovery time. Sudden rupture of a membrane may also produce a failure of the spectrometer.

Atmospheric pressure ionization (API), and atmospheric sampling glow discharge ionization (ASGDI) sources provide a means of directly introducing a continuous flow of air or vapors. Differential pumping maintains low pressure in the mass analyzer region of the spectrometer while supporting much higher pressure in the discharge source region. Mass spectrometers equipped with these types of ionization source/inlets are often used for continuous, on-line monitoring of airborne pollutants such as stack emissions and vehicle exhaust.

A widely used approach is to ionize at atmospheric pressure by using either a  $\beta$  emitter such as  $^{63}\text{Ni}$  (48, 49), or a corona discharge (50 - 52) as a source of ionizing electrons. Both methods are commonly referred to as API. A number of reviews are available that describe API as a sensitive means for detecting trace quantities of certain organics in air [53, 54]. ASGDI [37, 55, 56] ion source is based on the establishment of a glow discharge in a region of reduced pressure

with ambient air as the discharge support gas. Ionization occurs, as with conventional chemical ionization, primarily through ion-molecule reactions. In this case, however, the discharge supplies the ionizing electrons, and compounds present in the sampled air serve as the reagent molecules. This ion source has been proven to be very sensitive for a variety of heteroatom-containing organic molecules. It has a number of features that make it useful as an ion source for continuous monitoring of ambient air for trace organic contaminants.

Several characteristics are usually desirable for an ion source intended for monitoring trace organics in ambient air. These include the following: low detection limits for the compounds of interest, fast response, minimal memory effects, minimal interference from compounds that may also be present, the possibility of analyzing for either positive or negative ions, low maintenance requirements, and a wide dynamic range.

Each of the approaches to ionizing trace organics in ambient air has its own unique set of characteristics. Electron impact ionization has the advantage of allowing for the analysis of a wide range of compounds than the API approaches, but is not well suited for the analysis of negative ions. Depending on the design of the API or ASGDI source, positive or negative ions can be formed. Negative ions are especially useful for detecting compounds with a high electron affinity, such as explosives.

Unlike the other inlets for direct sampling mass spectrometry, API and ASGDI use special ion source for on-line monitoring of VOCs. Disadvantages of API and ASGDI include the need for complex pumping systems, high-voltage

power supplies for ionization, and tedious instrument operation. Formation of unwanted cluster ions can also be a problem when large amounts of water vapor are present in a sample. API has been shown to be extremely sensitive for many types of compounds but can be susceptible chemical interference. The chemical interference may compete for charge, resulting in poor ionization efficiency for the species of interest, or may complicate the mass spectrum by extensive clustering.

Other approaches such as silica-fiber micro-extraction for laser desorption [57], and inertial spray extraction [58] have also been reported. The other major type of inlet used in direct sampling mass spectrometry is a sorbent trap. In our previous studies, the microtrap interface had been explored for directly introducing air sample into a mass spectrometer (MTMS). Compared with other methods, microtrap offers the convenience of being both a sample concentrator and injection device. By trapping VOCs on a sorbent material to increase the sample amount for detection, the detection limits can be reduced to ppt level [59]. Sampling time varies from under one minute to several minutes depending on the detection level required by the application [60, 61]. Air monitoring by MTMS has the further advantage of reducing potential mass spectral interference caused by ion-molecule reactions from water, nitrogen, oxygen, and carbon dioxide. Unlike the other methods, the thermal desorption of the microtrap produces a concentration pulse into ionization chamber which generates a peak instead of a platform as detection signal. When selected ion monitoring is used, this peak signal is much easier to be distinguished from the baseline for trace level monitoring. For gases studied, it

appears that microtrap interface is much more efficient compared with membrane introduction to ion trap detector through a jet separator [47].

#### 1.4 Adsorption

Adsorption is a physical process that deals specifically with the concentration of dispersed material in a continuous phase (carrier stream) on the surface of a highly porous material. There have been many complex theoretical approaches taken to explain the adsorption phenomenon. Adsorption is not only a function of physical parameters such as temperature and pressure, but also of concentration and intermolecular interaction. To put the problem into a simple framework, the theories are presented on a broad basis that will hold true for most materials and conditions. It can be stated, therefore, that the amount of a given gas adsorbed at equilibrium is a function of the final pressure and temperature only:

$$A = f(p, T)$$

##### 1.4.1 Adsorbent and Adsorbate

The use of gas-solid chromatography (GSC) as a tool for the characterization of adsorbents evolved in the late 1940s and early 1950s [62]. In that era, the physicochemical measurements that could be obtained by GSC were established, and till today the technique remains a viable analytical tool. In the 1960s, since Hollis [63] reported the use of porous polymers as packing materials in gas

chromatography, various types of porous polymers have been developed. Considerable attention has been given to the development of adsorbents with physical (i.e., structural) and chemical (i.e., homogeneous or inert surface) properties that enabled them to be used as both GSC stationary phases and sample enrichment. These developments in sorbent characteristics led to the application of solid adsorbents in the field of environmental monitoring, specifically in air sampling, and for enrichment of contaminants from aqueous media.

Because adsorbates can possess one or more functional groups and can exist in many molecular sizes and shapes, choosing the adsorbent becomes a critical issue. The adsorbents most widely used are: activated charcoals, activated silica gels, porous polymers, carbon molecular sieves, and graphitized carbon blacks. Characterization of these adsorbents in the 1960s led to a classification scheme for both adsorbents and adsorbates, and laid the groundwork for understanding adsorption phenomena at the gas-solid interface. The use of this classification scheme and the principles characterizing these adsorbate/adsorbent interactions have assisted in constructing adsorbent devices currently used in sampling enrichment procedures.

Kiselev [64] first categorized the interactions between adsorbate and adsorbent, and developed a scheme that classified them into three classes: Class I, Class II, and Class III. Class I adsorbents are those that possess no ionic charges on the surface. This lack of ionic interaction, or nonspecific interaction, allows for predictable retention mechanism and also allows the sampling professional to choose sampling parameters based on the molecular size and shape of the



molecule(s) of interest. Class I adsorbents are hydrophobic. Examples of Class I adsorbents include the graphitized carbon blacks such as Carbopack C, Carbopack B and Carbotrap.

Class II adsorbents possess localized positive charges that interact specifically with the adsorbates. This specificity allows for a strong or weak electrostatic interaction between the adsorbate and the adsorbent. A characteristic shortcoming of these specific adsorbents is their affinity for water that can negate the specificity of the surface. An example of a Class II adsorbent is activated silica gel which is so hydrophilic that water vapor is adsorbed in preference to the organic of interest.

Class III adsorbents possess localized negative charges which as with the Class II adsorbents, interact specifically with the adsorbates. This specific interaction has similar positive and negative surface characteristics (i.e., specificity and hydrophilicity). Activated charcoal and porous polymers such as Tenax belong to Class III adsorbents.

Characteristics study has been published on several porous polymer adsorbents [65, 66]. The use of carbon as an adsorbent dates back to 1773 when Scheele described experiments on gases exposed to carbon [67]. It is only in the past 70 years that the technique of activation has been used with any great success. One of the earlier uses of carbon, in the form of wood charcoal, was for respirators and gas masks. Charcoal made from different types of wood exhibited marked differences in the adsorptive capacities. For carbon sieves, the adsorption strength is caused by the pyrolysis temperatures used in manufacturing. As the pyrolysis

temperature is increased, the microporous region of the sieve shrinks, because the loss of hydrogen, with an increase in the number of carbon-carbon bonds and, subsequently, with an increase in the aromatic properties of the sieve product [68].

Kiselev [64] also categorized adsorbates, according to electronic activity, into four groups: Group A – n-alkanes; Group B – aromatic hydrocarbons, chlorinated hydrocarbons, ketones, Group C – organometallics; and Group D – organic acids, organic bases, and aliphatic alcohols. Table 1-1 summarizes the interactions between the three classes of adsorbents and the four groups of adsorbates.

#### **1.4.2 Characteristics for Adsorption and Desorption**

The adsorbent must satisfy a number of requirements, such as total chemical inertness relative to the adsorbed compounds, a capacity for total desorption and an adsorption capacity as large as possible for a maximum number of compounds. Two of the most critical parameters for an adsorbent are breakthrough volume (BTV) and desorption efficiency.

The breakthrough volume (BTV) is defined as the volume of carrier gas per unit mass of adsorbent necessary to cause a mass of adsorbate molecules, introduced into the front of the sorbent tube to migrate to the back of the tube. The BTV is also defined as the sampled volume corresponding to the end of the linear domain. The extreme value of the linear domain is evaluated by calculation of the intersection between linear and non-linear domains. The preconcentration

**Table 1.1** Classification of adsorbents and adsorbates and their subsequent.

Adsorbate types	Adsorbent types				
	Class I Without ions or active groups	Class II Localized positive active groups	Class III Localized negative active Groups		
<b>Molecular groups</b>	Nonspecific interactions				
Group A (n-alkanes) Spherically symmetrical shells $\sigma$ -Bonds					
Group B (aromatic hydrocarbons, chlorinated hydrocarbons, ketones) Electron density concentrated on Bonds/links $\pi$ -Bonds					
Group C (organometallics) (+) Charge on peripheral links				Nonspecific interactions	Nonspecific and specific interactions
Group D (organic acids, organic bases, aliphatic alcohols) Concentrated electron densities (+) Charges on adjacent links					
Classification of Adsorbents					
Adsorbent	Surface	Classification (Kiselev)			
Graphitized carbon blacks Carbon molecular sieves	Graphitic carbon Amorphous carbon	Class I Weak Class III (can approach Class I)			
Activated silica gel Activated charcoal Porous polymers	Oxides of silica gel Oxides of amorphous carbon Organic "plastics"	Class II Class III Weak → Strong Class III			

Source: W. R. Betz et. al, "Sampling and Analysis of Airborne Pollutants", Lewis Publishers, 1993 [69].

of a compound on an adsorbent can only be quantitative at sampling volumes that do not exceed the BTV of the compound. Earlier studies suggested an empirical equation to estimate the breakthrough regarding the boiling point of the adsorbate [26]. It has been demonstrated that the BTV depends on numerous factors such as humidity, temperature and concentration of adsorbate. There are also some other parameters which may affect the BTV value such as the chemical composition of the gaseous mixture [70, 71], the flow-rate and linear velocity of the carrier gas [72, 73], the dimensions of the trap [74]. A number of parameters relating to the adsorbent can also effect BTV, such as mass, granulometry, pore diameter and specific surface area [75, 76], repeated re-use and thermal pretreatment [77,78].

When considering the effect of humidity, it is necessary to take into account the change in the adsorption due to the interactions of the substance with the adsorbed water itself. Hydrophobic, non-polar porous polymers adsorb small amounts of water, and the effect of water vapor on these materials is insignificant [79]. Anasorb 747 and Anasorb CMS are examples of this type of adsorbent [80]. As the moisture content of the air increases, cooperative interactions between water molecules take place on the surface and render it hydrophilic, causing a dramatic drop in capacity for hydrophobic organic molecules. The breakthrough study on Anasorb CMS showed the adsorbed methylene chloride did not appear to be lost at high humidity, and in this case breakthrough can be attributed solely to saturation. The organic and the moisture molecular can coexist as a mixed phase in the pore structure of a molecular sieve carbon, the composition of the mixed phase being related to the composition of the atmosphere with which it is in

equilibrium. Yoon et. al. [81] carried out experimental and modeling studies for effects of humidity and concentration on breakthrough. The experiments conducted in the absence of adsorbate showed that the amount of water adsorbed by activated carbon increased dramatically as the relative humidity increased above 50 - 60 %. They concluded that the effect of water vapor on contaminant adsorption is minimal for humidity in the range of 0 - 50 %. The deviation between experiment and theory increased with decreasing contaminant concentration and increasing humidity.

Temperature is another important parameter influencing breakthrough [82-84]. Adsorption is an exothermic phenomenon, the BTV being related to the temperature by Van't Hoff-type relationship:

$$\frac{d[\log(BTV)]}{d\left(\frac{1}{T}\right)} = -\frac{\Delta H_{ad}}{2.3R}$$

Where  $\Delta H_{ad}$  is the adsorption enthalpy, R is the gas constant and T is the absolute temperature. This equation can be expressed as

$$\log(BTV) = a + \frac{b}{T}$$

Using the equation the BTV can be estimated at a given temperature.

The BTV is also a function of concentration. Normally, the BTV data were obtained at infinite dilution (i.e., the extreme lower end of the Henry's Law region) and thus represent a migration volume rather than a saturation, or capacity, volume. This region of adsorbate coverage is applicable to sample enrichment modes for which trace level analyses are required. Under this circumstance, the concentration of adsorbate was always neglected when BTV was discussed.

However, sorbent traps used for air sampling are usually short and do not have as many theoretical plates as an analytical GC column. There are several reasons why the use of short columns is advantageous. They have low pressure drops and do not require complicated pumping equipment. This is especially true for field sampling. A high flow rate is often desired, as it permits the collection of a large volume sample. A small physical size is also advantageous in the desorption step. The sample enters the trap as a front instead of a narrow plug, as no separation is intended. For this short, low plate number sampling trap, the concentration effect on the front shape of the elution peak can not be neglected [85, 86]. The numerical solution expressed was found to be a good approximation of breakthrough volume as a function of plate number:

$$BTV = V_R \left( a_0 + \frac{a_1}{n} + \frac{a_2}{n^2} \right)^{-1/2}$$

where  $V_R$  is retention volume,  $n$  is theoretical plate number,  $a_0$ ,  $a_1$  and  $a_2$  are constants related to breakthrough level.

The dependence of equilibrium adsorption capacity on adsorbate concentration with all other factors held constant is usually described by an adsorption isotherm. Many equations have been proposed and fit to type I equilibrium adsorption isotherm data and data from breakthrough studies. The simplest ones, such as the Langmuir isotherm, contain only two adjustable parameters:

$$W_e = \frac{W_{\max} K_H C_0}{1 + K_H C_0}$$

where  $W_{\max}$  is the upper limit of capacity at very high vapor concentrations,  $K_H$  is Henry's law constant, and  $C_0$  is inlet concentration ( $\text{g}/\text{cm}^3$ ). This equation is often used in a linearized form by plotting  $C_0/W_e$  versus  $C_0$ .

Nelson et al. [87] demonstrated the application of a Freundlich isotherm in describing adsorption capacity as a function of concentration:

$$T_b = a C^{1/n}$$

where  $T_b$  is breakthrough time (min),  $C$  is concentration (ppm),  $a$  is constant for a given set of conditions, and  $n$  is constant ( $<1$ ). In practice, the logarithm of  $T_b$  is plotted against the logarithm of  $C$  in hopes of getting a straight line with slope of  $1/n$  and intercept of  $\log a$ .

Based on the theory of filling micropore volume, and the Polanyi concept of adsorption potential, the Dubinin/Radushkevick isotherm equation [88] was developed:

$$\ln W_v = \ln W_{vsat} - \left( \frac{KR^2T^2}{\beta^2} \right) \left[ \ln \left( \frac{P}{P_{sat}} \right) \right]^2$$

where  $W_v$  is volume capacity,  $W_{vsat}$  is volume capacity at saturation vapor pressure,  $P_{sat}$ ,  $T$  is absolute temperature,  $P/P_{sat}$  is relative vapor pressure,  $R$  is ideal gas constant,  $K$  is sorbent structural constant, and  $\beta$  is affinity coefficient. Hacskeylo and LeVan developed an adsorption isotherm equation based on analogy with the well-established Antoine equation for vapor pressures [89]:

$$\ln P = A + \ln \theta - \frac{B + b(1 - \theta)}{C + T}$$

Where  $A$ ,  $B$ ,  $C$  are Antoine constants,  $\theta$  is fraction of saturation capacity,  $P$  is equilibrium pressure and  $b$  is the constant for the linear variation of heat of adsorption with loading. In each case, the isotherm is favorable in the linear region at low concentrations [90, 91]. No observable effect of the particle mesh size on BTV has been reported [92]. Changes in BTV were observed in the presence of other compounds. Lewis et al. [93] carried out adsorption studies near the flat portion of the isotherm. Here, there is little additional adsorption capacity. Each



molecule of an additional chemical competes for adsorption space and will displace another potential adsorbate. Carbon adsorption capacity can be estimated for monolayer coverage using the cross-sectional surface area of an adsorbate molecule and the internal pore area of the carbon granule. Jonas et al. [94] demonstrated that one molecule of carbon tetrachloride occupies one active site, that there are no interactions among carbon tetrachloride molecules, and that the adsorption occurs as a single adsorption layer. This approach is useful in making estimates as to the total capacity of carbon for an adsorbate when adsorption isotherm data is unavailable. A number of models have been developed over the years under various assumptions. A comprehensive review of single-component adsorption modeling has been published by Schork [95]. Yang [96] has provided a review of multi-component adsorption, particularly based on equilibrium theory. In general, most reported studies have used Langmuir isotherm.

Several experimental and theoretical studies were done on the effect of the kinetics of adsorption/desorption on the shape of the desorption profiles [97, 98]. Two types of phenomena control these profiles, the nonlinear behavior of the equilibrium isotherms and finite rates of the kinetics of axial and radial mass transfers. The former phenomena, which are of thermodynamic origin, are properly accounted for the ideal model of chromatography [99 - 101]. The latter phenomena have an important effect on the production rate and recovery yields achieved in preparative chromatography. In many cases, when the kinetics of adsorption/desorption are fast, the equilibrium diffusive model can be used to predict accurately the shape of the band profiles [101-103]. There are cases of

importance when the kinetics of mass transfers and /or the kinetics of the retention mechanism are slow. They are explained by the progressive decoupling between the thermodynamics and kinetics influences on the band. It is not possible to separate simply the effects of the mass transfer kinetics and adsorption/desorption kinetics on a band profile [104-106].

Complete desorption of the adsorbed organics from the adsorbent is also critical for quantitative analysis. If an analyte is adsorbed on a very strong adsorbent, it may not be efficiently released during the desorption process. Also, analytes subject to thermal breakdown can not be held at high temperatures too long. Both of these occurrences can lead to poor recovery of the analyte. Desorption efficiency of several VOCs have been studied [107, 108]. For a symmetrical desorption peak, the maximum volume of carrier gas required for complete desorption is reported to be twice the retention volume [109].

## CHAPTER 2

### RESEARCH OBJECTIVES

The objective of this study is to develop a better microtrap, and also apply it in air monitoring. A better understanding of the breakthrough and desorption characteristics is needed. A goal is to develop an understanding of breakthrough as a function of analyte concentration. A measurement of microtrap temperature is necessary to understand desorption mechanisms. So, microtrap temperature during a few seconds pulse heating is measured.

When more adsorbent is packed inside the microtrap, the breakthrough volume increases. It is essential to have large breakthrough volume for analyzing volatile compounds. However, fast desorption of a large trap is difficult. Slow desorption causes poor chromatographic resolution by generating broad injection bands. A two-stage microtrap system comprising of a large trap in series with a microtrap is proposed. The objective is to minimize breakthrough while making sharp injection for gas chromatography.

Microtrap has been tested as injection device for directly sampling mass spectrometry. In this study, microtrap will be further studied for sampling volatile organic compounds at low concentrations (ppb levels). Microtrap mass spectrometry will be used for monitoring emission from a laboratory scale catalytic incinerator.

A continuous, non-methane organic carbon monitor has been previously developed using microtrap as an injection device. This instrument will be tested with real world air emission from a coating facility in North Carolina. The

instrument will be evaluated as a continuous emission monitor based on accuracy, precision and its ability to monitor emission transients.

In summary the objectives of this research was four folds:

- Study the breakthrough and desorption issues related to the microtrap
- Develop a two-stage microtrap
- Application of microtrap in direct sampling mass spectrometry
- Field validation of C-NMOC analyzer.

## CHAPTER 3

### BREAKTHROUGH AND DESORPTION CHARACTERISTICS OF A MICROTRAP

#### 3.1 Introduction

Air monitoring involves qualitative and quantitative analysis of a wide range of volatile organic compounds (VOCs). Normally VOCs exist at trace level (sub-parts per million); hence, preconcentration techniques are necessary for their analysis. Sorbent traps have been widely used for this purpose, where the concentrated organics are subsequently recovered via thermal desorption [26, 29, 30, 110]. The VOCs present in air sample have different molecular sizes, shapes, as well as functional groups. Therefore, choosing an adsorbent which is appropriate for all compounds is not an easy task. The ideal adsorbent would be one which has large breakthrough volume for the very volatile compounds while providing for complete, rapid desorption for larger compounds. It is impossible to find such an unique adsorbent because adsorption and desorption are opposing phenomena.

Several kinds of adsorbents have been studied for sampling organic contaminants in air. Graphitized carbon blacks such as Carbopack C and Carbopack B (Supelco Inc., Supelco Park, PA) are nonspecific, or Class I, adsorbents. They have been widely used for sampling VOCs in air [30, 64, 68, 92, 111]. Without ions or active groups, these adsorbents interact nonspecifically with all types of adsorbates. Silica gel is a Class II adsorbent. Its usage is restricted to some alcohols, phenols and amines. Despite its high surface area, the sorbent is

polar and hydrophilic, with a marked preference for binding water molecules at any humidity [112-114]. Anasorb 727 is a synthetic beaded microporous polymer with a hydrophobic surface. Tenax is a porous polymer based on 2,6 diphenyl-p-phenylene. They both belong to Class III adsorbents which possess localized negative charges that interact specifically with the adsorbates. They have been validated for sampling different organic contaminants in workplace air [115-118].

Microtrap is made by packing a narrow metal tubing with one or more adsorbents. In continuous, on-line monitoring, the microtrap can be directly placed in a sample stream as an interface cum injector for GC. This has been referred to as on-line microtrap (OLMT). The sample stream passes through the microtrap where the organics of interest are trapped while the background stream serves as a carrier gas. The microtrap is periodically desorbed by resistive heating with an electrical pulse that serves as a GC injection. A sequential valve microtrap system (SVM) combines a gas sampling valve and microtrap. The sample stream continuously flows through the sampling valve. When the valve is switched to the injection position, the sample is purged out by a carrier gas to the microtrap. Then, the microtrap is desorbed to make an injection to GC. In another configuration, the sample loop of a gas sampling valve is replaced by a microtrap. It is referred to as on-line microtrap with backflush desorption (OLMT-BF). In the sampling position, sample stream passes through the microtrap. When it is switched to the injection position, the microtrap is isolated from the sample stream and thermally desorbed. The carrier gas flows in an opposite direction and backflushes the sample into the GC. Multi-sorbent microtraps can be used in this mode of operation. For making

sharp injections while minimizing the breakthrough, a two-stage microtrap has been developed, where the first microtrap is packed with relatively more adsorbent to serve as a retention trap, and the second microtrap, with relatively small dimension, serves as an injection trap.

The capacities of adsorption in term of breakthrough and desorption efficiency are important characteristics of a microtrap. Because of its small dimensions only a small amount of adsorbent can be packed inside. Thus, the microtrap is prone to breakthrough. For quantitative sampling of VOCs using a sorbent trap, the sample volume can not exceed the breakthrough volume. Previous studies have suggested that for a trap of a large number of theoretical plates, the breakthrough is independent of the adsorbate concentration [85]. The microtraps are designed to be of small dimension, so that they can be heated rapidly. Therefore, they are packed with a small amount of adsorbent. Moreover, often they are designed to retain the organics only for a few seconds or minutes while allowing large flow rate with small pressure drop. Considering all this, breakthrough is a major issue in a microtrap and the effect of the adsorbate's concentrations can not be neglected [119].

The desorption of the microtrap is made by heating the microtrap resistively using an electrical current pulse. Rapid desorption is essential for producing a sharp concentration pulse to serve as an injection for high resolution gas chromatography. The rate of desorption depends mainly on the maximum temperature achievable and the heating rate. Accordingly, the thermal stability of the adsorbate must be considered because the thermally unstable VOCs can not be

held at high temperature for too long. It is not easy to estimate the temperature of the microtrap because the whole duration of electrical pulse is less than 5 second and the resistance of the microtrap changes with the temperature during the heat up period. However, it effects desorption efficiency and desorption peak shape. The measurement of temperature is also difficult because the whole heating cooling cycle is only a few seconds, and conventional thermocouples do not have such a fast response time. There is also the issue of heat transfer because the heat has to migrate through the tube and into the sorbent bed.

In this chapter, the breakthrough characteristics of the microtrap were estimated, and the factors that affect heating mechanism of the microtrap were studied.

### **3.2 Experimental**

The schematic diagram of the experimental system is shown in Figure 3.1. All experiments were carried out on a Hewlett Packard 5890 Series II gas chromatography (Hewlett Packard, Avondale, PA) equipped with a conventional flame ionization detector (FID). The microtraps used in the breakthrough studies were made by packing 10 cm long  $\times$  0.53 mm i.d. silica lined stainless steel tubing (Restek Co. Bellefonte, PA) with 20 – 40 mg of sorbent. For the desorption studies, larger microtraps were made by packing 10 cm long of 1.1 mm i.d. stainless steel tubing (Small Part Inc., Miami Lakes, FL, USA) with different adsorbents. The adsorbents used in this study were Carbopack C, Carbopack B, Carbosieve SIII, Tanex-TA and Anasorb 747.



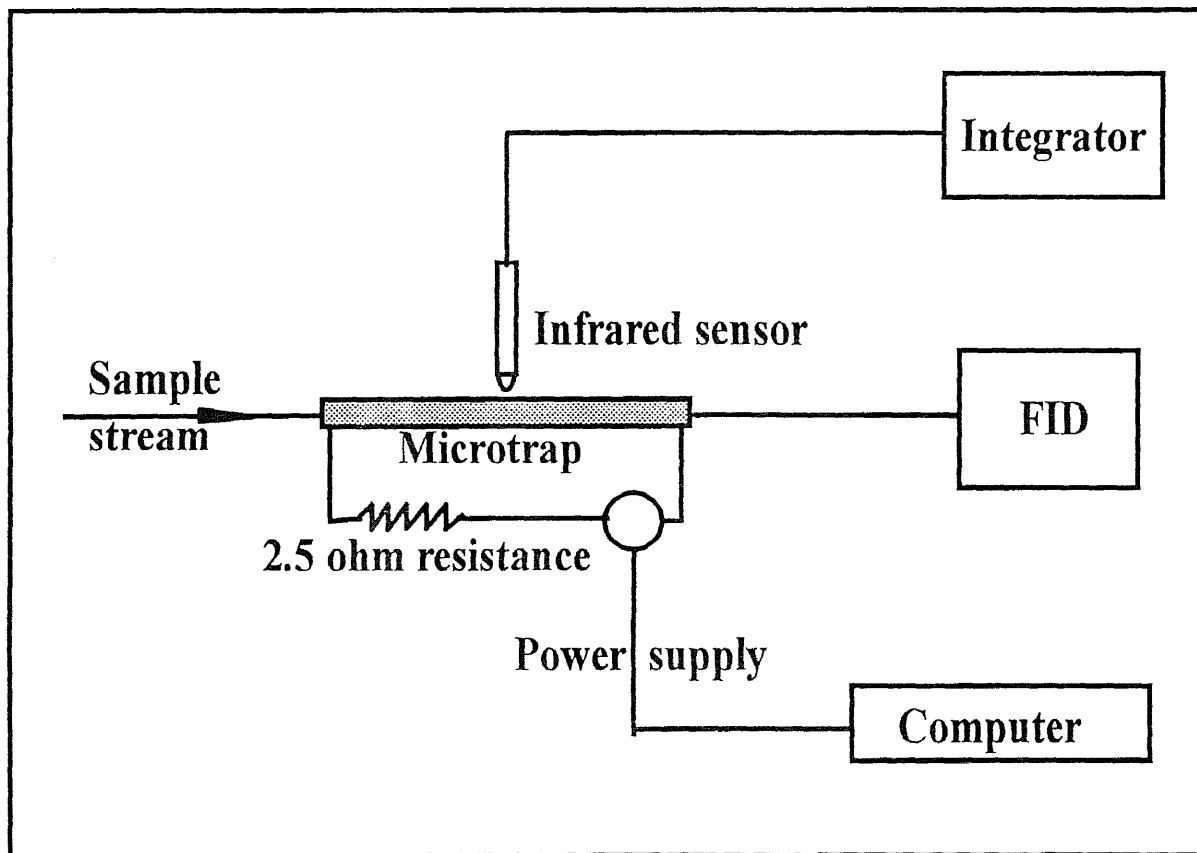


Figure 3.1 Schematic diagram of the experimental system.

A microprocessor controlled the interval, and duration of the electrical pulses to the microtrap. The different desorption temperatures were achieved by increasing either the voltage, or the duration of heating. For example, when the duration of heating was set to be 4 seconds, the energy supplied by the electrical current could be changed by altering the voltage. A higher voltage across the microtrap led to a higher desorption temperature. Desorption temperature could also be increased by increasing the pulse duration. For example, when the voltage was set to 50 volts, increasing the heating time provided more energy to reach higher temperatures.

Conventional thermocouples could not be used here because once contacted to the microtrap, the resistance of the microtrap would change. The resistance of the microtrap also changes when the temperature increases. Since the desorption was made by a short electrical pulse (3 – 5 second), the thermocouple did not have enough time to respond. Here an IRT/C K-440F infrared thermocouple (Exergen Corp. Watertown. MA) was used to measure the microtrap temperature. This non-invasive device measured temperature based on infrared radiation from the heated object. It was mounted at about 2 mm away from the microtrap. The response time of the infrared thermocouple was approximately 80 milisecond and it was able to monitor the microtrap heating profile. A GC integrator was used to record the response of the infrared sensor. The peak heights of the infrared sensor were converted to temperature. The infrared sensor was calibrated using a furnace whose temperature could be set at different levels.

Standard gases such as methanol, propane, toluene were purchased from Matheson Co., NJ. The standard gases containing acetone, benzene were made in the laboratory. An empty 13-liter tank was evacuated and then flush with zero grade air. This process was repeated several times to clean the tank. Then a predetermined quantity of each of the compounds was injected into the tank. Then tank was then filled with zero grade air to desired pressure.

The breakthrough time was measured by the peak shape. The sample flowed continuously through the microtrap. When the microtrap was heated, a desorption peak occurred. The analytes were re-adsorbed in the microtrap as the microtrap cooled. This lowered the base line into the negative territory appearing as a negative peak. As the sample began to breakthrough, the detector response increased again. The width of the negative peak has been shown to be equal to the breakthrough time measured by frontal chromatography [29].

### 3.3 Results and Discussions

#### 3.3.1 Breakthrough as a Function of Adsorbate Concentration

A log-log plot of the breakthrough volumes for methanol and acetone on Carbopack B are shown in Figure 3.2 as a function of the concentration. Linear relationship between breakthrough volume and concentration was observed when the concentration of acetone was below 168 ppm, and that of methanol was less than 232 ppm. The linear rang followed Freundlich's equation [120]:

$$\log(BTV) = a \log C + b$$

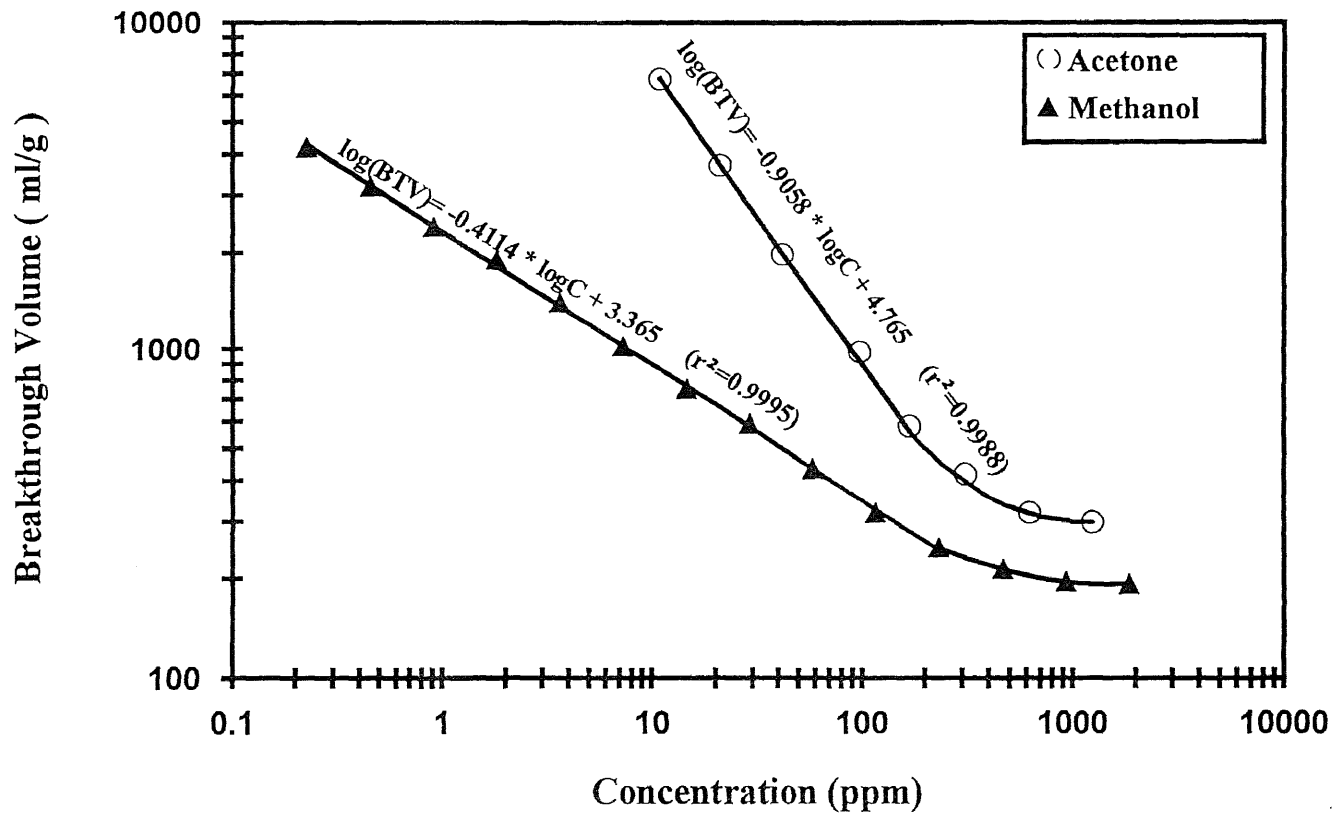
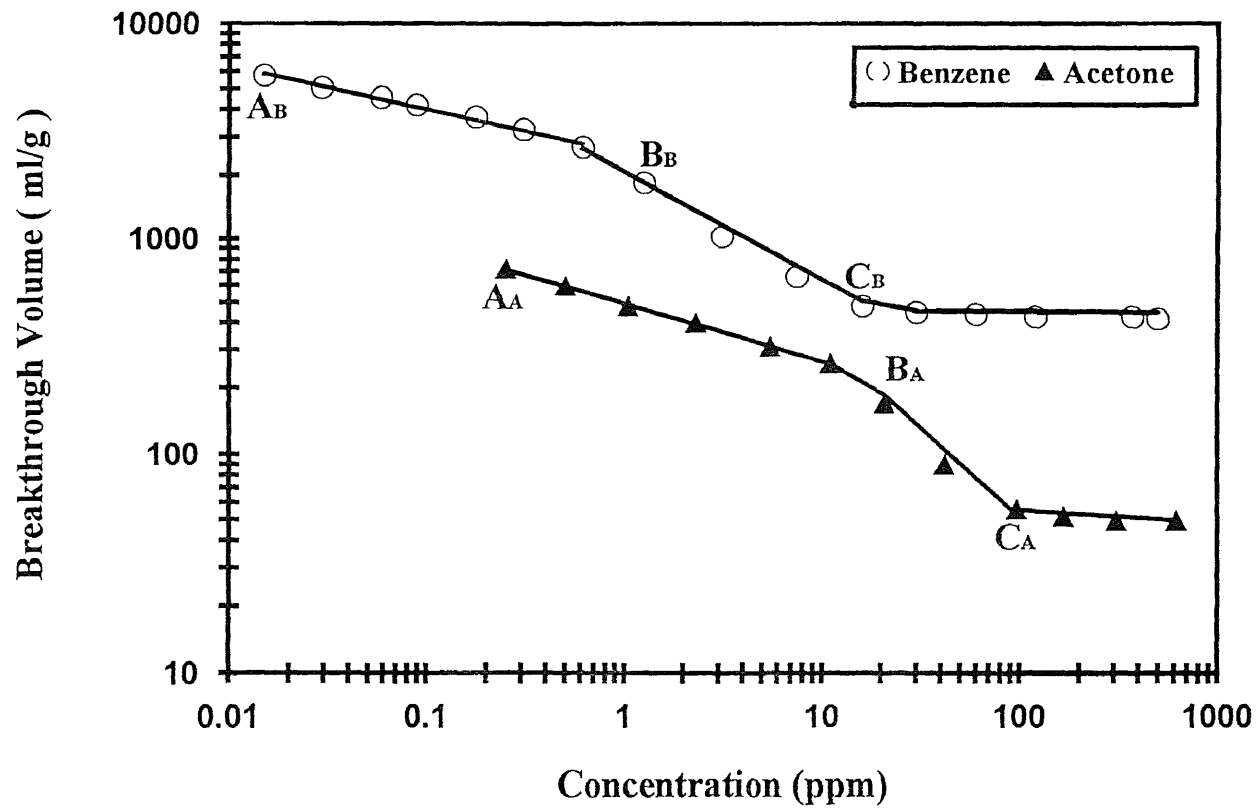


Figure 3.2 Breakthrough volumes (ml/g) as a function of concentrations of methanol, acetone on Carbopack B.

where, BTV is breakthrough volume, C is the adsorbate concentration. The intercept b is related to the adsorbent capacity, and the slope is related to the intensity of adsorption [121]. In this region breakthrough volume increased rapidly as concentration decreased.

At high concentrations, the breakthrough volume did not show any variation with concentration. There was only a limited amount of adsorbent (30 mg) inside the microtrap. When a large number of adsorbate molecules are present in the sample, the adsorbent capacity is reached rapidly. Each molecule of the adsorbate is competing for adsorption site and, if adsorbed, displaces another potential adsorbate. The breakthrough volume was independent of the adsorbate concentrations. Most environmental monitoring work is done at very low concentration where the curve is not flat. This region is applicable to sample enrichment modes. When an adsorbent is chosen for air sampling, especially when the concentrations of adsorbates are high, exceeding of the linear range should be avoided in order to have a large sampling volume before breakthrough occurs. Otherwise, the adsorbent trap will not yield good enrichment of the contaminants.

The logarithm of breakthrough volume for acetone and benzene on Carbopack C are plotted against the logarithm of the adsorbate concentrations in Figure 3.3. The flat portion was also observed when the concentration of benzene was over 30 ppm and acetone above 168 ppm. In case of Carbopack B, these points were at a significantly higher concentration. This is because the surface of Carbopack B is higher, 86 m<sup>2</sup>/g as compared to 10 m<sup>2</sup>/g from Carbopack C. The breakthrough volume as a function of concentration showed



**Figure 3.3** Breakthrough volumes (ml/g) as a function of concentrations of acetone, benzene on Carbopack C.

two linear regions for Carbopack C. The first linear region extended up to 20.8 ppm for acetone and 1.25 ppm for benzene.

To study the underlying mechanism, adsorption isotherms were plotted as adsorption capacity (gram of adsorbate/gram of adsorbent) against concentration. Figure 3.4 and 3.5 are adsorption isotherms for benzene and acetone on Carbopack C. The isotherm showed classic “type II” adsorption. Here first the adsorption occurs as a monolayer up to the point of inflection (P in Figure 3.4 and 3.5). This corresponds to points B<sub>B</sub> and B<sub>A</sub> in Figure 3.3. Beyond that, the slope of the line changes as the adsorption took place as multilayer from B<sub>A</sub> to C<sub>A</sub>, and B<sub>B</sub> to C<sub>B</sub>.

The adsorption isotherms for acetone and methanol on Carbopack B are shown in Figure 3.6. It showed “type I” [121] mechanism. Here the adsorption is via a monolayer.

### 3.3.2 Desorption as a Function of Temperature

Sample streams were passed through the microtrap at 5.0 ml/min and desorption pulses were made at 1 minute intervals. Then desorption peak areas were measured at different desorption temperatures. Desorption efficiency was calculated as the percentage of the maximum achievable peak area at high temperatures:

$$D.E._i(\%) = \left( \frac{PA_{i,1} - PA_{Bi}}{PA_{i,2} - PA_{Bi}} \right) \times 100$$

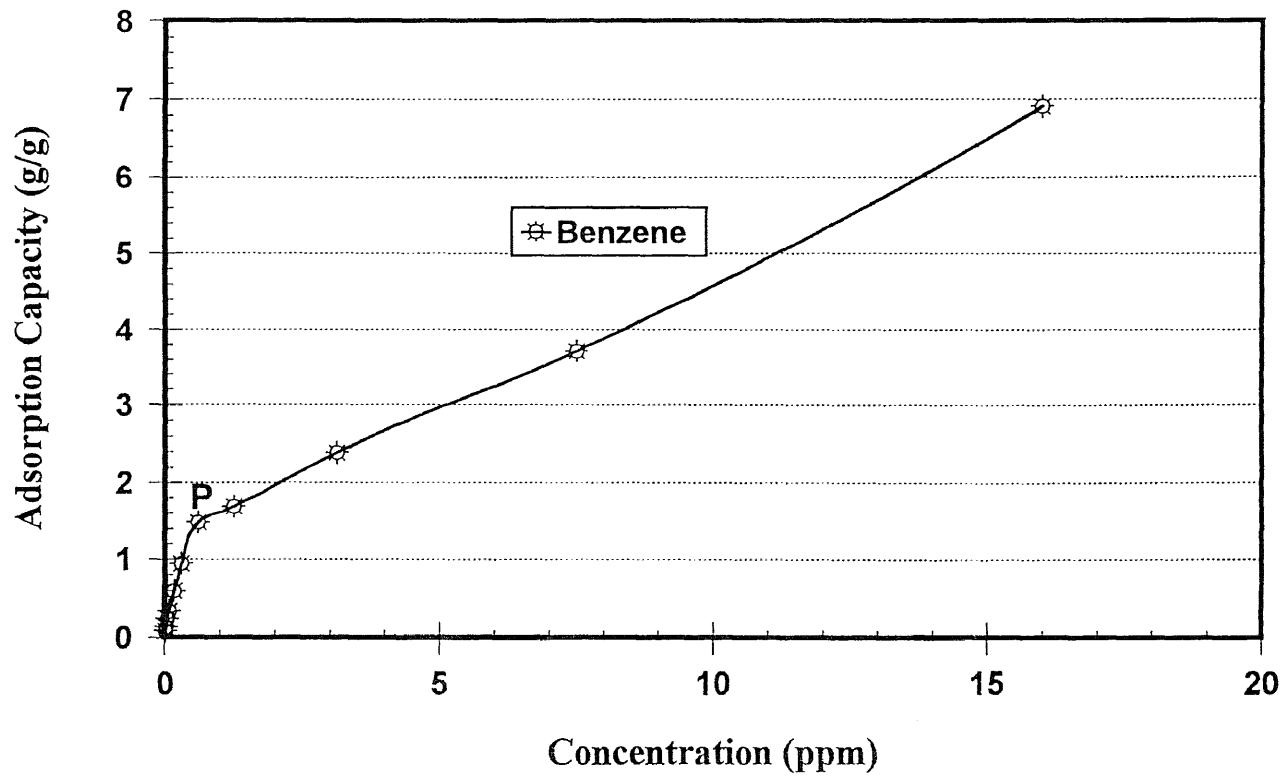


Figure 3.4 Adsorption isotherm for benzene on Carbopack C.



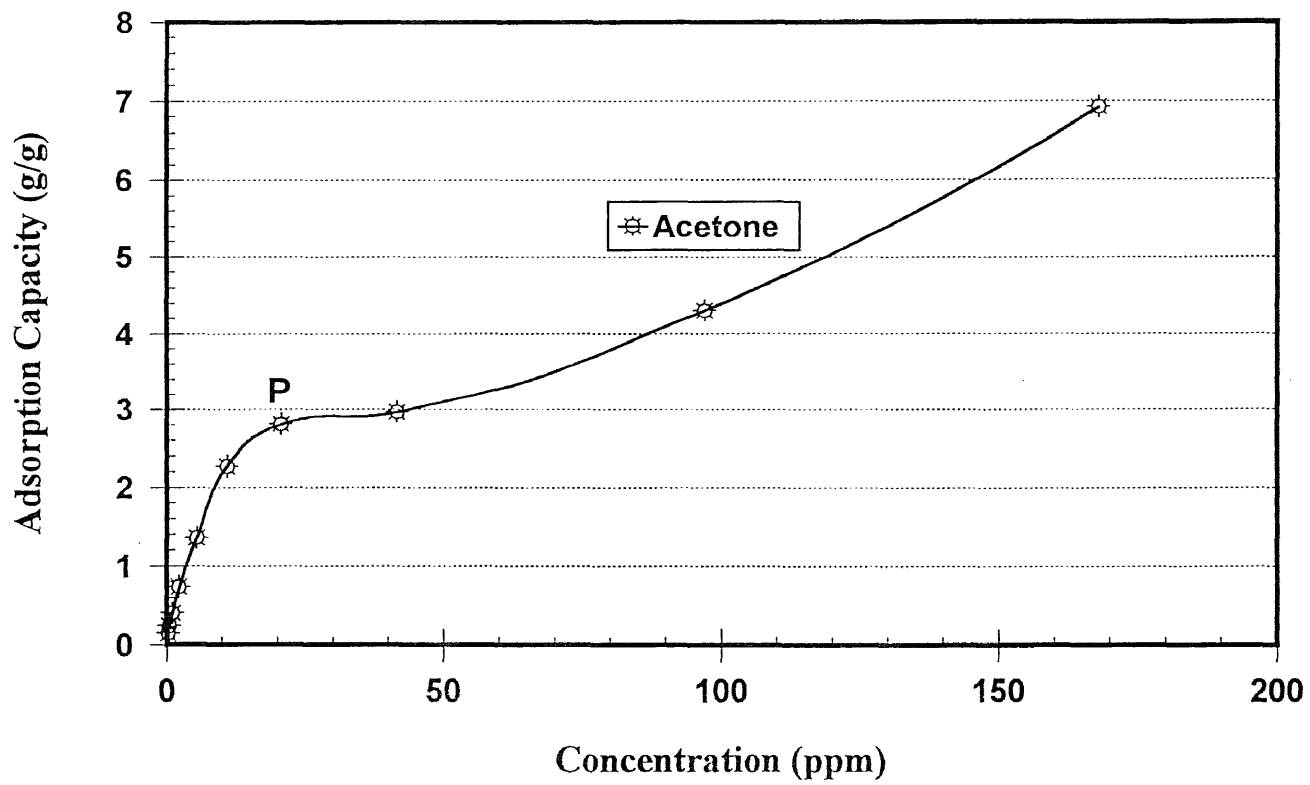


Figure 3.5 Adsorption isotherm for acetone on Carbopack C.

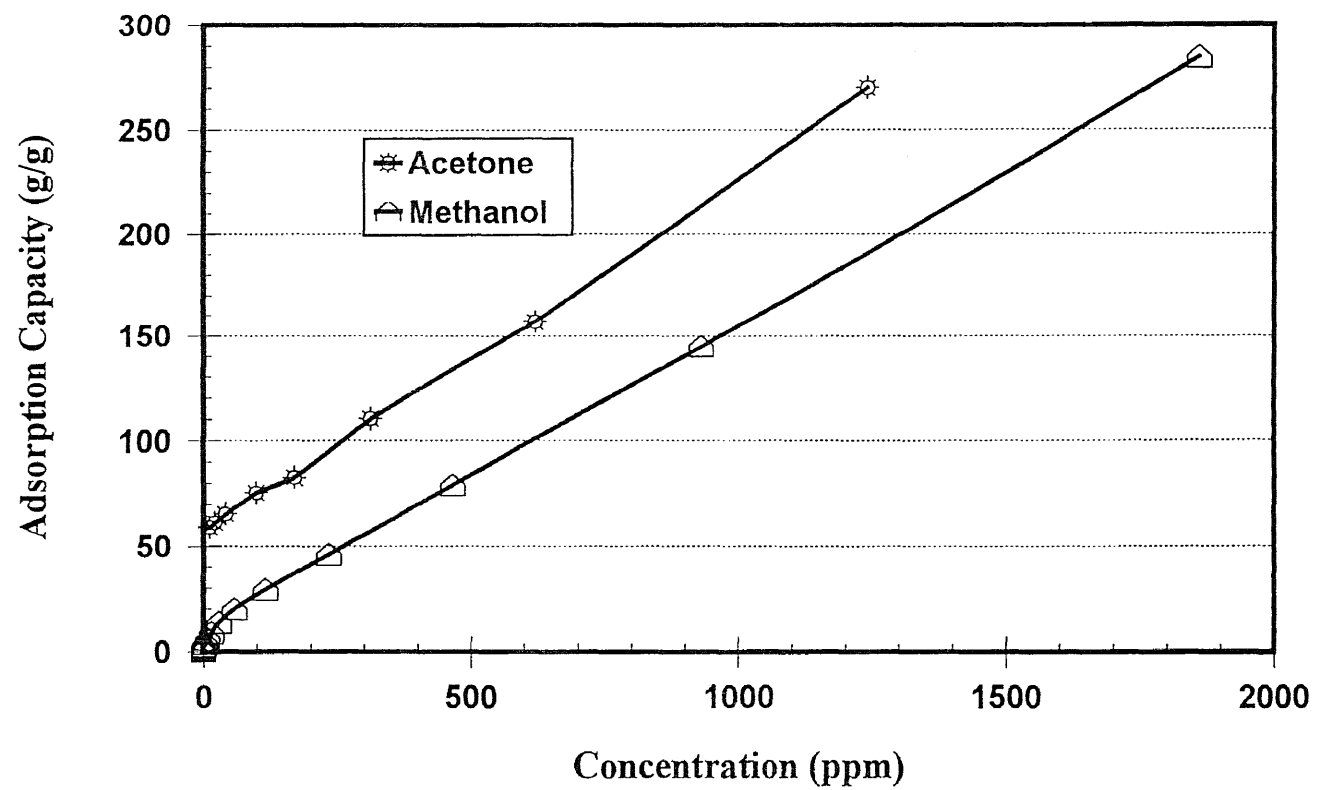


Figure 3.6 Adsorption isotherms for acetone and methanol on Carbopack B.

where,  $D.E._i$  is the desorption efficiency for analyte  $i$ ;  
 $PA_{i,1}$  is the area count of analyte  $i$  at certain temperature;  
 $PA_{i,2}$  is the maximum area count of analyte  $i$  at high temperature;  
 $PA_{B,i}$  is the area count of the adsorbent blank for analyte  $i$  (if any).

The desorption efficiencies for methanol, propane and toluene as a function of desorption temperatures from different adsorbents are listed in Table 3.1, 3.2 and 3.3, respectively. Desorption required more energy when the specific surface area of the adsorbent increased. At 145 °C, 97 % methanol could be desorbed from Carbo-pack C, 76 % from Tenax-TA, 65 % from Anasorb, 72 % from Carbo-pack B, and 75 % from Carbosieve SIII. For methanol, propane and toluene, Carbo-pack C was the weakest sorbent. The complete desorption of these compounds occurred at 215 °C, 215 °C and 265 °C respectively. The Carbosieve SIII was the strongest sorbent of all the ones studied here. Complete desorption of toluene from Carbosieve SIII became very difficult. Anasorb 747 is a bead polymer. It could not be used to pack a microtrap with a diameter of less than 1 mm. Among the sorbents studied here, Carbo-pack C and Carbo-pack B were nonspecific adsorbents which can be used to trap all kinds of adsorbates. The desorption study showed that the test molecules mentioned above could be desorbed at 256 °C from Carbo-pack C and 296 °C from Carbo-pack B.

A higher desorption temperature could be obtained either by increasing the voltage across the microtrap, or by a longer heating time. The maximum temperatures reached at different microtrap voltages, and at different heating times are plotted in Figure 3.7. These results show that 296 °C could be reached either by pulsing the microtrap for 5 seconds at 60 volts, or for 4 seconds at 70 volts.

**Table 3.1** The Desorption efficiencies (%) of methanol as a function of temperature.

Desorption Temperatures °C	Carbopack C	Tenax-TA	Anasorb 747	Carbopack B	Carbosieve SIII
65	42	20	18	20	12
80	63	30	24	35	24
105	80	52	44	50	52
145	97	76	65	72	75
215	100	94	85	93	90
256		100	100	100	97
296					100

**Table 3.2** The Desorption efficiencies (%) of propane as a function of temperature.

Desorption Temperatures °C	Carbopack C	Tenax-TA	Anasorb 747	Carbopack B	Carbosieve SIII
65	33	15	24	19	17
80	57	33	44	40	31
105	80	56	65	65	50
145	96	80	85	86	74
215	100	96	98	96	86
256		100	100	100	96
296					100

**Table 3.3** The Desorption efficiencies (%) of toluene as a function of temperature.

Desorption Temperatures °C	Carbopack C	Tenax-TA	Anasorb 747	Carbopack B	Carbosieve SIII
65	20	15	12	10	
80	43	35	22	19	9
105	66	59	49	40	20
145	85	79	70	63	41
215	97	92	87	83	68
256	100	100	95	93	80
296			100	100	91
350					100

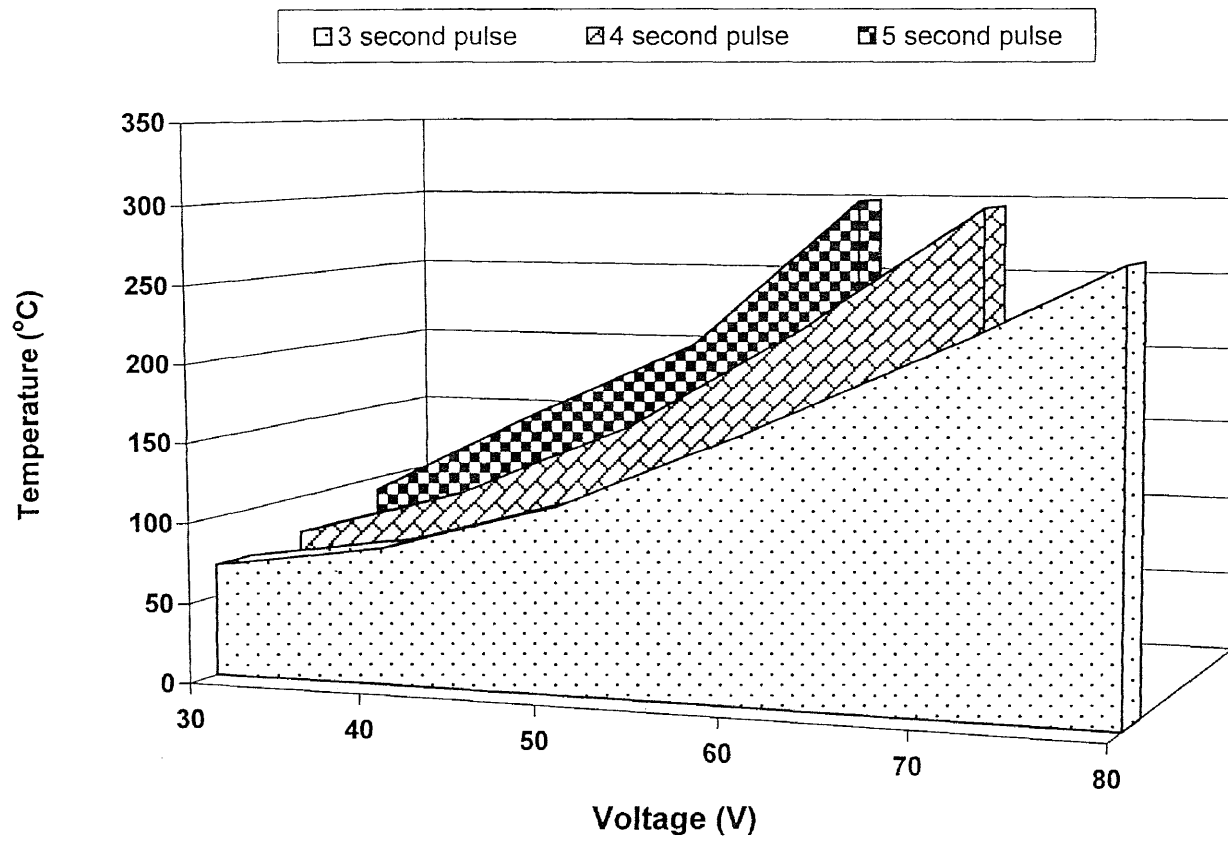
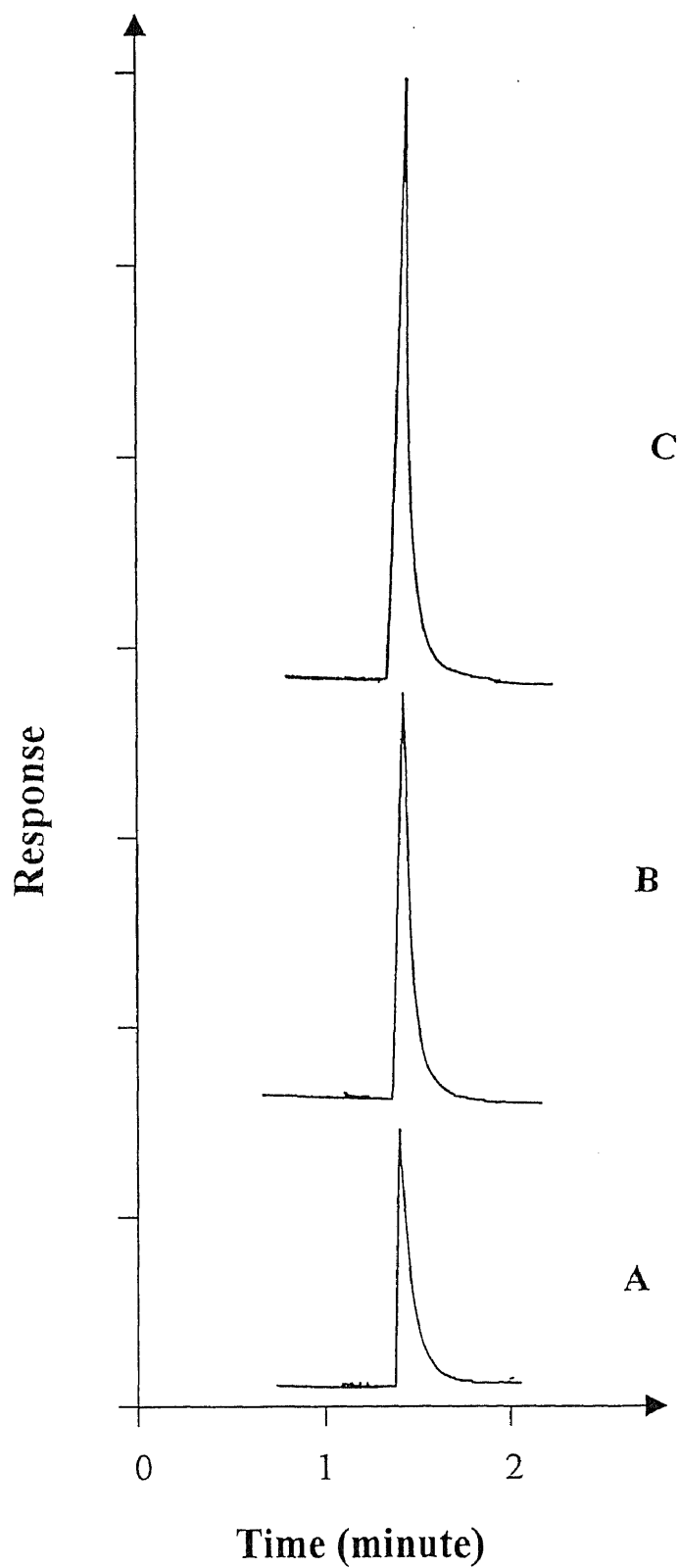


Figure 3.7 Maximum temperatures reached at different microtrap voltages and applying pulse of different durations.

Theoretical prediction of heating rate and energy input was not possible because during pulse heating, the temperature of the microtrap increases, which resulted in increased resistance.

Typical temperature profiles recorded by the IR sensors during microtrap pulses are shown in Figure 3.8. It was observed that at a given voltage, the maximum temperature reached increased with increase in pulse duration. However, the duration of heat pulse did not change significantly with the pulse time. This is because the microtrap heats up instantly (sharp rise in the temperature profile of Figure 3.8), but cools down more slowly. Consequently, the duration of the heating-cooling cycle is determined by the cool down period.

The pulse of analytes desorbed from the microtrap depends upon the sorbent temperature rather than the external measured temperature. Here no measurements were made in the sorbent core. Enough energy needs to be put into the microtrap for quantitative desorption. When enough energy was not put in, the desorption peak was found to be broad and of low magnitude. This can be seen in Figure 3.9. The microtrap may be modeled as a short GC column. When the microtrap is heated, the capacity factor drops to near a zero value. The latter part of the microtrap serves as column for the analyte molecules desorbed at the head of the microtrap. At low voltages, when the microtrap temperature is not high enough, the latter part of the microtrap serves as a column with a fairly high capacity factor. This results in generating a broad desorption profile. At high voltages, this is not encountered because the temperature of the microtrap is high and its capacity factor is low.



**Figure 3.8** Temperature profiles of a microtrap heated with a 60 V power supply. A: pulse duration of 3 seconds; B: pulse duration of 4 seconds; C: pulse duration of 5 seconds.

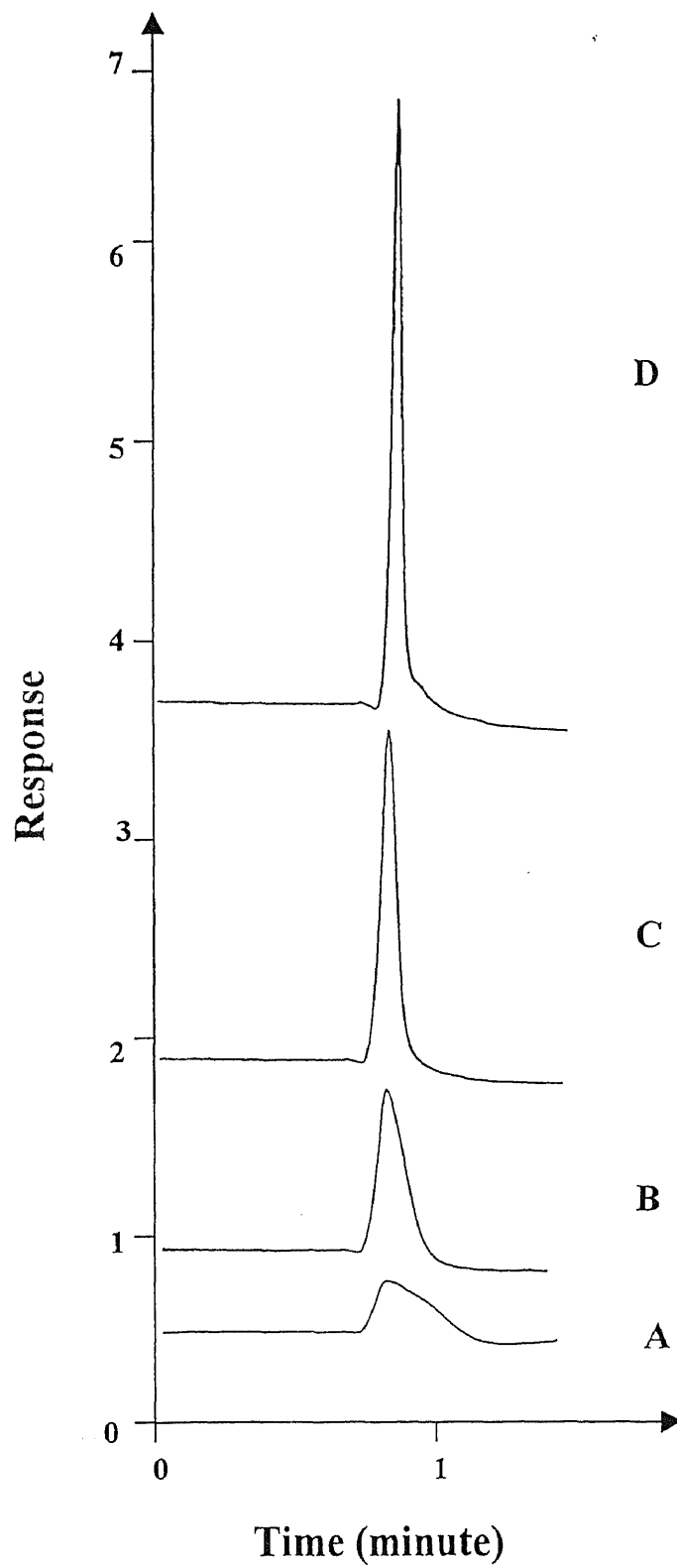


**Figure 3.9** Desorption profiles of toluene from Carbpac C. The pulse duration was fixed at 3 seconds and voltage varied, A: 30 V; B: 40 V; C: 50 V; D: 60 V.



The desorption is a function of sorbent temperature. The resistive heating occurs in the metal tubing, and the energy is transferred to the sorbent by conduction. This takes a finite amount of time. Consequently, a longer pulse time may have the advantage of more uniform heating of the microtrap and higher desorption efficiency. The range of pulse times studied were between 3 to 5 seconds and within this range the analyte desorption peak width did not show significant variations. However, the pulse time can not be increased indefinitely because the microtrap temperature rises to a point where the sorbent phase could be destroyed. For example, increasing the pulse time to the order of 8 seconds made the microtrap glow red hot. In general, some trial and error optimization of voltage and pulse time are needed.

The analyte desorption profile and the microtrap temperature profile are plotted against the microtrap voltages in Figure 3.10. The increase in microtrap voltage did not have significant impact on the duration of the heat pulse. When the microtrap voltage increased from 20 volts to 80 volts, the duration of the heat pulse (measured at half the maximum temperature) showed no significant variation (range of 3.4 to 5 seconds). However, the analyte desorption peak width at half height decreased from 12 seconds to 1.5 seconds.

As the microtrap voltage was increased, the area of analyte desorption peak increased. At low voltages, not enough energy was supplied for quantitative desorption. It was seen that at 50 volts, the microtrap reached a temperature high enough for quantitative desorption. Beyond this, the peak area did not increase significantly with voltage.

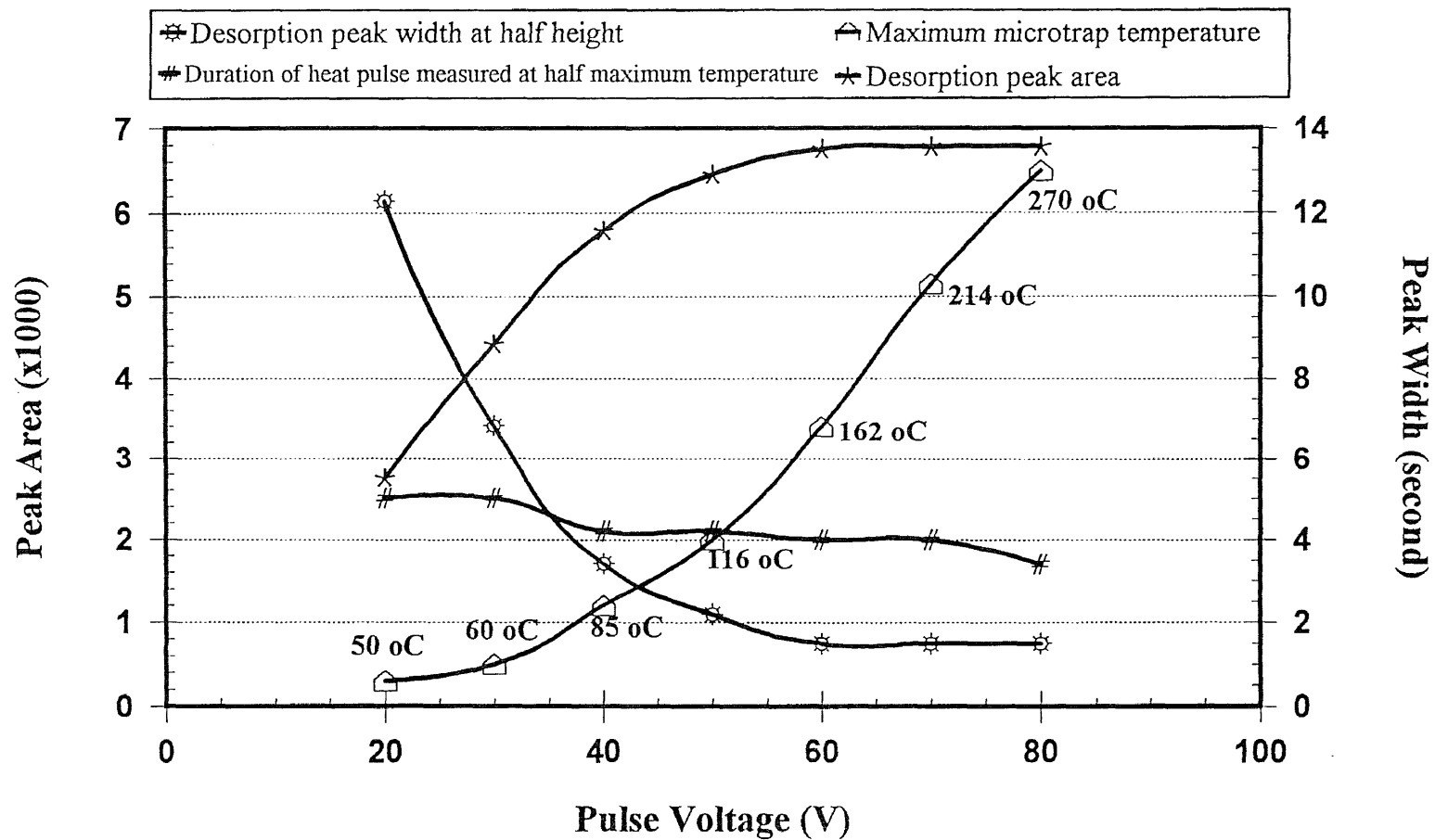


**Figure 3.10** Effect of increasing microtrap voltage on analyte desorption profile (pulse time of 3 seconds, and sample flow rate of 5.0 ml/mim).

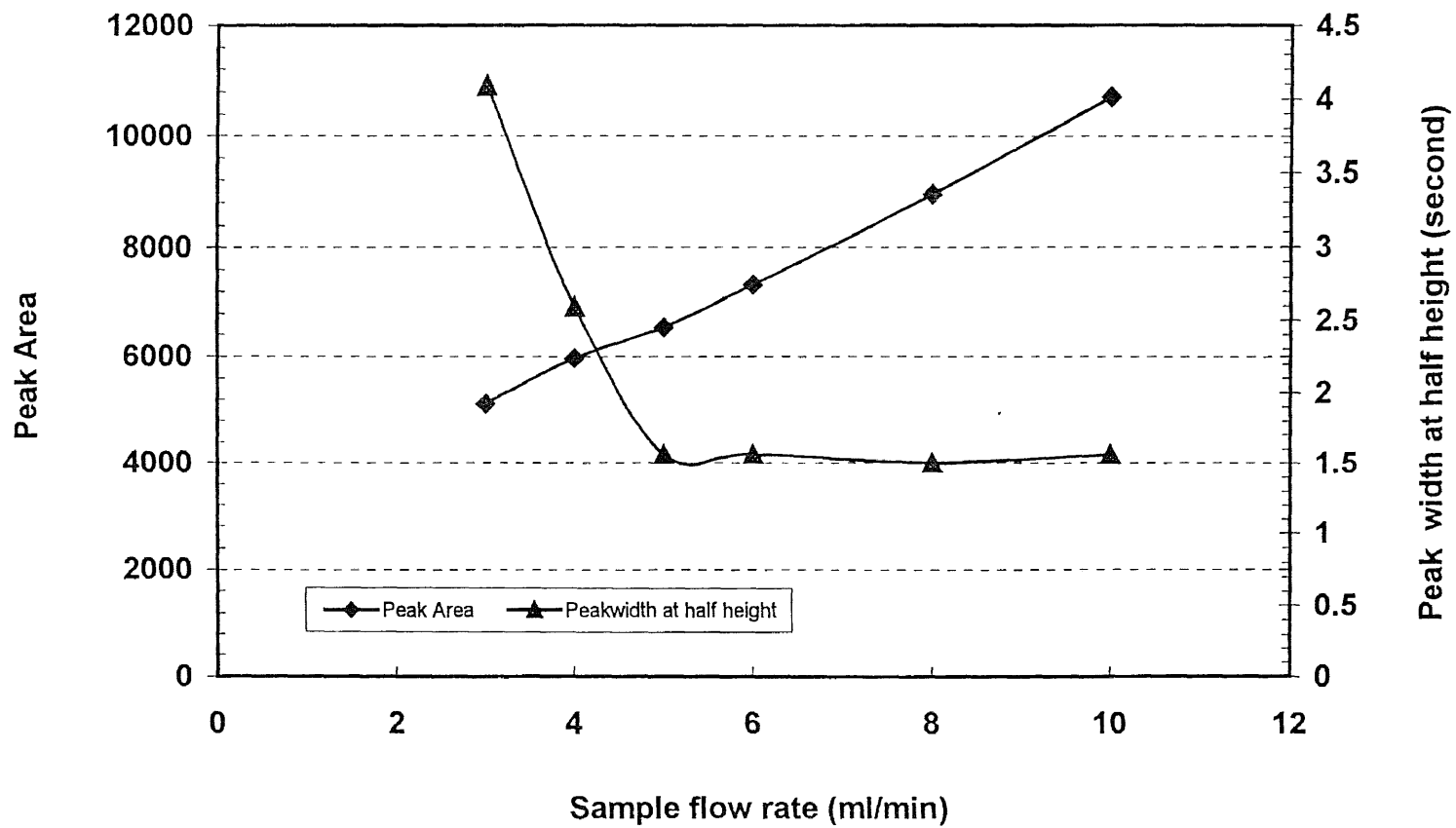


**Figure 3.11** The desorption peak changing with sample flow rate (micortrap voltage at 60 volts, pulse duration at 4 seconds).

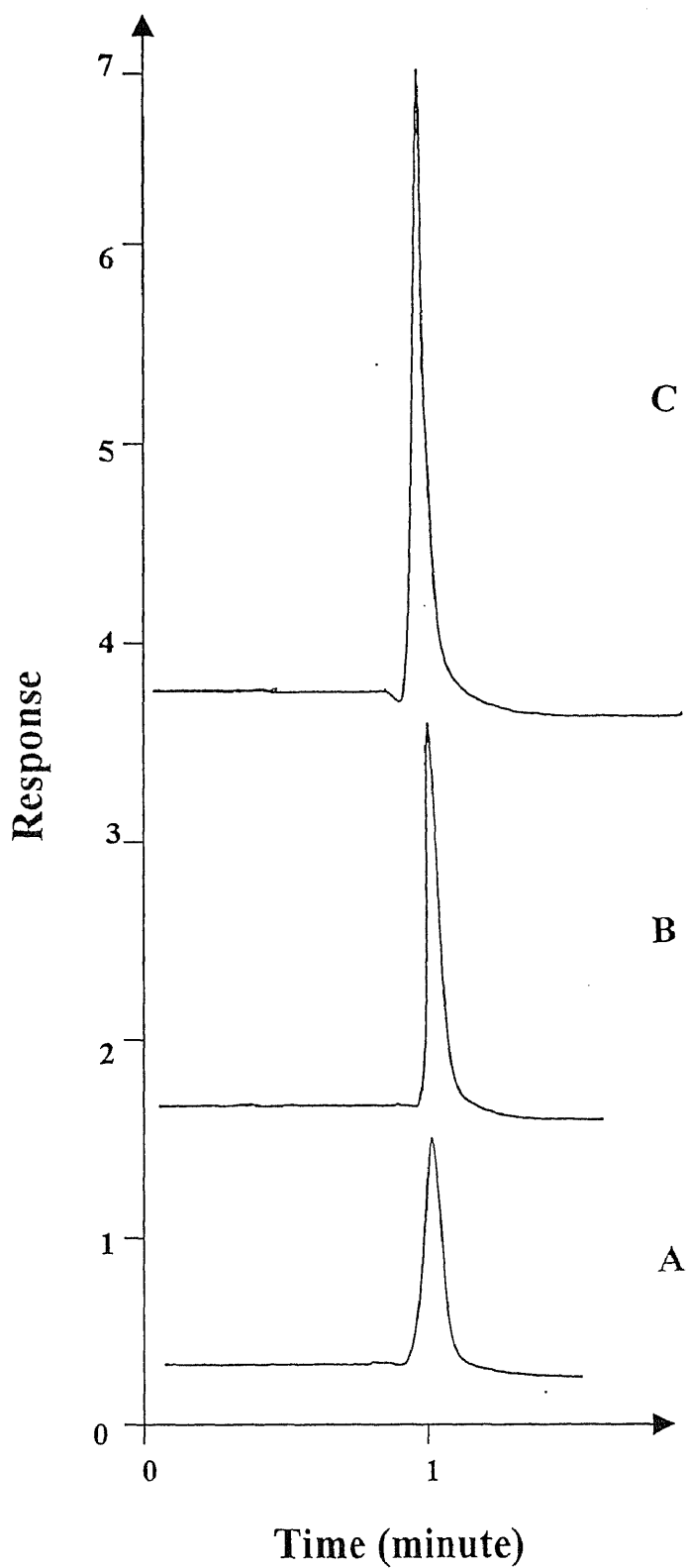


**Figure 3.12** Toluene desorption peaks from Carbopack C at different sample flow rates. The microtrap was desorbed at 60 V for 4 seconds. A: sample flow rate at 3 ml/min; B: sample flow rate at 5 ml/min; C: sample flow rate at 8 ml/min.

The area of the desorption peak and its width are plotted in Figure 3.11 as a function of flow rate at a pulse time of 4 seconds, and a microtrap voltage of 60 volts. Typical desorption profiles are given in Figure 3.12. It is seen that the area of the desorption peak increased linearly with flow rate. This is because more sample is brought into the microtrap resulting in a larger desorption peak as flow rate increases. The desorption peak width decreased with increase in flow rate and eventually reached a constant value. As mentioned before, the latter part of the microtrap served as a GC column. At low flow rates, the desorbed analyte pulse moved slowly. By that time the microtrap had begun to cool down, it encountered a cool sorbent bed of a high capacity factor that broadened the desorption peak. At high flow rates, this pulse escaped the microtrap before it began to cool down.

## CHAPTER 4

### TWO-STAGE MICROTRAP AS INJECTION DEVICE FOR ON-LINE VOCS MONITORING BY GC

#### 4.1 Introduction

Conventional approach to measurement of volatile organic compounds requires sampling of the organics using a sorbent trap or into a whole air sampler (for example canisters). This is followed by laboratory analysis using GC or GC/MS. Recently there has been much effort in development of analytical techniques for continuous, on-line measurement of these species in air emissions and in ambient air. The on-site (or on-line) analysis not only provides instantaneous results but also provides higher accuracy by eliminating the errors associated with the delay between sampling and laboratory analysis. During transport and storage of sample, the sample can degrade and contamination can occur. For example many organic compounds, especially the polar compounds are known to be unstable in electro-polished canisters. Extensive quality control steps are also necessary for these measurements to ensure that there is no error introduced at each step of the process. Consequently these methods are more expensive in term of time and effort required for analysis.

To develop gas chromatographic systems that can perform on-line measurements, it is important to have a device to perform sampling and sample introduction on-line as the air is taken in. The most common sample introduction device is a gas sampling valve. It withdraws a small portion of the sample stream

for injection into the GC which results in a small sample quantity and decreasing sensitivity. The typical injection volumes for using valves vary from a few microliters to 1 or 2 ml. Gaseous sample streams with low concentrations of organic compounds can not be effectively analyzed using valves because the small injection volume contains a small quantity of analyte which results in low sensitivity. The injection volume can not be increased by using a larger sample loop because the injection band becomes wide, reducing chromatographic resolution.

The microtrap has been developed as an automatic sampling and injection device for on-line, continuous GC analysis of volatile organic compounds (VOCs) in air [20, 29]. The major advantage of using microtrap as injection device over sample valves is that the microtrap is not only an automatic injection device but also the sample preconcentrator which allows a large volume injection for trace analysis. Using a microtrap as an injection device makes the analysis of VOCs in air possible on-line and continuously. The microtrap is made small in dimension so that it has low heat capacity and can be heated/cooled very rapidly. The trap is heated resistively, so heat has to migrate from the external tube wall into the sorbent. The heat transfer in larger diameter traps takes long time and desorption of organics is very slow. Fast desorption is essential for generating a narrow injection band so that high resolution separation can be achieved. However, due to its micro dimension, it can be packed with only a small quantity (fraction of mg) of adsorbent. The ideal adsorbent for microtrap would be one which has a large sampling capacity or breakthrough volume for the very volatile species, at the same time providing rapid quantitative desorption for the large molecular weight

compounds. Several studies have been performed to determine the breakthrough characteristics of different compounds on different sorbents [30, 86]. There still no single commercial adsorbent can satisfy the above mentioned criteria of efficient trapping the lightest molecules and high desorption efficiency of heavier ones. Conventional sorbent traps which are used for sampling usually use layers of different sorbents to trap the wide range of compounds. These traps are also designed to sample several liters of air and breakthrough time in the order of an hour or so is required. On the contrary, the microtrap is required to retain the sample for a few seconds to a few minutes. It is desirable to accumulate as much sample as possible in the microtrap prior to making an injection for maximum sensitivity. If a component breakthroughs, only a fraction of the sample is desorbed during injection and a small signal is generated at the detector. As the microtrap contains a small quantity of adsorbent, it is prone to breakthrough problem. The breakthrough volume (defined as L/gm of sorbent) is a function of the amount of the adsorbent, increasing the mass of material sorbent in the microtrap is a way to increasing the breakthrough time of the microtrap. A larger diameter trap can hold more adsorbent, but requires longer desorption time and coupled with slower heat transfer results in poor peak shape. Therefore, on one hand we have the problem of sample breakthrough in small diameter traps, and on the other hand we have the problem of broad desorption band in larger diameter traps.

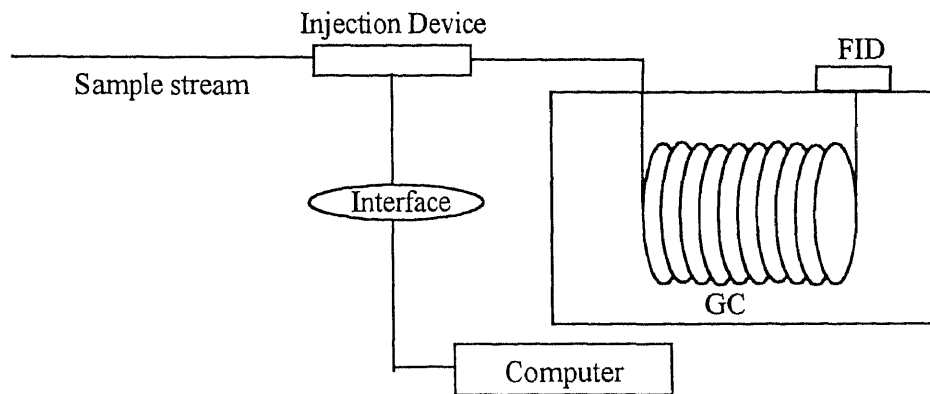
These problems can be solved by using two traps in series and operating sequentially. The first, a larger diameter trap is referred to as the retention trap is packed with more material to increase the breakthrough volume/time. The



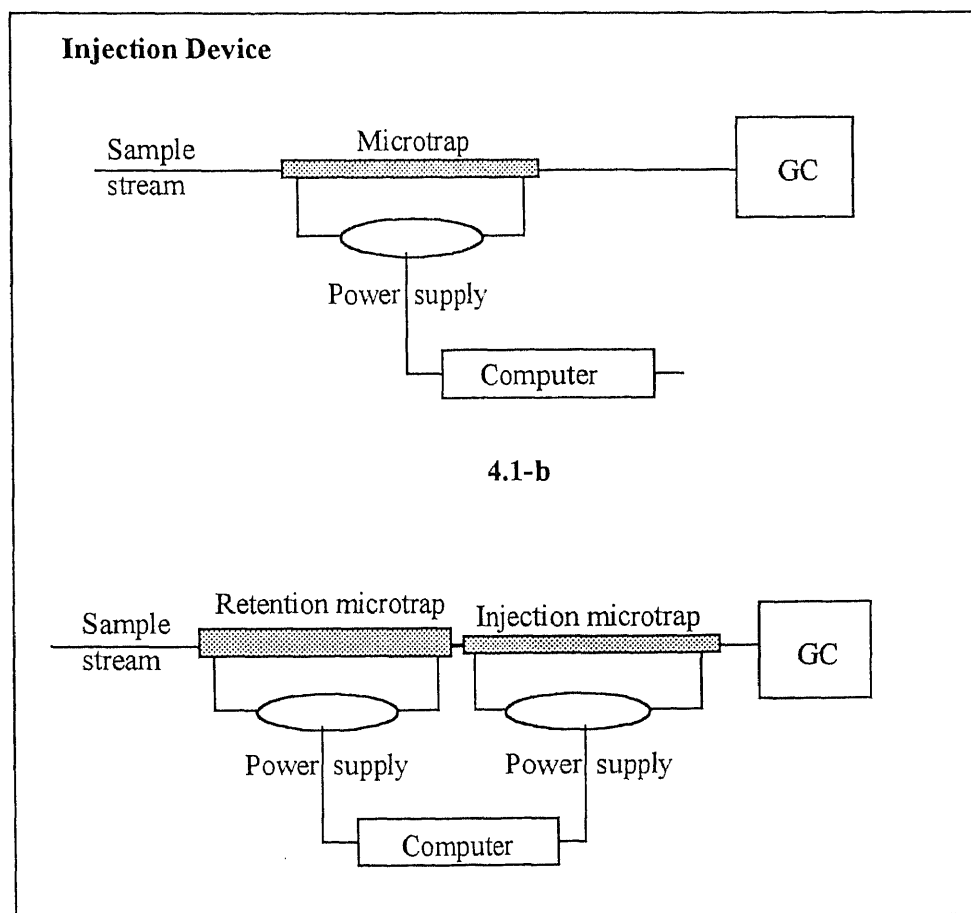
retention trap is desorbed and the analytes are refocused onto the smaller diameter microtrap referred to as the injection trap. A few seconds delay is provided and then the injection microtrap is desorbed to generate a sharp band injection for GC separation. The objective of this study was to demonstrate the effectiveness of using two microtraps in series to enhance the breakthrough time as well as perform on-line analysis by making a series of injections from a flowing sample stream.

## 4.2 Experimental

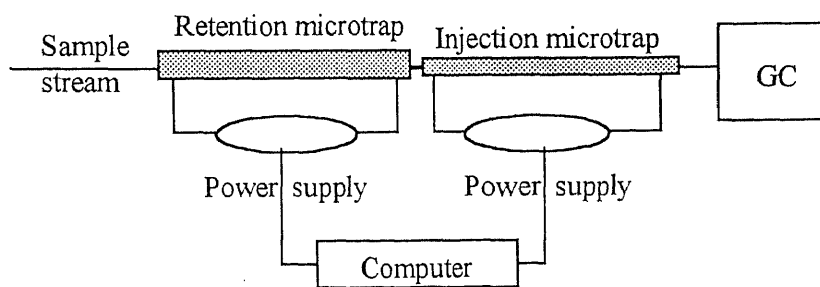
The experimental system is as shown in the Figure 4.1. A Varian GC (Model 3700) equipped with a flame ionization detector was used in the study. A DB-624 column (J &W Scientific, Folsom, CA, USA) was used for separation. Data were collected by a computer with Minichrom chromatography data system (Cheshire, England). Oven temperature was set at 80 °C and the sample flow rates were 6.0 ml/min for all experiments. The microtraps were made by packing Carbopack C (Supelco, Supelco Park, PA, USA) in 0.53 mm i.d. silcosteel tubing (Restek Co., Bellefonte, PA, USA) and 1.1 mm i.d. and 1.3 mm i.d. stainless-steel tubing (Small Part Inc., Miami Lakes, FL, USA). The microtrap was resistively heated by passing current directly through the wall of the metal tubing. The interval between injections and the duration of microtrap pulse were controlled using a microprocessor. The sample stream consisted of gas standards prepared in the laboratory. A variety of compounds were used in this study. Particular attention was given to oxygenated volatile organics which typically have low breakthrough times. Combinations of different microtraps in series were tried. The 1.1 mm, and



4.1-a



4.1-b



4.1-c

**Figure 4.1** Schematic diagram of the experiment system. 4.1-a: instrument system, 4.1-b: one microtrap injection system. 4.1-c: two-stage microtrap injection system.

1.3 mm i.d. microtrap were packed with 0.4 g, 0.8 g adsorbent, respectively. These served as the retention trap. The second or the injection microtrap had a small diameter of 0.53 mm i.d. silcosteel tubing, packed with only 0.02 g of sorbent. First the retention trap was heated at the end of sampling, then after a 5 second delays the injection microtrap was desorbed.

### **4.3 Results and Discussions**

#### **4.3.1 Breakthrough Characteristics of Retention and Injection Microtrap**

The breakthrough volume (specific retention volume) is defined as the calculated volume of carrier gas per unit mass of adsorbent necessary to cause a mass of adsorbate molecules, introduced into the front of the adsorbent trap, to migrate to the back of the trap [69]. The volume of sample that may be quantitatively sampled (greater than 99% collection efficiency) is always less than the breakthrough volume of the least retained component.

Breakthrough was measured by three different methods. The first was to measure response for the microtrap pulse as a function of injection interval [27]. Increasing the interval time increases the response as more samples are accumulated by the microtrap. Once the sample begins to breakthrough, the response does not increase anymore because no further sample accumulation occurs. The breakthrough can be found at the maximum response.

The second method uses the peak shape of the microtrap injections as the sample flows continuously through [29]. When the microtrap is heated, a desorption peak occurs. As the sample flows continuously, the analytes are

readsorbed in the microtrap. This lowers the base line into the negative territory appearing as a negative peak. As sample begins to breakthrough, the detector response increases and the response increases again. The width of the negative peak at the base line equals the breakthrough time.

The conventional method is using frontal chromatography. When a sample stream containing organics is introduced, initially the response stays constant and then as the sample front breakthroughs, the response increases to a steady value. Here the breakthrough volume is calculated based on the time required for breakthrough. The breakthrough time of acetone on a 1.1 mm i.d. Carbo-pack C microtrap was measured to be approximately 1.5 min by all three methods. The data in Figure 4.2 showed that these three methods were equivalent. For the rest of the study, the first method was chosen because it was the operationally simplest method.

#### **4.3.2 Quantitative Desorption from the Microtrap**

The desorption of adsorbate from the microtrap is achieved by passing a pulse of electric current directly through the wall of the microtrap. Figure 4.3 is the plot of peak area as a function of pulse time for the three microtraps of different diameters. The thicker wall of the larger diameter tubing further slow down the flow of heat. The pulse time required for 0.53 mm i.d. microtrap was 1.5 second as compared to 4 second for 1.1 mm i.d. and 5 second for 1.3 mm i.d. microtraps. With the increasing of the diameter of trap, the packing amount of the adsorbent also increased. The pulse time for complete desorption of adsorbate became

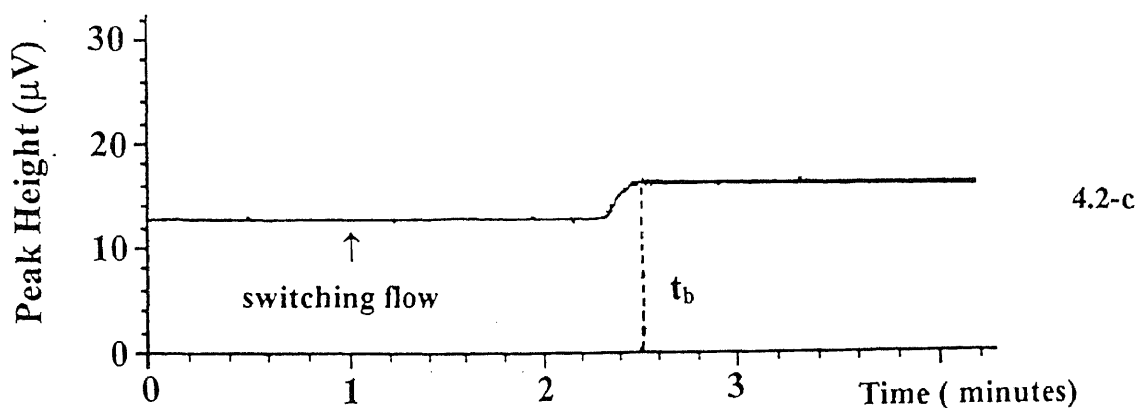
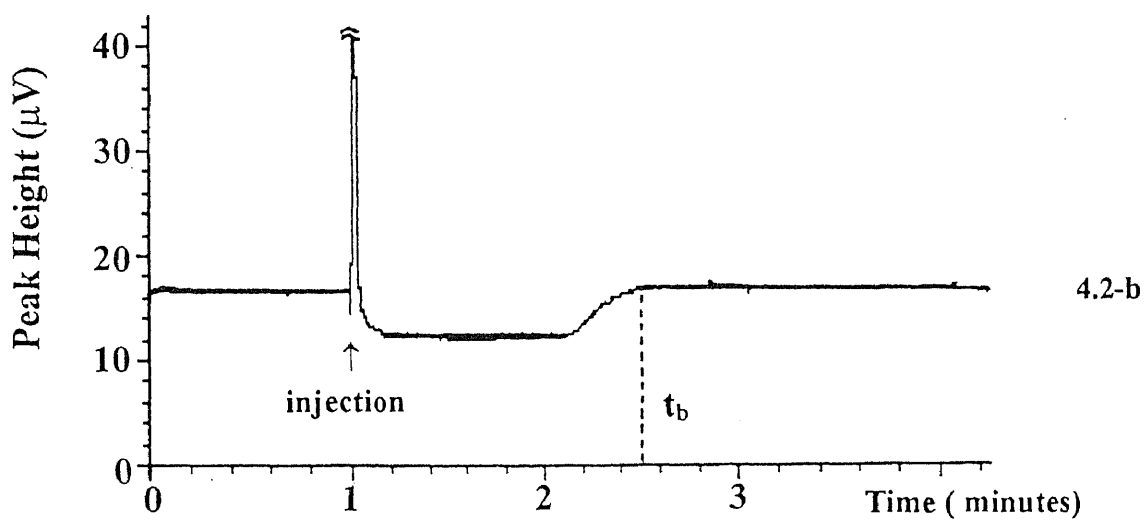
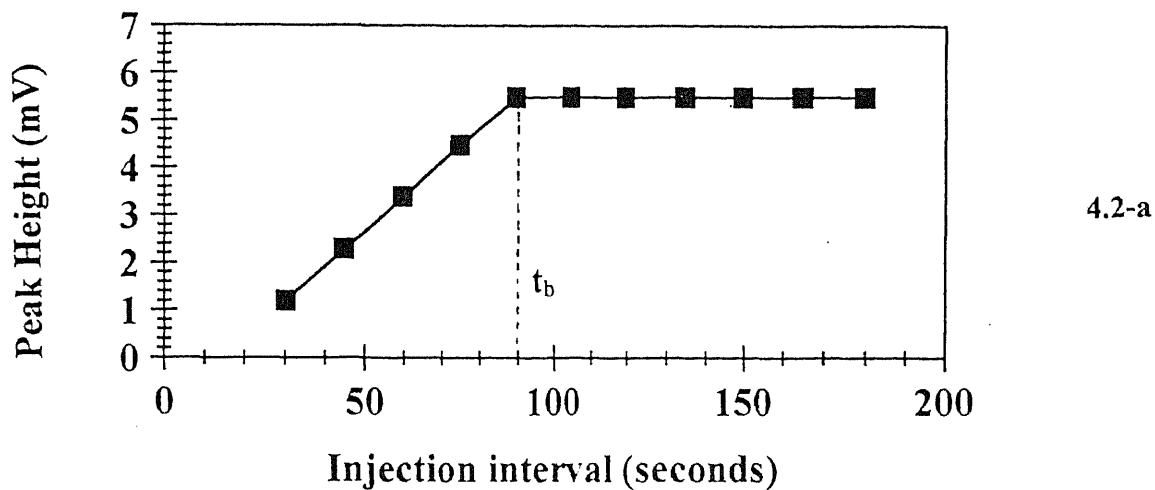


Figure 4.2 Acetone breakthrough on 1.1mm i.d. stainless steel microtrap measured by three different methods (sample flow rate 6.0 ml/min). 4.2-a: Response of the analytical system as a function of interval between microtrap pulses, 4.2-b: Characteristic peak from a microtrap, 4.2-c: Chromatogram generated by frontal chromatography.

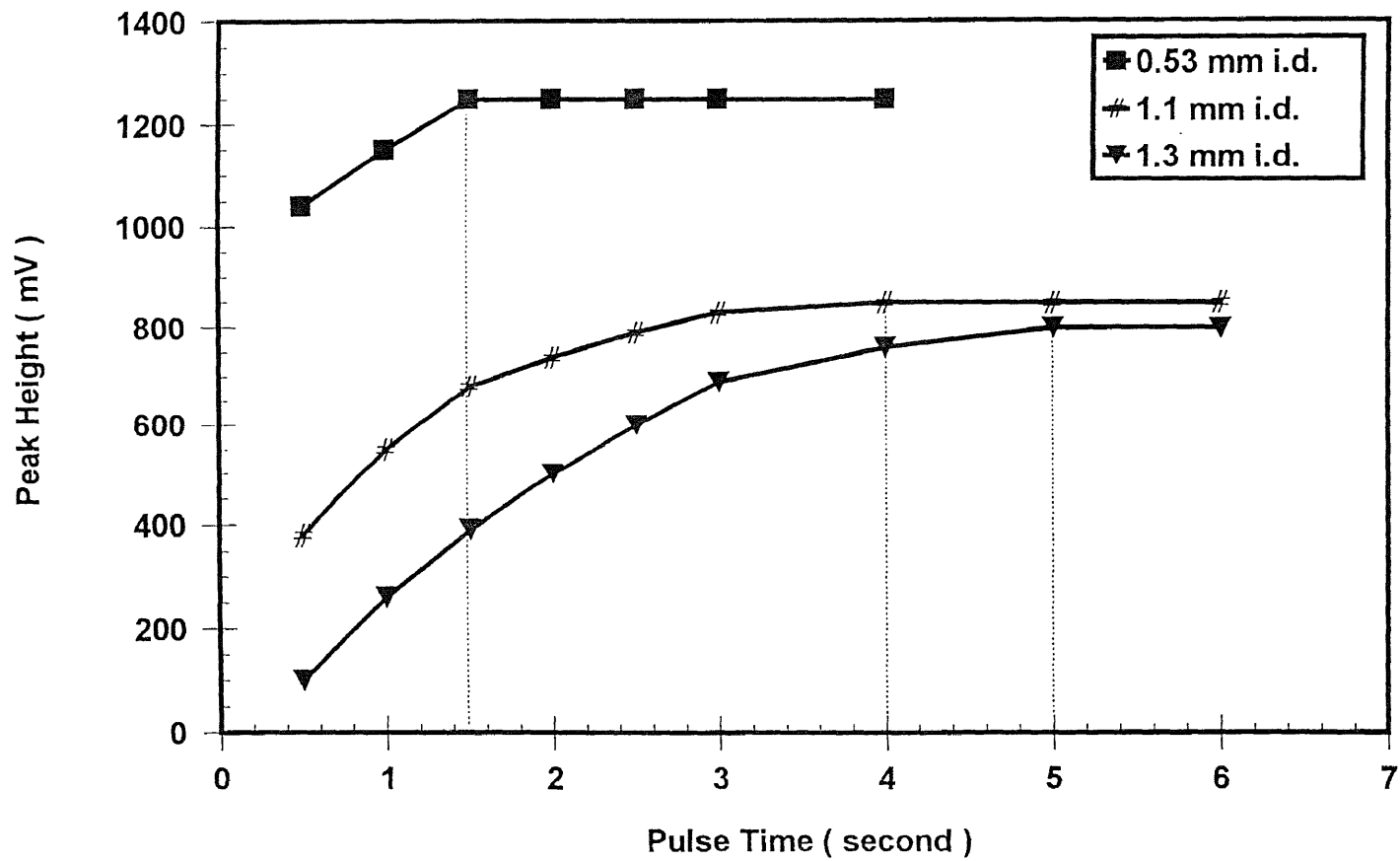


Figure 4.3 The plot of peak height as a function of pulse time for different size microtraps.

longer. If they are used as injections for GC, the peaks in chromatogram will become broad. As expected, the larger microtraps due to their slower heating rate generate broad chromatographic bands. The chromatograms generated by each microtrap are presented in Figure 4.4. The 0.53 mm i.d. microtrap generated a high resolution chromatogram where all components were well separated. For the larger microtraps the resolution was significantly lower. For example 1-propanol and 2-butanone were not well separated. The methanol peak was broadened to the point that it could not be distinguished from the baseline noise. The peak widths at half height for different components are listed in Table 4.1. All the peaks generated by larger traps became two times broader than those generated by small diameter traps. When components are present at low concentration in an unknown sample, poor peak shape and low peak height may cause misidentification. The peak heights of methanol were 0.11, 0.06, 0.07 mV for trap 1, trap 2 and trap 3, respectively. The method sensitivity will be dramatically decreased by a broadened injection band. If the GC separation can not be done within very short time, a longer sampling time will be needed. For low concentration streams, larger sampling time results in more preconcentration and lower detection limits can be achieved.

#### **4.3.3 Performance of Two-stage Microtrap**

The objective of using two microtraps in series was to enhance the breakthrough time by using a larger diameter trap while retaining high resolution. The first microtrap, namely the retention trap, prevents breakthrough while the second

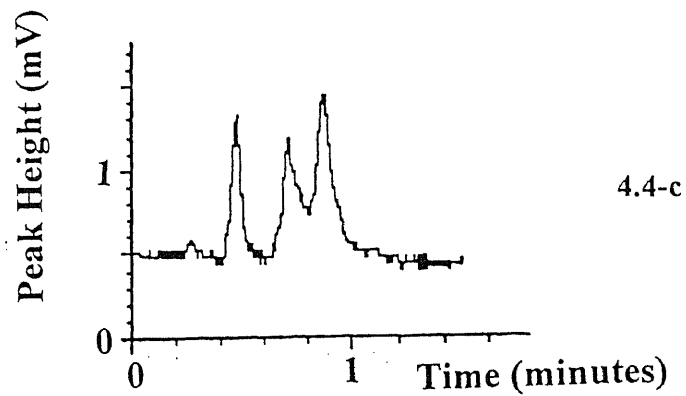
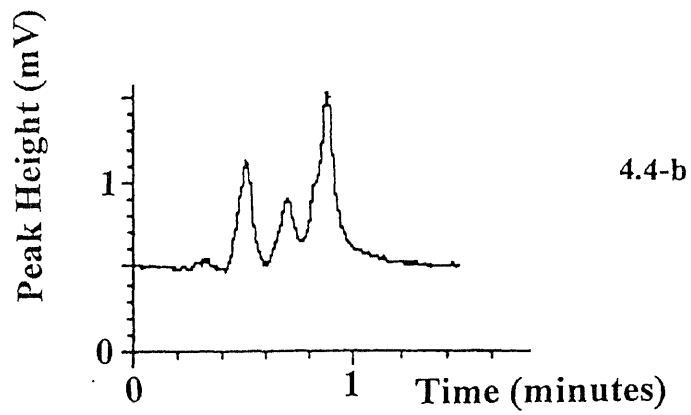
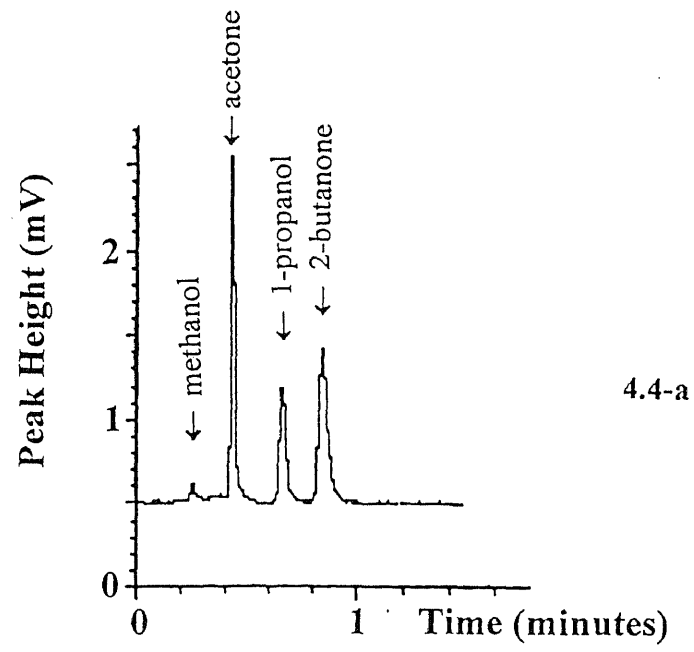


Figure 4.4 Chromatograms generated by using different sizes of microtrap as injection device. 4.4-a: 0.53 mm i.d. microtrap, 4.4-b: 1.1 mm i.d. microtrap, 4.4-c: 1.3 i.d. microtrap.



microtrap serves as an injector. For example from Table 4.2, the breakthrough times for trap 1 and trap 3 for methanol are 0.5 and 1.9 minute respectively. When the two microtraps are used in sequence, the breakthrough time will increase to 2.5 minute.

**Table 4.1** Peak width (minute) at half height in chromatograms generated using different size microtraps.

Peak width at half height (min)	Methanol	Acetone	1-Propanol	2-Butanone
Trap 1 (0.53 mm i.d.)	0.02	0.025	0.035	0.045
Trap 2 (1.1 mm i.d.)	0.07	0.05	0.075	0.075
Trap 3 (1.3 mm i.d.)	0.12	0.07	0.085	0.09

The same sample stream presented in Figure 4.4 was analyzed using two-stage microtrap injection and the chromatograms are shown in Figure 4.5. In both cases, trap 1 was used as the injector. A five seconds delay between the desorptions of the first and second microtrap was found to be adequate for readsorb the trapped organics from retention trap onto the injection trap. Figure 4.5 demonstrates the application of the two-stage microtrap as the sample stream flows continuously through. The chromatograms had excellent resolution and the

methanol peak was clearly distinguishable. Peaks of 1-propanol and 2-butanone were also well resolved.

**Table 4.2** Breakthrough times of different size microtraps.

<i>Breakthrough Time (min)</i>	<i>Trap 1</i>	<i>Trap 2</i>	<i>Trap 3</i>
<b>Methanol</b>	0.51	1.2	1.9
<b>Acetone</b>	0.81	1.5	2.1
<b>1-Propanol</b>	1.4	1.8	2.5
<b>2-Butanone</b>	2.3	3.7	6.3

Trap 1: Silcosteel trap, 0.53 mm i.d. packed with Carbopack C 0.02g;

Trap 2: Stainless steel trap, 1.1 mm i.d. packed with Carbopack C 0.08g;

Trap 3: Stainless steel trap, 1.3 mm i.d. packed with Carbopack C 0.13g.

In Figure 4.5-a, peak heights were 0.24, 3.65, 1.41, 3.36 mV for methanol, acetone, 1-propanol and 2-butanone, respectively. Peak heights of these four components increased significantly, comparing to the chromatogram showed in Figure 4.4-a where the peak heights were 0.11, 1.96, 0.71 and 0.95 mV for the components respectively and breakthrough occurred in the small diameter microtrap. The peak width at half peak height for methanol was significantly decreased to 0.02 min when using two-stage microtrap injection comparing to one using one stainless microtrap. Figure 4.5-a and 4.5-b showed that slight increase of microtrap diameter for retention microtrap did not have a significant influence on

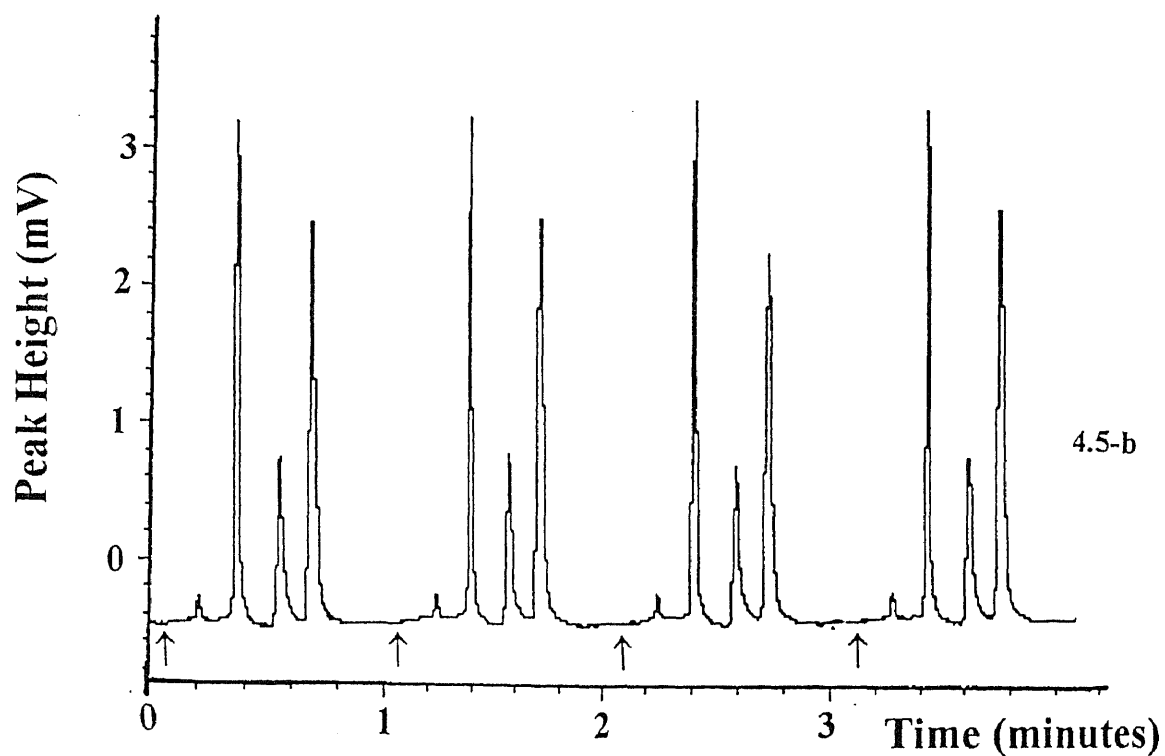
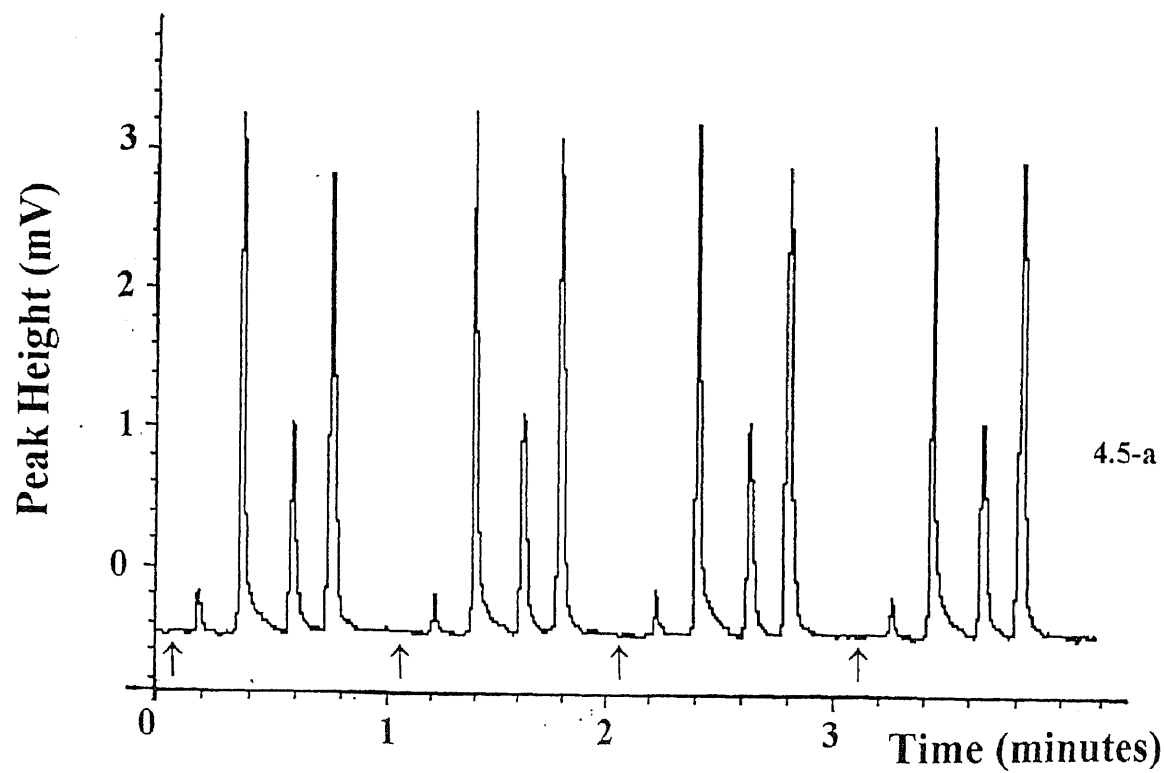


Figure 4.5 Chromatograms generated by using two-stage microtrap as injection device. 4.5-a: 1.1 mm i.d. microtrap as first trap and 0.53 mm i.d. microtrap as second trap, 4.5-b: 1.3 mm i.d. microtrap as first trap and 0.53 mm i.d. microtrap as second trap.

resolution because there was only a 1 second difference between the desorption time for these two traps. The results showed that using two-stage microtrap for injection will gain not only sampling time either for column separation or increasing sensitivity, but also good resolution in chromatogram with a good peak shape resulting in high sensitivity and low detection limit for the trace components presented in environmental samples.

#### **4.4 Conclusion**

The results demonstrated that the two-stage microtrap system was effective in reducing (if not eliminating) the breakthrough problem in microtrap. The two-stage microtrap produced high resolution chromatograms and increased sensitivity by accumulating sample for a longer period of time.

## CHAPTER 5

### A MICROTRAP INTERFACE FOR ON-LINE MASS SPECTROMETRY

#### 5.1 Introduction

In conventional VOCs analysis, the air is sampled by canister or sorbent trap, then cryogenically enriched, followed by thermal desorption and analysis using GC equipped with flame ionization detector (FID) or GC/MS. Volatile organic compounds (VOCs) concentrations can degrade caused by analyte losses from microbial degradation, absorption, and volatilization. Most of the errors in VOCs analysis may be attributed to the delay between the collection of an environmental sample and its chemical analysis [9]. Recently, much research on continuous, on-line monitoring has been reported. Continuous, on-line monitoring of pollutants in ambient air and emissions provides diagnostic information in field analysis where immediate results may have important health and safety benefits. Since it eliminates the time for transportation and storage between sampling and analysis, not only can the cost be significantly reduced [8], but also more accurate results can be obtained. In the lab analysis, the separation capacity of a capillary column in GC makes the separation of individual compounds feasible and hence increases the accuracy of the identification and quantification. However, the time required for column separation can be fairly long. Mass spectrometry provides fast response, excellent quantitative and qualitative information. The high sensitivity and rich spectral information of MS measurement are particularly attractive for trace analysis [9, 122-125].

The main challenge for using mass spectrometer for continuous, on-line analysis in air monitoring application is the interface between the sample collection system and the ionization chamber. Normally, VOCs are present in trace concentration (ppm to ppb levels) while permanent gases such as H<sub>2</sub>O, oxygen and CO<sub>2</sub> are present at percent levels. Moisture, in particular, is a source of serious interference in on-line mass spectrometry [123]. Small inorganic molecules can absorb energy in the ionization chamber of a mass spectrometer and hence reduce the measurement sensitivity for the target organic compounds. Large quantities of interfering species can also cause a failure of the vacuum pump and damage the instrument. Consequently, a sensitive on-line mass spectrometry requires an effective sampling technique to eliminate the moisture and other permanent gases such as CO<sub>2</sub>, H<sub>2</sub>O and CH<sub>4</sub> from the sample before the entrance into the ionization chamber. Several kinds of approaches have been reported for on-line mass spectrometry analysis of VOCs. They are direct introduction [124], membrane introduction [41, 42, 50, 125], atmospheric pressure ionization or atmospheric sampling glow discharge ionization [48, 56] and sorbent trap introduction [126].

Direct introduction of air emissions into a mass spectrometer provides nearly instantaneous response. Normally, it requires a moisture filter to dry the sample especially when a large amount of moisture is present in the sample stream. However, large quantities of other permanent gases such as CO<sub>2</sub> still cause interference. Moreover, in the moisture filtering techniques, along with moisture, organic molecules are also partially removed. This technique is not suitable for efficient detection of trace level of VOCs because the limits of the gas flow into

the instrument are typically under 1.0 ml/min. In the membrane introduction mass spectrometry (MIMS), air emissions are introduced through a membrane that provides some selectivity towards the organics while blocking the flow of background gases. The limitations of membrane include that permeation efficiency may not be very high and the response time may be long. Sudden rupture of a membrane may also produce a catastrophic failure of the spectrometer. The designs of atmospheric pressure ionization and atmospheric sampling glow discharge ionization facilitate the continuous, on-line monitoring. The disadvantages are that complex pumping systems and high-voltage power supplies for ionization and tedious instrument operation are required. Sampling and injection devices based on microtrap preconcentrator have shown advantages in continuous, on-line monitoring of VOCs in air [20, 27, 32]. The microtrap which served as an interface for direct sampling mass spectrometry was tested in our previous study. Several configurations of combination of microtrap and gas sampling valve have been studied. On-line microtrap with back-flushed desorption (OLMT-BF), with the microtrap replacing the loop of sampling valve, showed encouraging performance for analysis of VOCs in air.

In this research, microtrap based sampling systems were further studied for sampling low concentration, and multiple VOCs directly into a mass spectrometer. This technique is referred to as microtrap mass spectrometry or MTMS. The performance of MTMS was also demonstrated for monitoring VOCs in catalytic incinerator emission.

## 5.2 Experimental

The microtrap was configured in several ways with the mass spectrometer. Three kinds of sampling and injection systems were compared. The schematic diagrams of these configurations studied for continuous monitoring of VOCs are presented in Figure 5.1. They are direct injection by sampling valve without microtrap; sequential valve microtrap (SVMT) directly connected to MS; and on-line microtrap with back-flushed desorption (OLMT-BF). In this study, the performances of these sampling systems were evaluated at a low concentration of toluene (5 ppm). In direct sampling mode, sample stream was first collected by a sampling valve with 5 ml loop. Helium purged out the sample from the loop directly into ionization chamber through a jet separator. The sampling valve and the jet separator were connected by fused silica tubing. In the SVMT mode, helium purged out the sample from the loop of sampling valve to the microtrap that was directly connected to the jet separator. The sample air stream passed through the microtrap into the MS while the organic components were retained by the adsorbent packed in the microtrap. The microtrap was desorbed to make injections into the MS after the inorganic peak. In the OLMT-BF mode, a microtrap replaced the sample loop of a six port gas sampling valve. First, the air stream passed through the microtrap. The VOCs were trapped, and the matrix gases such as moisture, N<sub>2</sub>, and CO<sub>2</sub> were vented to the outside without entering the MS. When the valve was switched to the injection position, carrier gas, helium passed through microtrap to the mass spectrometer. The flow direction of He was



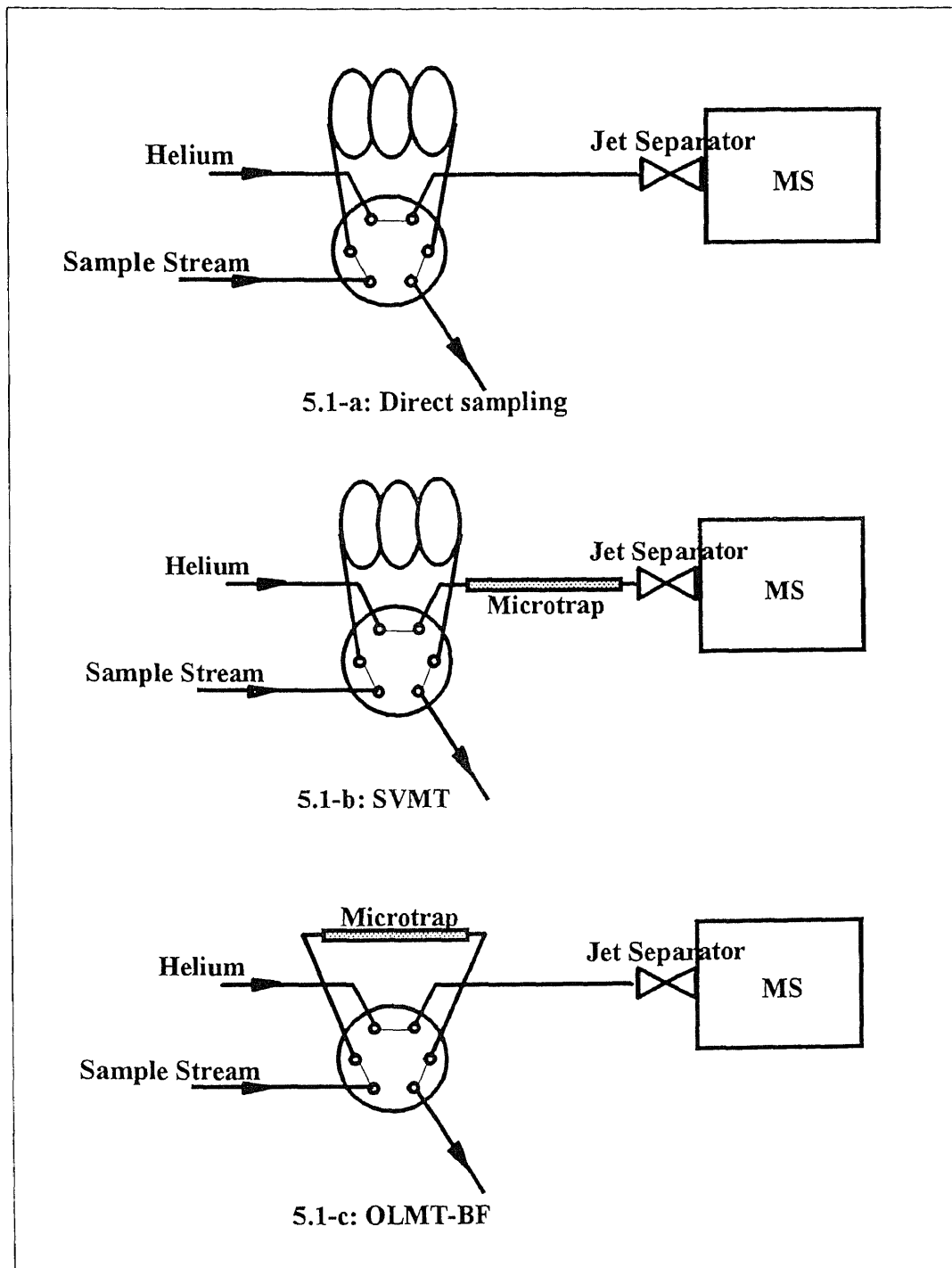


**Figure 5.1** Schematic diagram of the experimental system. 5.1-a: Direct sampling, 5.1-b: Sequential valve microtrap, 5.1-c: On-line microtrap with backflush.

reversed to backflush the microtrap. The microtrap was then heated and VOCs were desorbed/injected into the MS.

The microtrap was made by packing Carbopack C (Supelco, Supelco Park, PA) into a 10 cm long, 0.53 mm i.d. silica lined stainless steel tubing (Restek Co. Bellefonte, PA). The injection was performed by heating the microtrap with a pulse of electric current. A seven to ten amperes of current was supplied using a Variac. A microprocessor-based timer was used to control the current at a short pulse time of 1.5 seconds. Each electric pulse generated an analytes concentration pulse that was analyzed with the MS.

A six-port gas sampling valve (Valco Instruments Co. Inc., Houston, TX) was used to switch between sampling and injection. A Hewlett Packard (Avondale, PA) quadruple MS model 5988A was used for the detection of VOCs. A jet separator was used to limit the flow into the MS at 1.5 ml/min. Evaluations were done using a laboratory-made mixture containing 5 ppm toluene, 3.0 % H<sub>2</sub>O, 8.0 % CO<sub>2</sub>, and in an air balanced. The m/z of interest were 91, 44, and 17 to represent characteristic fragments of toluene, CO<sub>2</sub>, and H<sub>2</sub>O, respectively. The sample stream contained 2-butanone (90 ppm), hexane (40 ppm), benzene (57 ppm), toluene (16 ppm) and tetra-chloroethylene (TCE) (16.7 ppm), 3.0 % H<sub>2</sub>O, 8.0 % CO<sub>2</sub> was used as feeding stream for catalytic incinerator. The detection limits and low ppb level standard calibration curves were measured on a Varian Saturn Ion Trap Mass Spectrometer using standard gas (ALPHAGAZ, Walnut Creek, CA) containing 625 ppt of benzene, toluene, ethylbenzene and tri-chloroethylene.

Monitoring of incinerator emission was demonstrated. The experimental system was sketched in Figure 5-2. The catalytic reactor employed in the experiment was a 2.5 cm o.d. stainless tubular reactor placed in a temperature controlled horizontal furnace (Lindberg, Watertown, WI). The catalyst (Engelhard Corporation, Edison, NJ) was 1.5 % platinum deposited on an Y-alumina washcoat and carried on a 400 cells per square inch cordierite honeycomb. The length of catalyst bed was 0.5 cm. The sample stream containing VOCs was passed through the catalytic incinerator at 20 ml/min. The temperature of the incinerator was changed by 50 °C from room temperature to 400 °C for measurement of VOC's residues in emission.

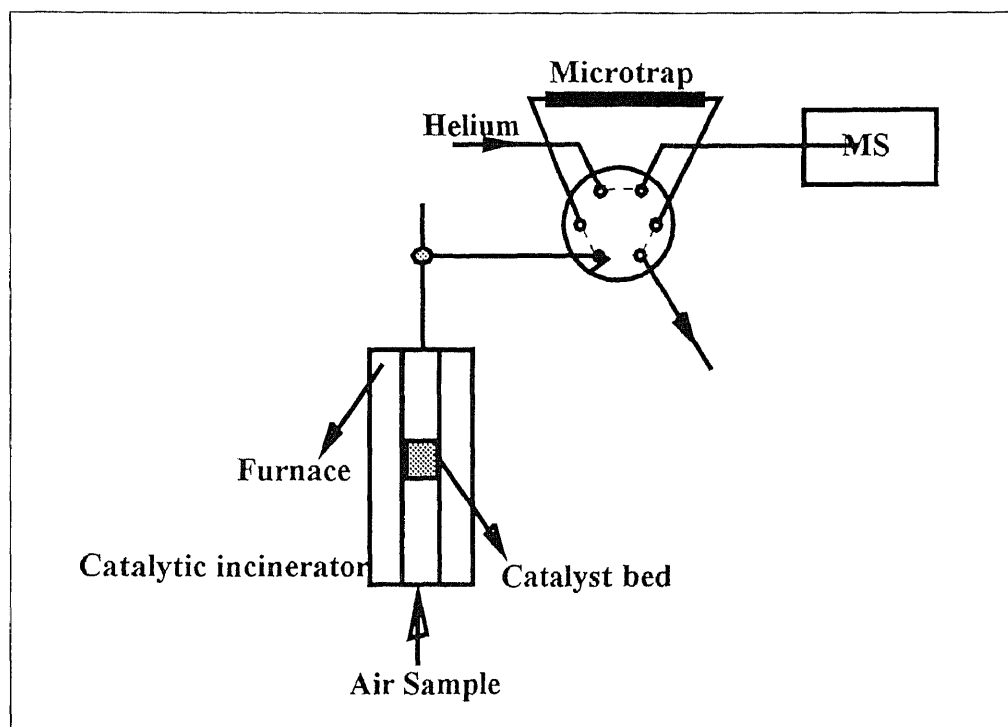


**Figure 5.2** Schematic diagram of experimental system for catalytic incinerator emission monitoring.

### 5.3 Results and Discussions

#### *Direct Sampling*

Direct sampling allowed all the sample stream enter the ionization chamber of mass spectrometry. The total ion current (TIC) and mass spectrum obtained from direct sampling system were given in Figure 5.3. Figure 5.3-a is TIC as a function of time and Figure 5.3-b is a set of spectrum at point A. Even the sample stream generated high intensity in TIC, only moisture ( $m/z:17$ ) and  $\text{CO}_2$  ( $m/z:44$ ) can be seen from mass spectrum when all ions greater than 10 were measured. In this case, 5 ppm toluene was not detected. It is very common for incinerator emissions containing high concentrations of  $\text{CO}_2$  as well as moisture. When the emission sample stream was introduced to the instrument, the large peak of inorganic gases caused difficulties of identification of low concentration organic components. The large amount of small inorganic molecular can adsorb most energy in ionization chamber and results in reducing the measurement sensitivity. Further more, exceed amount of these molecular may cause secondary ionization of organic molecules and interfere in the mass spectral analysis. They may also cause deterioration of the instrument. It is difficult to detect low concentration of organics from sample matrix containing a high concentration of inorganic interference gases using direct sampling mode. Even changing the mass scan range can efficiently eliminate all the inorganic mass spectra, the low concentration organic still can not be detected by quadruple mass spectrometer without sample enrichment because the limitation of the detection limit of the instrument. Ion-trap mass spectrometer has low detection limit, but most of them are not designed for direct sample stream introduction. By

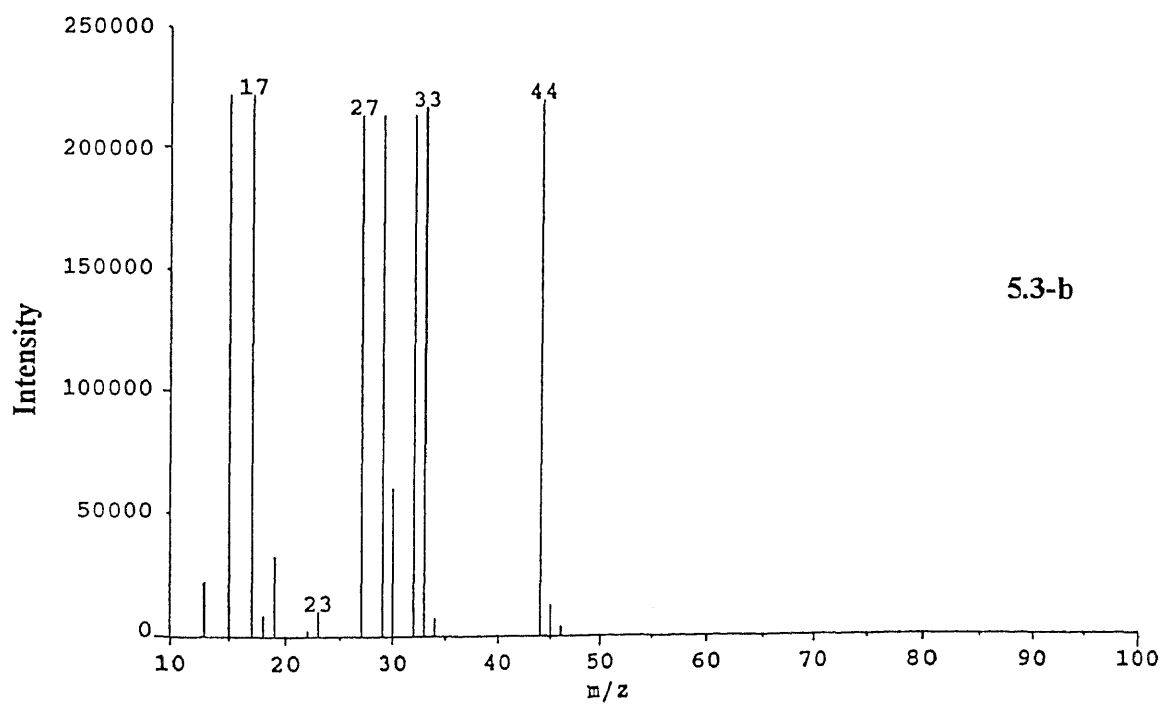
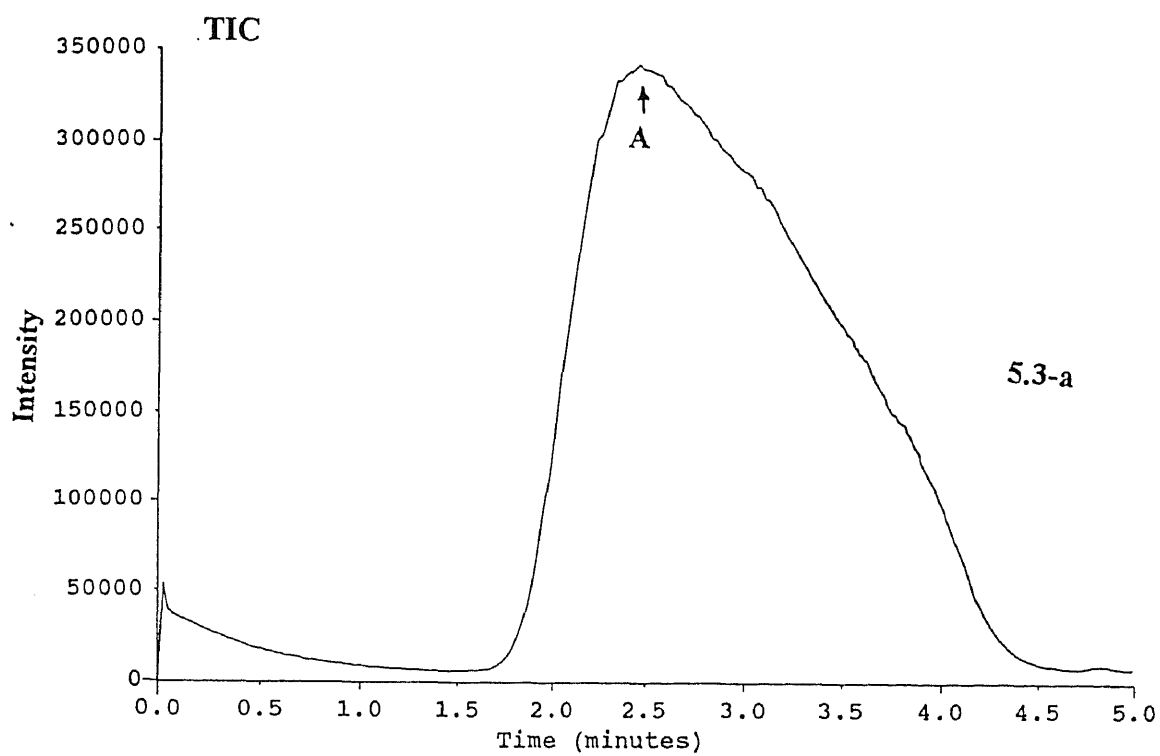
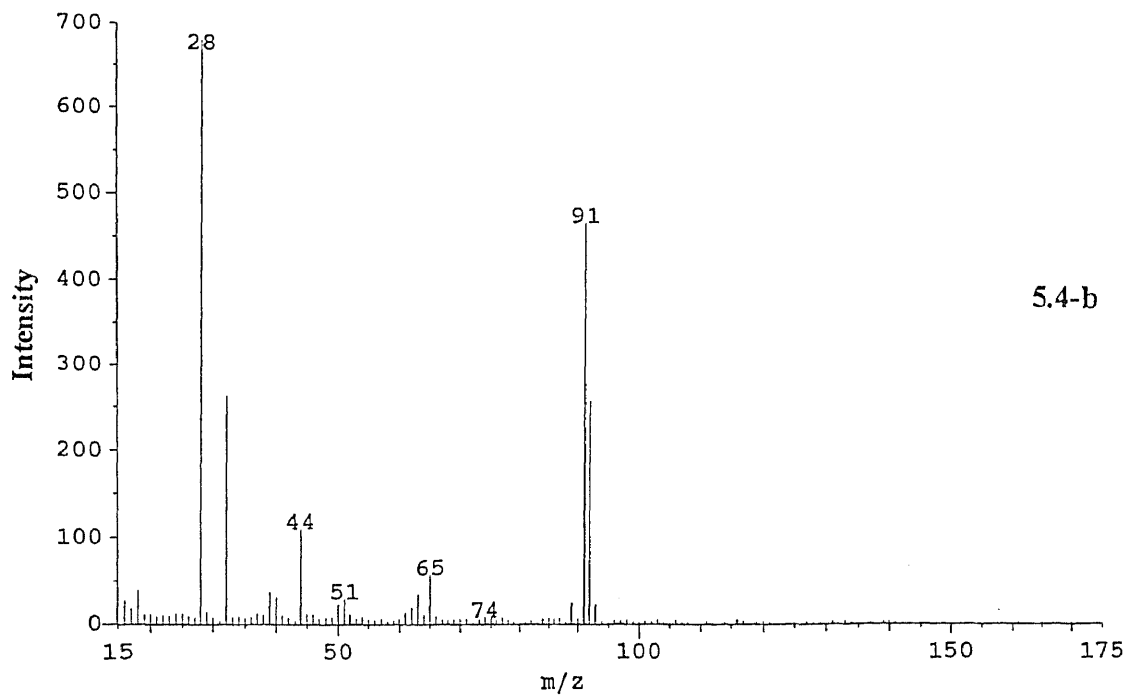
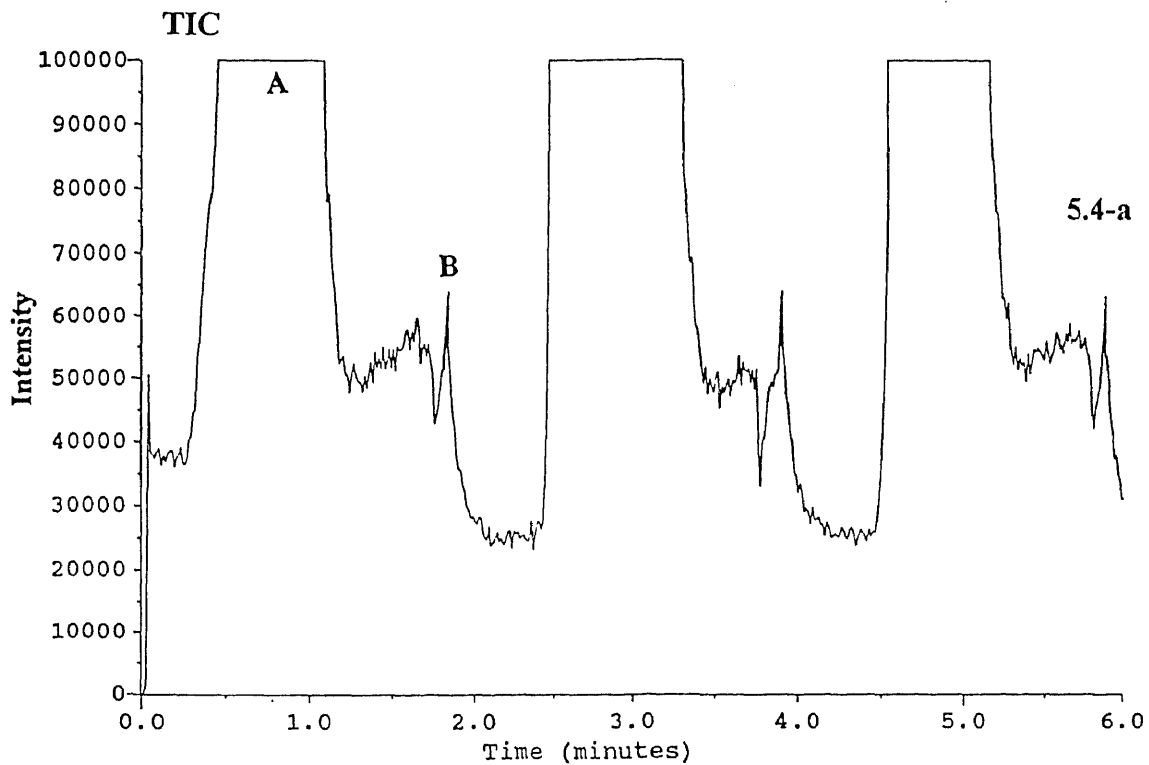


Figure 5.3 The chromatogram generated by direct sampling. 5.3-a: TIC as function of time, 5.3-b: Spectrum at point A.

employing the sampling valve in this experiment, helium, instead of emission sample stream, was used to carry the sample into the instrument. However, the data collection system for Varian Saturn ion-trap mass spectrometer was still not capable to handle such large intensity when the sample was injected into the instrument.

### *Sequential Valve Microtrap (SVMT)*

In our previous studies, the microtrap has been successfully used to concentrate organics and inject into a GC (14, 16). The microtrap can also be used as a sample concentrator and injector for a mass spectrometer. The TIC generated by SVMT injection system was given in Figure 5.4. In the SVMT mode, helium purged out the sample in the loop flowing through the microtrap while the organic components was retained by the adsorbent packed inside of the microtrap. After the sample matrix passed through the microtrap, the trap was pulsed in presence of He to desorb the organics. Here the background gases were separated from toluene in time. The large intensity of peak A was mainly due to the background gases. When the response came down, the microtrap was pulsed to generate the desorption peak B. The mass spectrum at point B (Figure 5.4-b) clearly shows the mass spectrum corresponding to toluene with significantly less background species. By using the microtrap, the organics present in the sample stream were concentrated and the background gases were separated. The major drawback for this configuration is that all the background gases were still sampled into the ionization chamber. The limitation can be overcome by selectively trapping the



**Figure 5.4** The chromatogram generated by SVMT. 5.4-a: TIC as function of time, 5.4-b: Spectrum at point B.

organics while venting the background gases, and then introducing the organics into the MS.

### *On-line Microtrap with Backflush Desorption*

The OLMT-BF configuration was most effective in removal of interference and enhancement of sensitivity in the measurement of VOCs in air. During sampling, most of the background gases were vented to the outside, while the organics were retained in the microtrap. At the end of each sampling period, the microtrap was desorbed when the valve was switched to injection position that is showed in Figure 5.5. In Figure 5.5-a, peak B was generated by desorption of the microtrap. The peak A was generated by the residue of sample matrix left in the microtrap. The selected ion monitoring at  $m/z:91$  was given in Figure 5.5-b where the toluene peaks were corresponding to the desorption of the microtrap. The mass spectrum of one of these peaks was given in Figure 5.5-c.

Figure 5.6 was also generated by the OLMT-BF. Here, before the valve was switched to injection position, the sample stream was switched to helium to remove any remaining background gases especially  $H_2O$ . Consequently, the MS was never loaded with any sample matrix, and the base line remained stable and constant. When the microtrap was desorbed, a concentrated pulse of organics was introduced into the MS. The TIC trace as a function of time and the associated mass spectrum are shown in Figure 5.6. Peak A corresponds to a point in time right after the valve was switched to the inject position. The peak B was generated from the thermal desorption of the microtrap. The main component here is toluene.



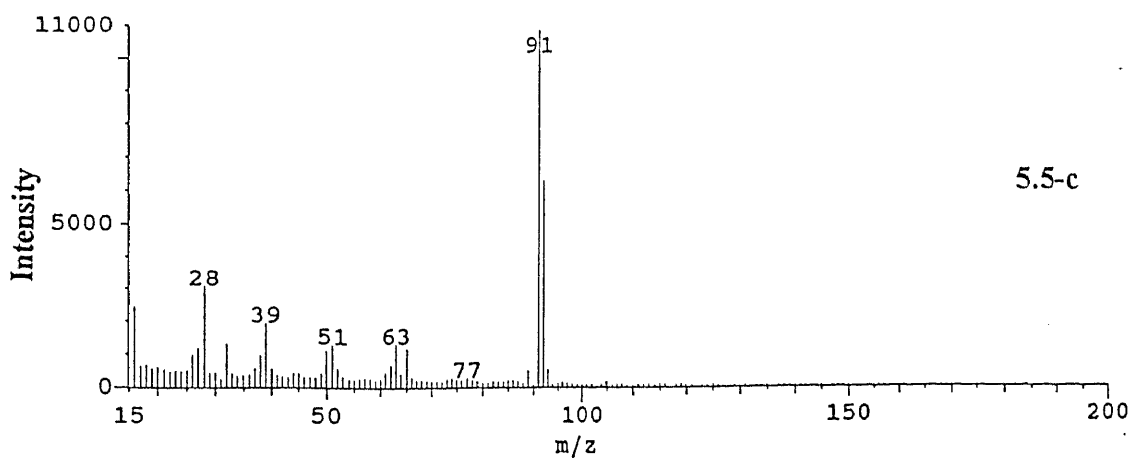
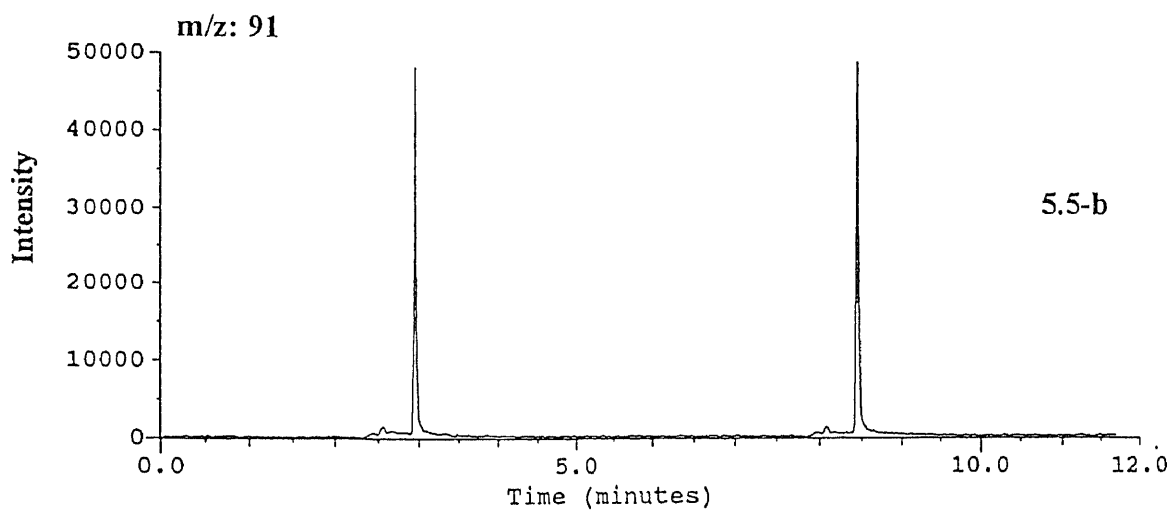
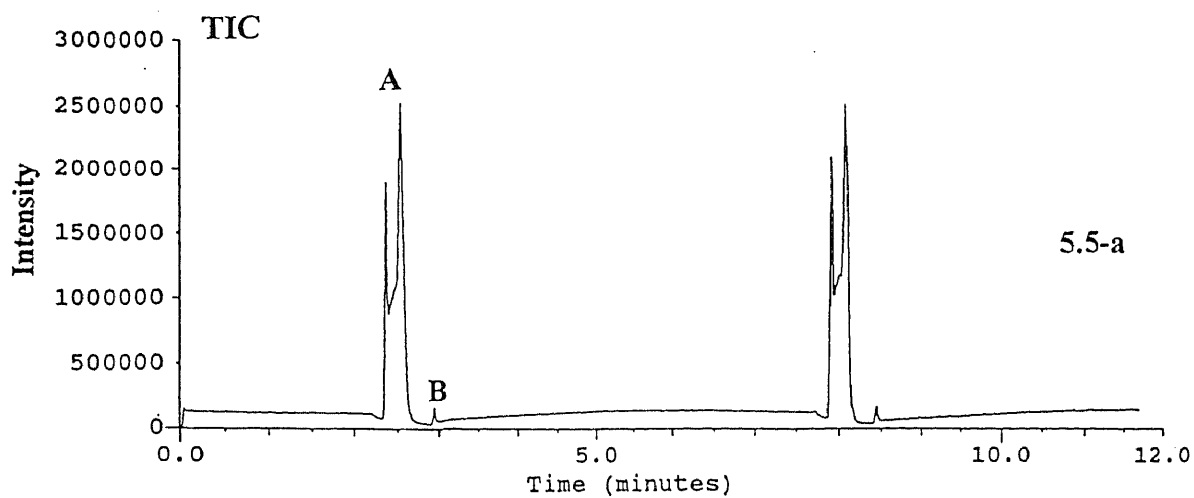


**Figure 5.5** The chromatogram generated by OLMT-BF without helium purge. 5.5-a: TIC as function of time, 5.5-b: Selected ion chromatogram at m/z: 91, 5.5-c: Spectrum at point B.

Practically none of the background species are seen here. The  $m/z$  peaks of 91, 65, 51, 39 and their relative intensities were well matched with the standard spectrum from the NIST library. High precision was obtained. The relative standard deviation (RSD) was 3.4 % based on the intensity at position B of five consecutive measurements.

In the OLMT-BF mode, the air does not go into the MS. The sampling volume is only limited by the breakthrough of organics on the microtrap. The backflush mode also facilitates the multiple bed microtrap when sampling a wide range of VOCs. By comparison of the different sampling configurations, it is clear that the highest response was obtained when the background gases were vented out. The advantages of the MTMS in the enhancement of measurement sensitivity and in interference elimination are clearly demonstrated.

Based on the above results, the OMLT-BF mode was used for the rest of the experiments. The determination of the sample with multiple components was carried out. Each component was identified by its highest intensity characteristic fragment. Figure 5.7 is a typical mass spectrum of the studied sample stream containing 2-butanone ( $m/z$  43), hexane ( $m/z$  57), benzene ( $m/z$  78), toluene ( $m/z$  91) and tetra-chloroethylene ( $m/z$  166). The dynamic range for the analysis for these VOCs using OLMT-BF can be from low ppb level to ppm. The calibration curves of different VOCs were given in Figure 5.8 and 5.9. The relative standard deviations for 2-butanone, hexane, benzene, toluene and tetra-chloroethylene were 3.77 %, 6.59 %, 4.48 %, 3.73 % and 4.89 %, respectively based on six measurements. The detection limits are listed in Table 5.1 for one minute sampling

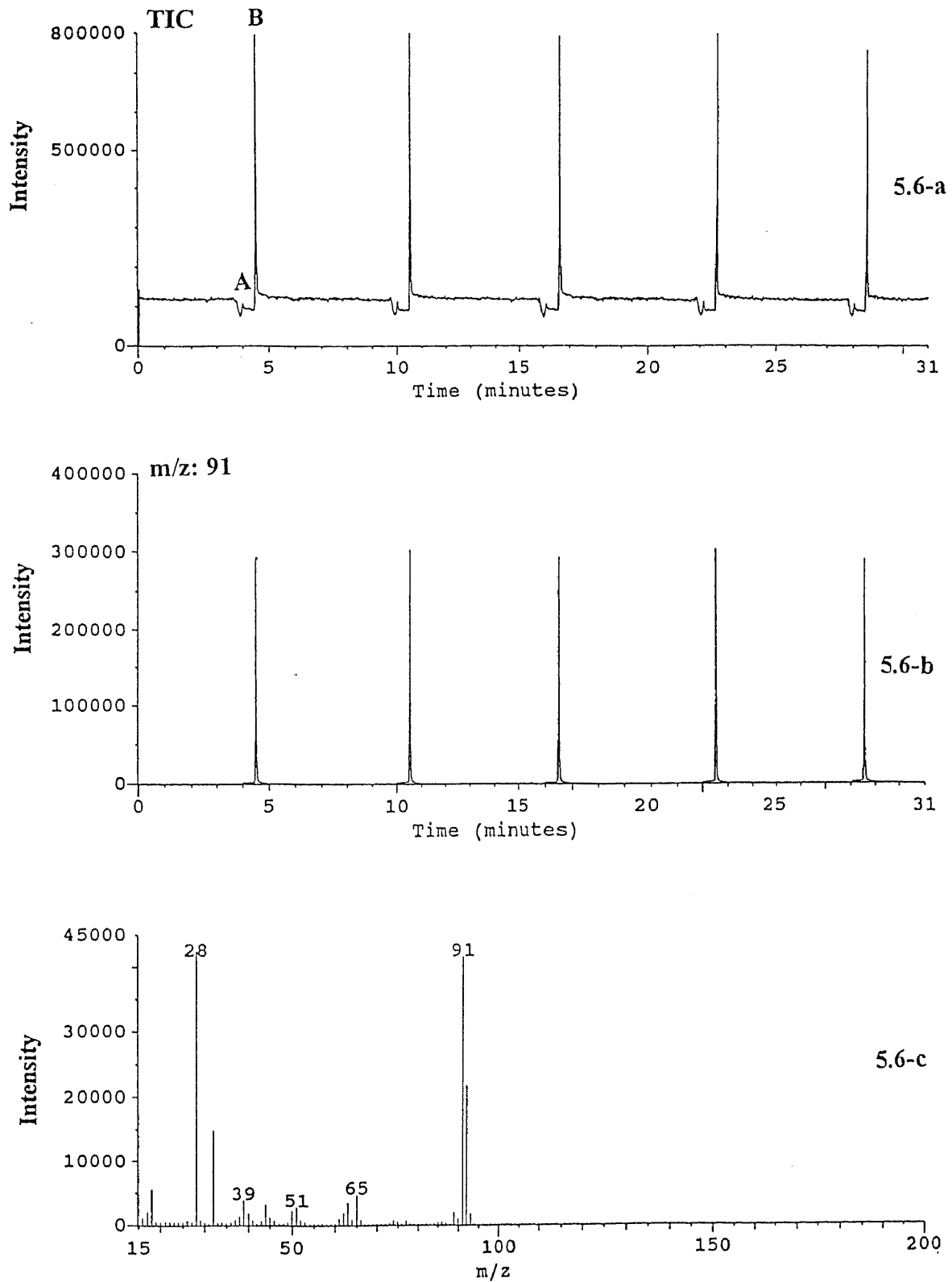
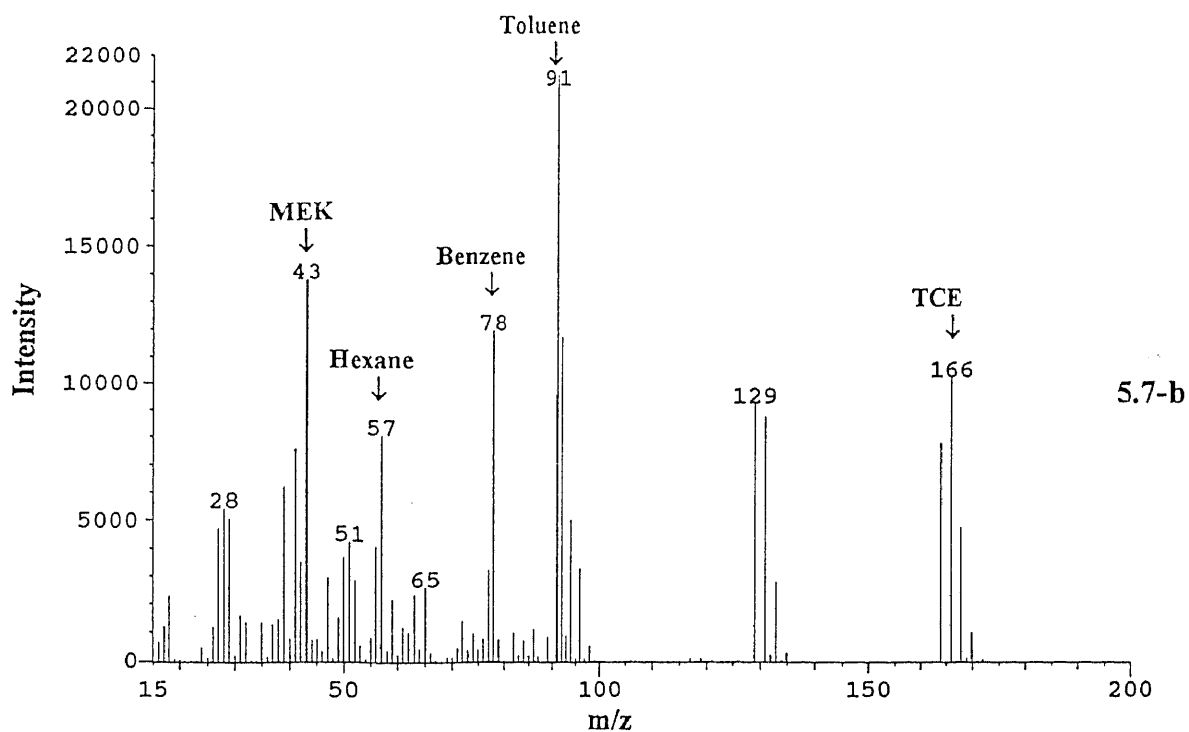
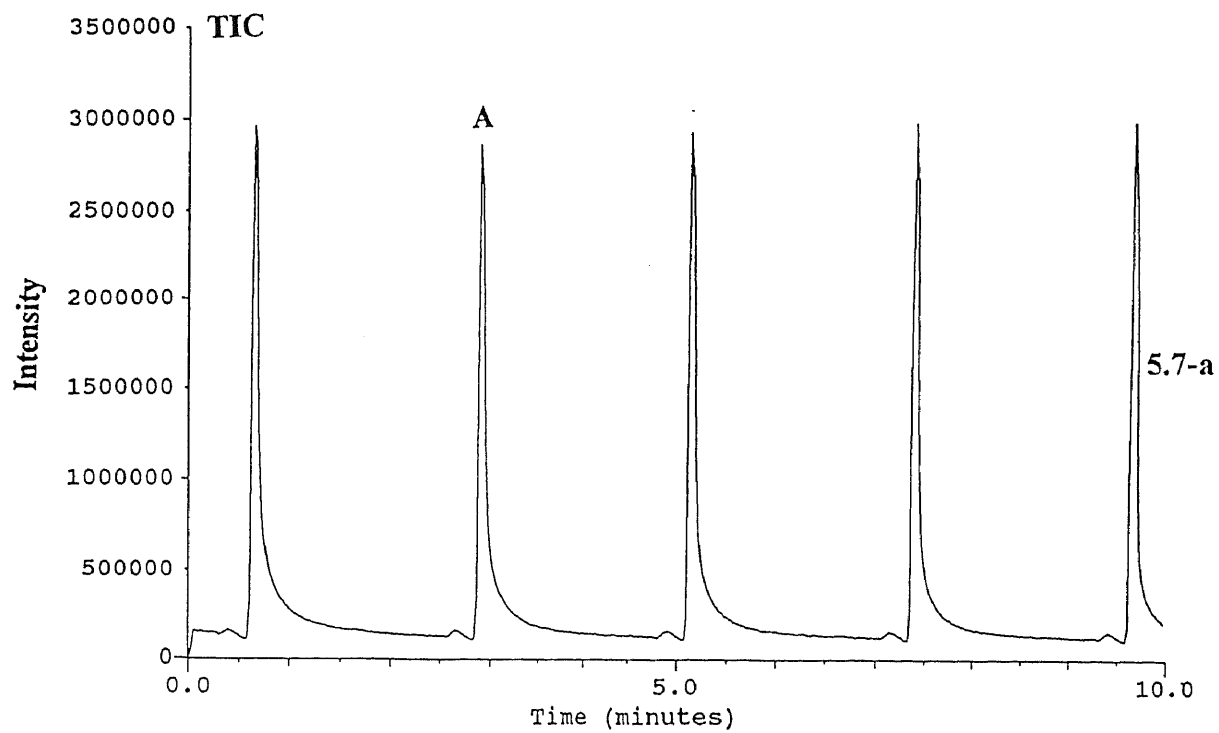


Figure 5.6 The chromatogram generated by OLMT-BF with helium purge. 5.6-a: TIC as function of time, 5.6-b: Selected ion chromatogram at m/z: 91, 5.6-c: Spectrum at point B.



**Figure 5.7** The chromatogram generated by OLMT-BF with helium purge for multiple compounds. 5.7-a: TIC as function of time, 5.7-b: Spectrum at point A.

at 10 ml/min sample flow rate. The detection limits can be further lowered by increasing sampling time or sample flow rate until the breakthrough of the lightest component, 2-butanone in this case. For demonstration, low ppb level calibration curves were obtained for benzene and toluene on Varian Saturn ion trap MS and given in Figure 5.10. The detection limits for 1 min sampling at 20 ml/min sample flow rate were 100 ppt for benzene and 35 ppt for toluene. The selected ion chromatograms at  $m/z$ :78, 91 and corresponding spectrum generated by multiple compounds at low concentrations are showed in Figure 5.11 where benzene ( $m/z$ :78), toluene ( $m/z$ :91), ethylbenzene ( $m/z$ :105) and tri-chloroethylene ( $m/z$ :130) were 625 ppt, sample volume was 20 ml. The turn over time for one analysis using MTMS can be shorted to few minutes even for trace analysis. All the experiments successfully demonstrated that OLMT-BF mode MTMS is a sensitive method for continuous, on-line monitoring of VOCs.

The catalytic incinerator emission was monitored using OLMT-BF. The change in concentration profile of test compounds changing with incinerator temperature was plotted in Figure 5.12. When the incinerator operation temperature was increased to 200 °C, all the VOCs were well converted except chloroorganic compounds (TCE) which was still stable under that temperature. At 250 °C, the concentration of TCE in emission started to decrease. 99 % of all the VOCs were decomposed when the operating temperature was higher than 350 °C.

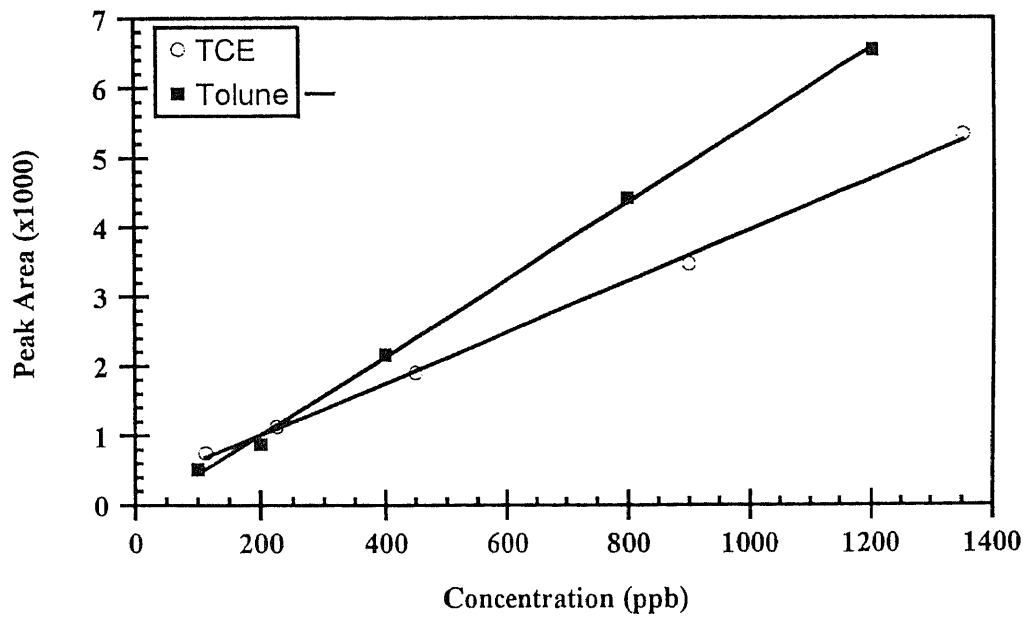


Figure 5.8 Calibration curves for toluene and TCE.

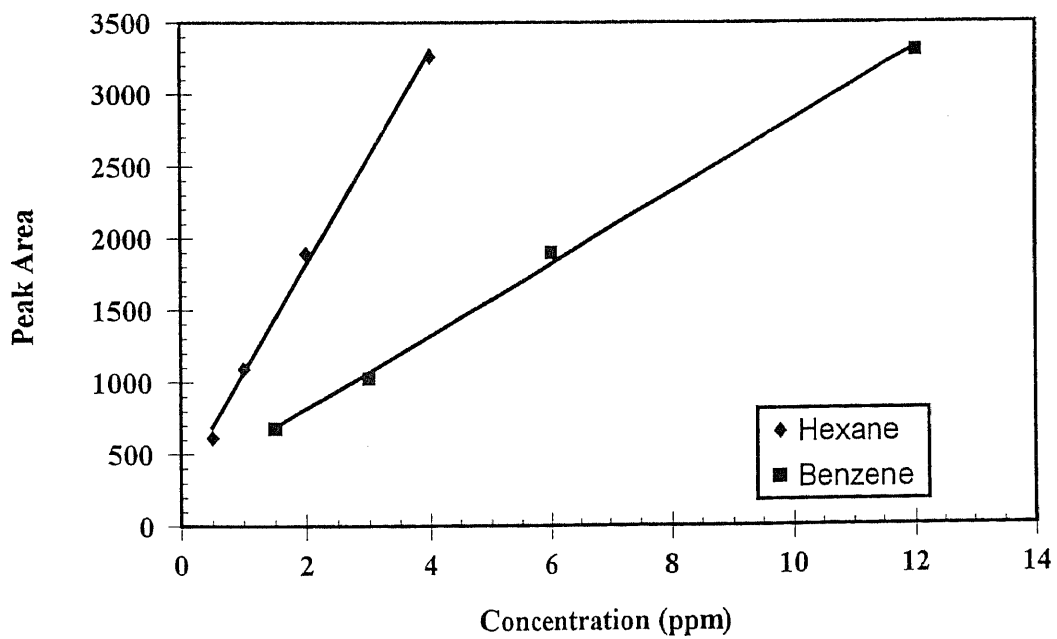
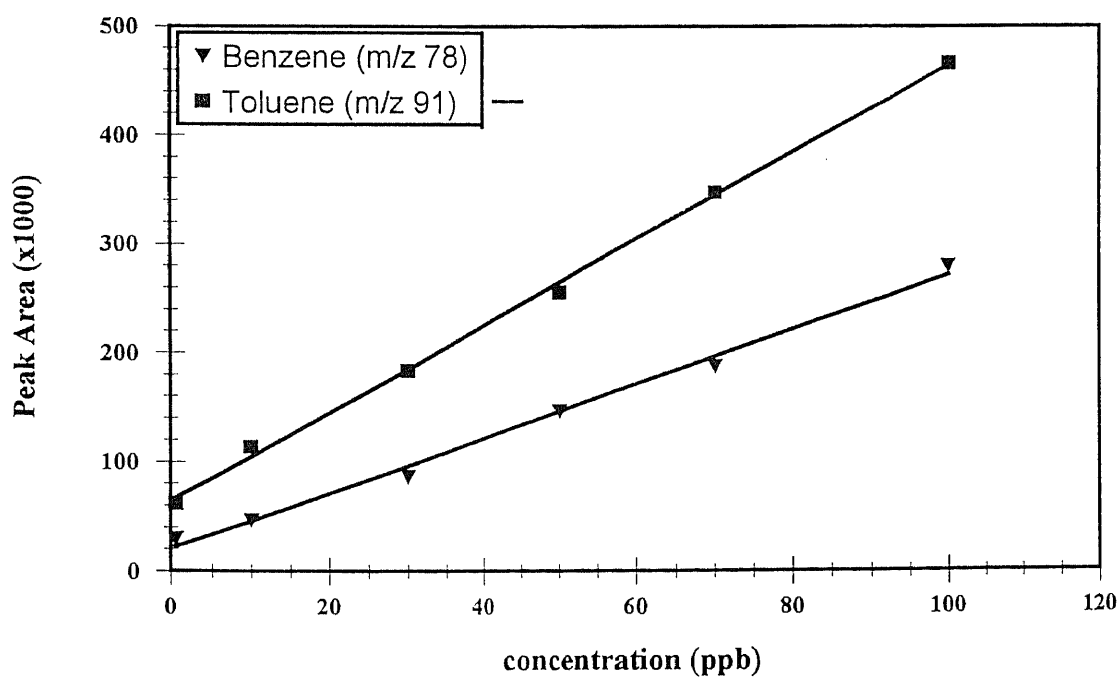


Figure 5.9 Calibration curves for hexane and benzene.

**Table 5.1** Detection limits for the different substances (sampling time: 1 minute, sample flow rate: 10 ml/min, helium purge time: 1 minute)

<i>Substance</i>	<i>Detection Limits (ppb)</i>
2-Butanone	25
Hexane	20
Benzene	10
Toluene	4
TCE	6



**Figure 5.10** Calibration curves for benzene and toluene measured by ion trap mass spectrometry.

Scan: 1202 Seg: -- Group: -- Retention: 10.01 RIC: 45705 Masses: 40-134  
Plotted: 1 to 2400 Range: 1 to 1266 100% = 397036

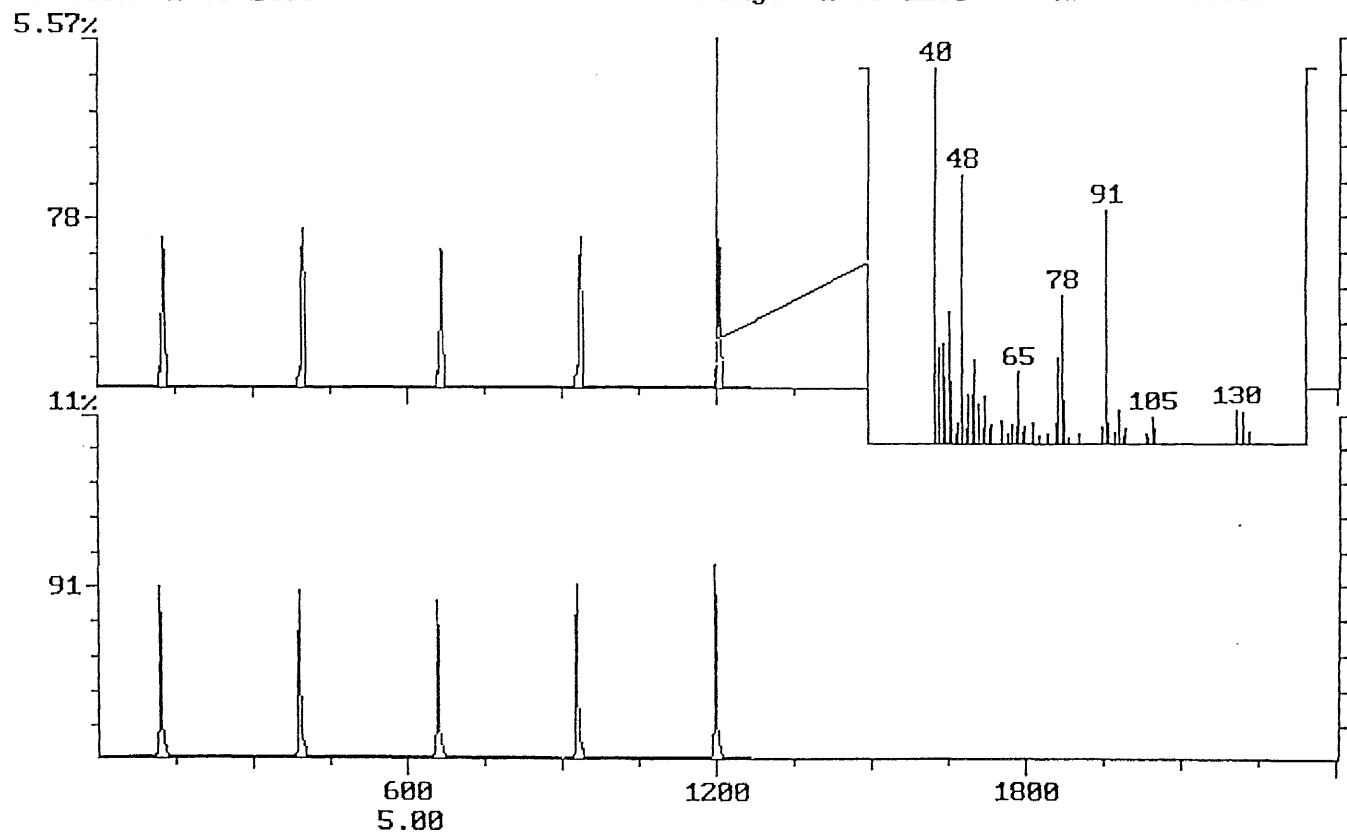


Figure 5.11 The chromatogram generated by Varian Saturn ion-trap mass spectrometer with selected ion monitoring at m/z: 78 and 91.



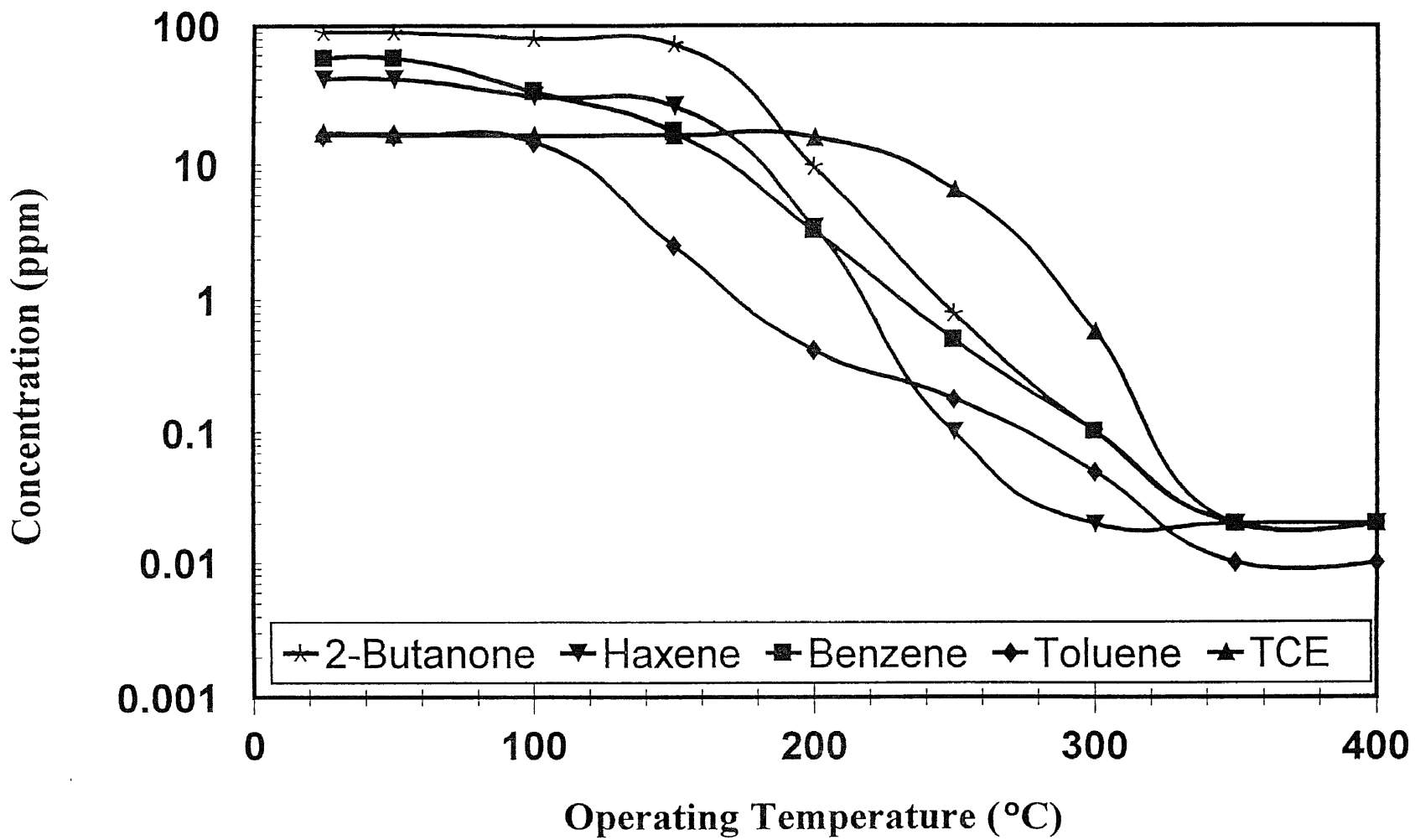


Figure 5.12 The concentration profiles of test compounds changing with incinerator temperature.

#### 5.4 Conclusion

Microtrap mass spectrometry for continuous, on-line monitoring of pollutants in air emission was developed. Large amount background gases commonly present in air emissions such as CO<sub>2</sub>, H<sub>2</sub>O. This results in a high background and also interference during MS analysis. OLMT-BF with helium purge showed best performance for eliminating background interference. Direct sampling mass spectrometry based on microtrap as sampling interface increased the measurement sensitivity because of the sample enrichment by microtrap. High precision was also obtained. The detection limits were at low ppb levels or even ppt levels. Monitoring of catalytic incinerator emission using microtrap mass spectrometry had also been demonstrated.

## CHAPTER 6

### FIELD VALIDATION OF CONTINUOUS NON METHANE ORGANIC CARBON ANALYZER FOR AIR EMISSION MONITORING

#### 6.1 Introduction

Non-methane organic carbon (NMOC) is a measure of total organic carbon except that from methane. Thus, its measurement represents organic pollutants that play an important role in the formation of photochemical oxidants at urban and regional scale. NMOC measurements have been used to study emission sources as well as ambient air [127 - 130].

EPA standard method 25 employs a non-methane organic carbon analyzer, which use oxidation/reduction and gas chromatography as means of quantifying NMOC emission from stationary sources such as incinerators and coatings facilities [131]. In this method, air is sampled into a chilled condensate trap, and the unretained compounds are collected in an evacuated canister. After sampling is completed, the NMOC are determined by combining the analytical results of the condensate trap and the canister. The trapped CO<sub>2</sub> in the condensate trap is removed first by warming the condensate trap to room temperature. Then the NMOC is transferred to an intermediate collection vessel by heating the condensate trap to 200 °C. The sample is injected using a sampling valve into a column to separate CH<sub>4</sub>, CO and CO<sub>2</sub>. Once the detector response returns to the baseline following the CO<sub>2</sub> peak, the column is backflushed while the column temperature is raised to 195 °C. The NMOC is determined by oxidizing the organics to CO<sub>2</sub> and then reducing the CO<sub>2</sub> to CH<sub>4</sub>, which is measured by a

conventional FID. The NMOC content of the canister sample is analyzed the same way. The major challenge has been measuring NMOC in samples that have high concentration of moisture and CO<sub>2</sub>. During sampling, CO<sub>2</sub> gas bubbles are trapped inside the ice that is formed in cryogenically cooled condensate traps. It is difficult to purge out the CO<sub>2</sub> prior to recovery of the condensate. Since the organics are also oxidized to CO<sub>2</sub> in the analysis step, any CO<sub>2</sub> from air generates a bias in the analysis. The other problem is that polar oxygenated organics that not condense in condensate trap are collected in the canister and it is difficult to accurately analyze these compounds in the non-methane organic analyzer [132]. Furthermore this method can not be used for continuous on-line monitoring of air emissions.

Continuous emission monitors (CEM) are being used more and more for regulatory compliance [133]. They can eliminate/minimize the errors associated with transportation and storage of samples and also because there is no manual handling involved. Normally, on-line monitors have three main components, namely, a sampling interface, sample conditioning and an analyzer [134]. The sampling interface either transports or separates the flue gas for the analyzer. CEM systems are often classified by their interface into three groups: extractive, in-situ and remote sensor. In the extractive system, the interface extracts and conditions the gas prior to entering the analyzer. In in-situ systems, the interface is composed of flanges designed to align or support the monitor. Remote sensing systems have no interface between the stack gases and the sensing instrument other than the ambient atmosphere. CEMs are commercially available today. A major challenge is to perform on-line preconcentration for trace analysis, and to be able to complete

the analytical cycle fast enough that information about process transients can be obtained. For example, the monitoring system for automobile engines needs to have a sampling time less than 2 ms to monitor the start up emission [135]. For stationary sources, data reported on hourly or even daily basis are sufficient [136-137].

On-line injection devices based on microtrap have been developed for continuous monitoring of volatile organic compounds using GC and mass spectrometry [20, 27, 29]. The microtrap comprises of a capillary tubing packed with a sorbent. As the sample passes through the microtrap, organics are trapped by the adsorbent and background gases pass unretained. The microtrap can be rapidly desorbed by heating with a few seconds (1 to 5 second) pulse of electric current. The desorption band is sharp enough to serve as an injection for GC separation, or MS analysis. High precision, fast response time and low detection limits of microtrap devices have been demonstrated.

Recently we have reported the development of instrumentation for continuous NMOC monitoring [138]. This instrument referred to as C-NMOC uses the microtrap in combination with a sampling valve, and conventional oxidation/reduction NMOC detector. Besides being an on-line concentrator and injector, the microtrap serves as a separator that isolates NMOC from H<sub>2</sub>O, CO, CO<sub>2</sub>, CH<sub>4</sub> and other background gases. After these gases have passed through, the microtrap is desorbed, and the trapped NMOC are released into the oxidation reactor to be converted to carbon dioxide. Then the carbon dioxide is reduced to methane and quantified by the FID.

The preconcentration of organics in the microtrap results in ppb levels detection limit. The C-NMOC analyzer had been successfully used to evaluate the performance of a laboratory scale catalytic incinerator. These details have been published in the literature [139]. The objective of this research was to field test the C-NMOC system at an industrial site and evaluate its viability as a CEM. The field test was a collaborative effort between US EPA, Mid-west Research Institute, and Research Triangle Institute. The test was carried out at a coatings facility in North Carolina.

The present paper reports the results of two consecutive days of testing. On the first day, the process was coating metal sheets with PVC products. According to the material safety data sheet, the main organic ingredients were diisodecyl phthalate, 2,2,4-trimethyl-1,3-pentanediol di-isobutyrate, di-(2-ethylhexyl) azelate, and aromatic naphtha. On the second testing day, the process was coating polyester, and the main organic ingredients were xylene isomers, 1,2,4-trimethylbenzen, ethyl benzene and aromatic naphtha. These two coating substances produced widely different NMOC emission concentrations. The sampling manifold and the C-NMOC analyzer was installed in a mobile laboratory located next to the emission stack as illustrated in Figure 6.1. The stack was equipped with an air toxic control device that comprised of a methane burner followed by a catalytic incinerator. The effluent from the incinerator was sampled using a heated sample line to the mobile laboratory.

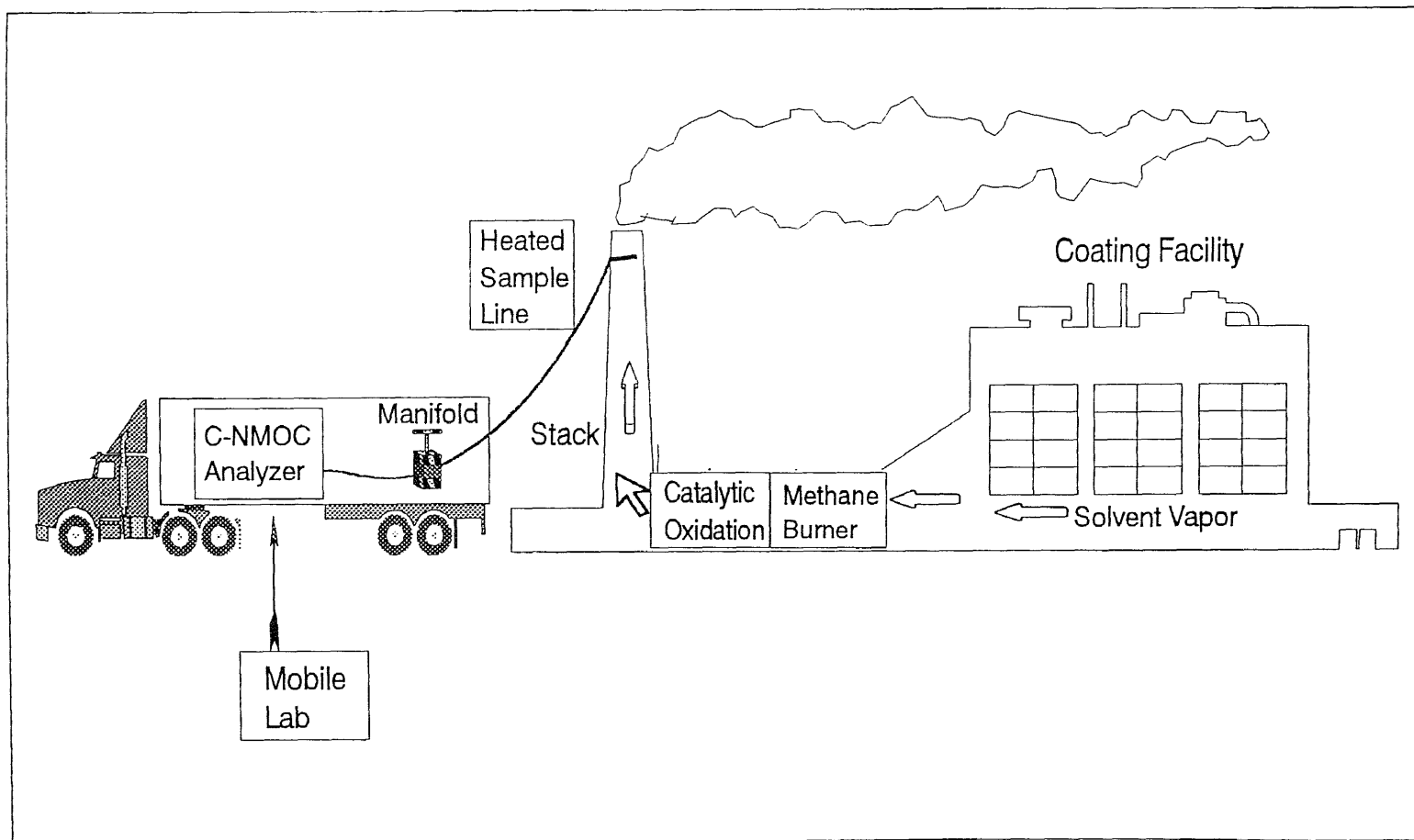


**Figure 6.1** Schematic diagram of the field analytical system.

## 6.2 Experimental Approach

A schematic diagram of the sampling system in this study is shown in Figure 6.2. Emissions from the catalytic incinerator outlet were extracted from a single point near the stack centroid. A heated sample pump drew the flue gases at approximately 7 liters per minute. The sample gas stream was transported to a heated manifold (~127 °C) via heat traced sample tube. The heated manifold contained three exit ports that distributed identical gas samples. One of those was used for the C-NMOC analyzer.

The sampling/injection system for the C-NMOC consisted of a gas sampling valve in series with the microtrap. The emission stream continuously flowed through the sample loop of the sampling valve. At predetermined intervals, the sampling valve was switched to the injection position. Carrier gas injected the sample into the microtrap where the organics were trapped. The background gases passed directly into the NMOC detector. After a two minutes of delay, the microtrap was thermally desorbed by electrical pulse. The gas sample valve was a six-port air actuated valve with a digital interface (Valco Instruments Co. Inc., College Station, Texas). The microtrap was made by 1.1 mm ID, 150 mm long stainless steel tubing and packed with Carbopack C (Supelco, PA). This microtrap was relatively larger than those reported previously [138]. This was packed with 300 mg of Carbopack C to prevent breakthrough of polar compounds. A microprocessor based controller developed in house controlled the operation of the valve and the interval between pulses, and the pulse duration during desorption of the microtrap.



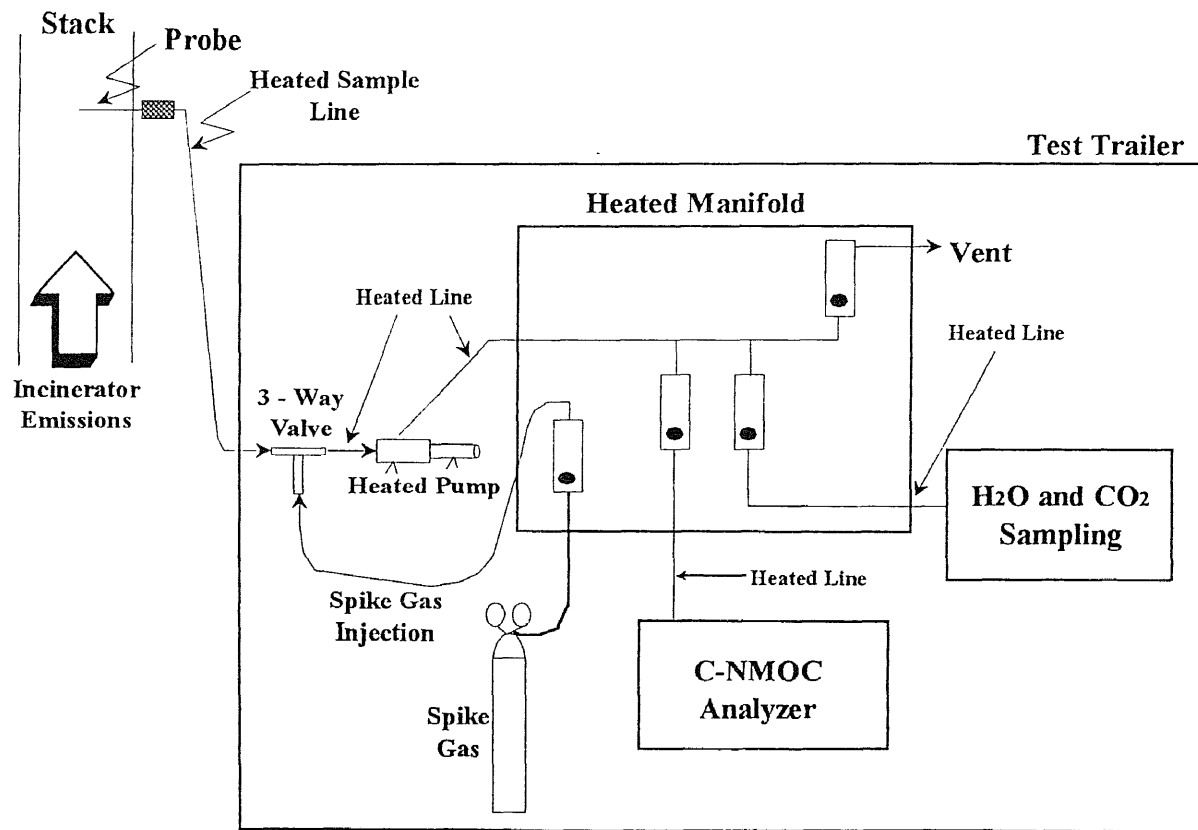


Figure 6.2 Schematic diagram of the sampling system.

The oxidant reactor in the NMOC detector was a ¼ inch stainless steel tubing packed with Chrome Alumina. The catalyst bed was 4 inch long. This reactor was put in a furnace (Lindberg, Watertown, WI). The reduction unit was a ¼ inch OD quartz tube installed in the GC injection port. The reducing catalyst was nickel powder. The typical operation temperature for the oxidation unit and reduction unit was 650 °C and 380 °C, respectively. A flame ionization detector (FID) from an Hewlett Packard 5890 Series II gas chromatograph (Hewlett Packard, Avondale, PA) was used as the final detector. A 5 ml sample loop was used for injection. Nitrogen was used as the carrier gas to elute the air sample from the sample loop and inject into the NMOC detector. The schematic diagram of C-NMOC analyzer is given in Figure 6.3.

For estimating the relative bias of the method, the analyte spike and audit samples were used. The process exhaust gas was spiked with a gas mixture containing toluene, isopropanol, carbon monoxide, and carbon dioxide. The spike gas was blended with the stack gas by injecting the spike into the sample stream just ahead of the sample pump. The emission and the spike were monitored each alternative hour. The percent NMOC spike recovery was calculated. Two audit gases, the first containing 20.2 ppm ethanol (40.4 ppm<sub>C</sub>) and the second containing 17.9 percent CO<sub>2</sub>, and 46 ppm hexane (276 ppm<sub>C</sub>) were also used to test the method accuracy. The audit gases were certified working standards with an analytical accuracy of ± 5 %.

Testing the deactivation of oxidation and reduction catalysts in the NMOC detector was an important issue during continuous, on-line operation. To test the

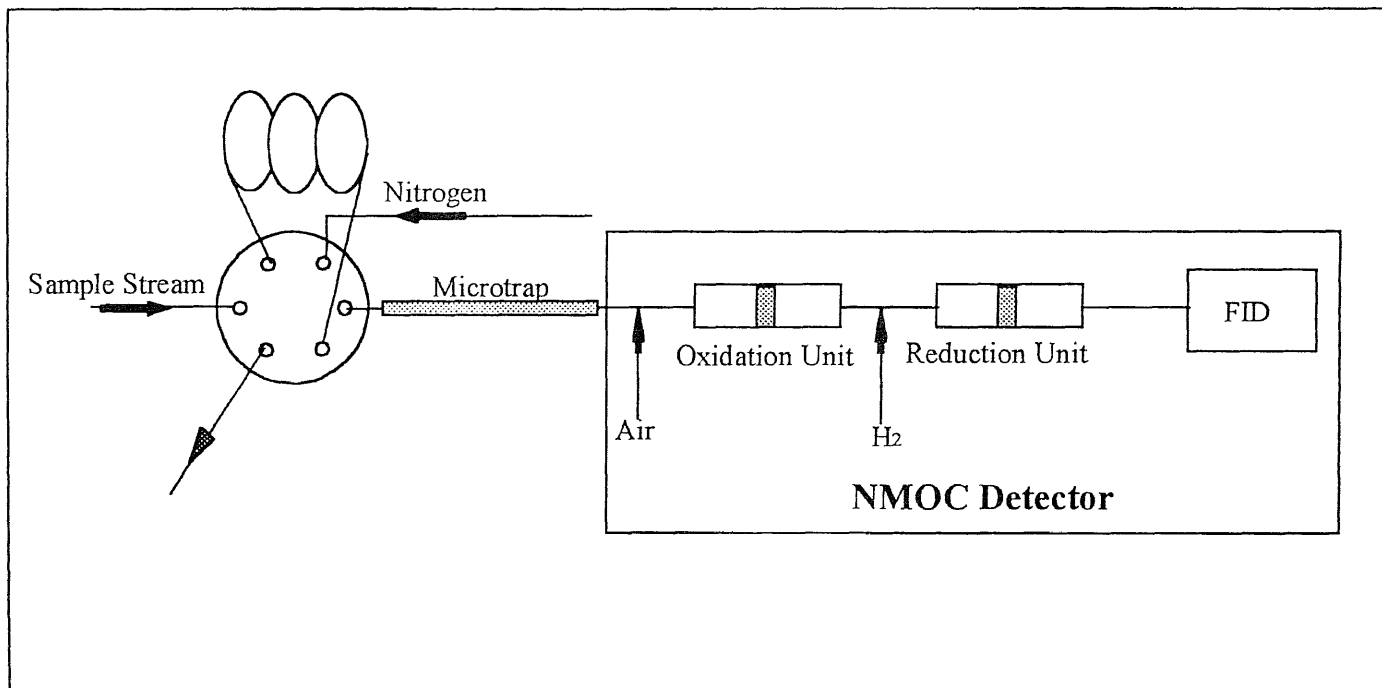


Figure 6.3 Schematic diagram of the C-NMOC analyzer.

oxidation catalyst, a gas standard containing 0.997 percent  $\text{CH}_4$  was injected into the C-NMOC while the oxidation unit was at its operating temperature, while the temperature of the reduction unit was lowered to 100 °C. During this check, the  $\text{CH}_4$  was oxidized to  $\text{CO}_2$ , and the FID showed no response. Then the temperature of the reduction unit was increased to its operating temperature (380 °C), and the  $\text{CH}_4$  peak reappeared. Next, a gas standard containing 0.990 percent of  $\text{CO}_2$  was injected through the oxidation and reduction catalysts when both were at their operating temperatures. If the area of the  $\text{CO}_2$  peak was within 15 percent of that of the  $\text{CH}_4$  peak, then it was concluded that both the oxidation and reduction catalysts were working effectively. The catalyst deactivation was checked on a daily basis.

A four-point calibration (zero, 112 ppm<sub>C</sub>, 224 ppm<sub>C</sub>, 336 ppm<sub>C</sub>) was performed each morning before the start of sampling. The standard gas was made of toluene. Ultra high pure nitrogen was used as the zero gas, and it is also served as the system blank.

### 6.3 Results and Discussion

During the check for catalyst deactivation, the percentage deviation between 0.997%  $\text{CH}_4$  and 0.990%  $\text{CO}_2$  peak areas were 12.0, 4.6 and 8.1, respectively on three consecutive days. This showed high activities of both catalysts. The catalysts showed no signs of deactivation over periods of operation. All the check results are listed in Table 6.1. The instrument blank values from Table 6.1 were negligible during the field study and no instrument contamination was detected. The

instrument precision was checked by repeat injection of 112 ppm<sub>C</sub> standard five times. The RSD was 7.6 % on the first day right after instrument setup. This was relatively higher than what was commonly encountered in the laboratory (less than 5 %). On the subsequent testing RSD dropped to 0.933 % and 2.9 % respectively. This demonstrated that precision of the instrument in the field was as good as those reported in the laboratory studies [138]. A four-point calibration was performed on the instrument each morning prior to the start of sampling. A typical calibration curve is shown in Figure 6.4. It shows linear response ( $r^2$  is 0.9995) and near zero blank.

The typical output of C-NMOC for emission monitoring is given in Figure 6.5. Each group of peaks was generated by one injection. Peak A in each injection was from by CO, CO<sub>2</sub> and CH<sub>4</sub>, while peak B was from the thermal desorption of the microtrap. The air sample collected in the loop of sampling valve was swept into the NMOC detector when it was switched to the injection position. The inorganic gases and methane went through the microtrap while all the organic components were retained in it. Desorption of microtrap was made after a certain predetermined delay (2 minutes). Based on the concentration of inorganic species and methane in the emission, this delay could be adjusted to ensure the separation of NMOC from these gases. Also, peak A could be used to estimate the combined concentration of CO, CO<sub>2</sub> and CH<sub>4</sub>. Separate calibration would be necessary for that measurement. It can be seen from Figure 6.5 that NMOC was successfully separated from all the inorganic gases in the emission.

**Table 6.1** QC Data: Checking the catalyst activity and system blank.

<b>Results in the day of instrument setup</b>				
	Blank (Nitrogen)	0.997 % Methane	0.990 % CO <sub>2</sub>	112 ppm <sub>c</sub> (standard)
Peak Area	2654	911726	816008	19695
	2444	937031	861341	19850
	2268	954490	833986	16974
	2188	936587	855341	17937
	2246	954490	838095	17937
Average	2360	933679	804954	18308
R.S.D (%)	8.0	1.7	2.1	7.6

<b>Testing day one</b>				
	Blank (Nitrogen)	0.997 % Methane	0.990 % CO <sub>2</sub>	112 ppm <sub>c</sub> (standard)
Average	1314	931459	856664	18858
R.S.D %	4.6	2.1	0.88	0.933

<b>Testing day two</b>				
	Blank (Nitrogen)	0.997 % Methane	0.990 % CO <sub>2</sub>	112 ppm <sub>c</sub> (standard)
Average	1214	1435762	1368985	19432
R.S.D %	4.9	3.0	2.1	2.9

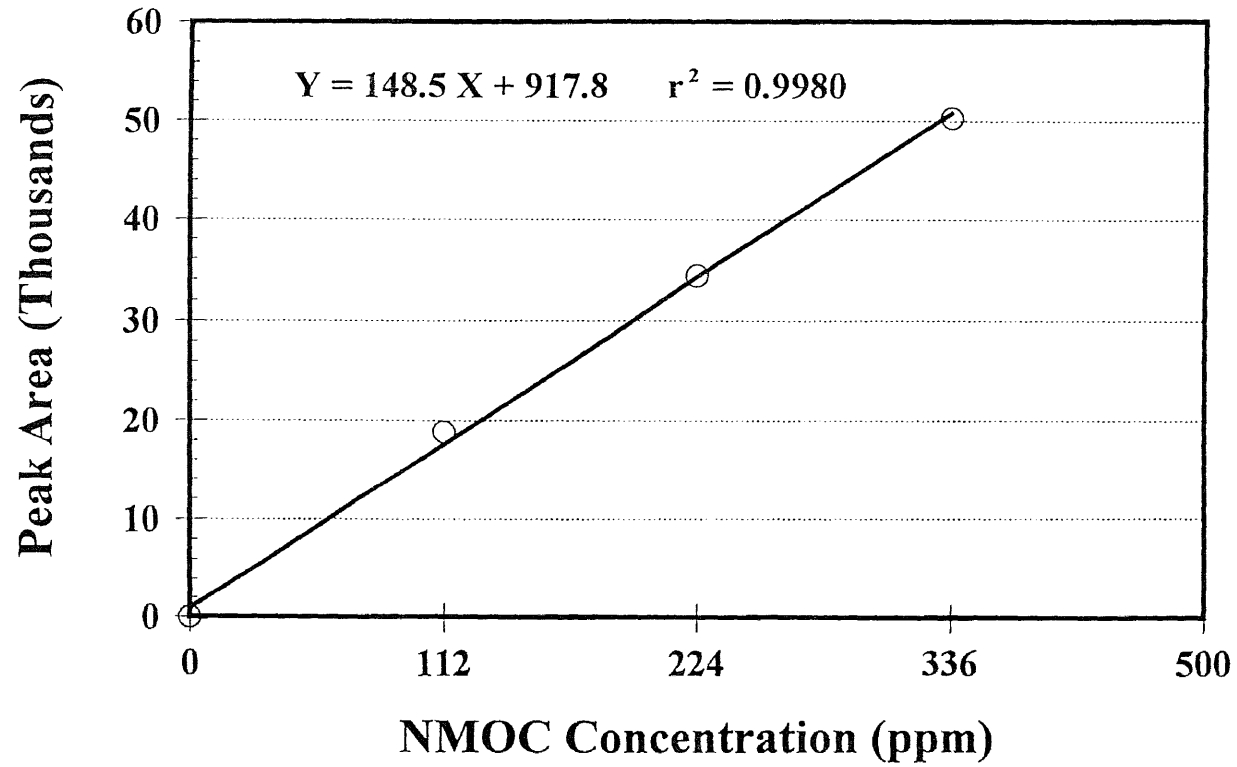
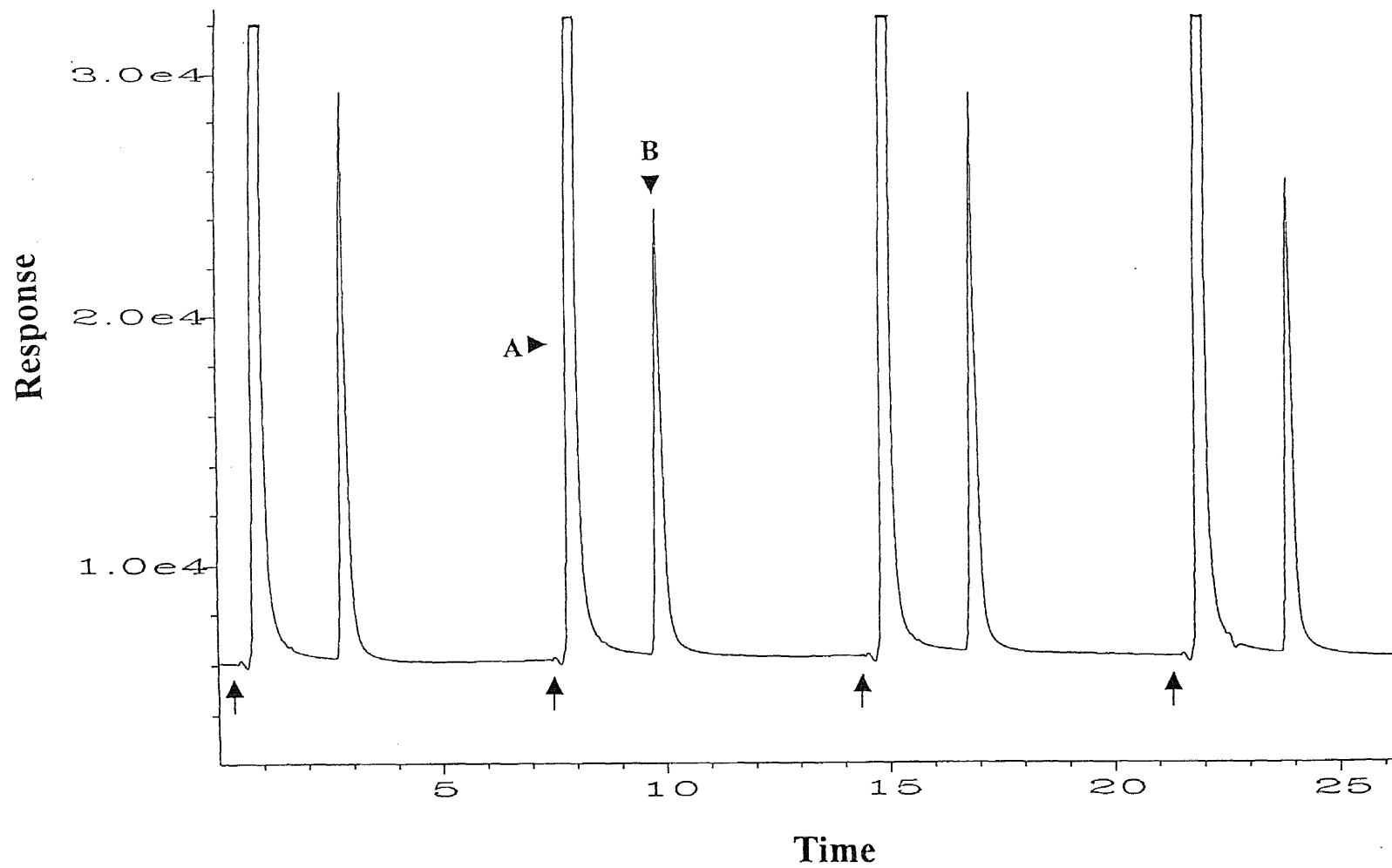


Figure 6.4 Typical calibration curve for NMOC monitoring.

Continuous analysis was done by making injection every 10 minute. It was possible to carry out the analysis even faster, but was not necessary here. The results from day one are plotted in Figure 6.6. Test runs 1A, 2A and 3A were monitoring the emission stream, test runs 1B, 2B and 3B were from the spiked sample stream. The NMOC concentrations and relative standard deviation (RSD) of six injections in each test run are presented in Table 6.2. The emission source was relatively stable except the test run 1A where the RSD of the six monitoring results was 33.9 %. This was probably caused by the change of coating material. In Figure 6.6, The highest NMOC was 790.7 ppm<sub>C</sub> at the first injection in run 1A. In general, on this day, the NMOC concentration was within 356.7 to 790.7 ppm<sub>C</sub>. A crude estimation of combined concentration of CO, CO<sub>2</sub> and CH<sub>4</sub> was between 1.3 –3.2 %. This was based on the area of peak A in Figure 6.5, and using a one point calibration with a 0.997 % CH<sub>4</sub> certified standard.

The calculated spike recoveries are listed in Table 6.3. They were between 83 - 113 % for all test runs on the first test day. No parallel measurement of the source was made during the spiked run. The spike recovery was computed assuming that the NMOC concentration remained the same as the previous unspiked run. The calculation was also based on the average concentration during the one hour runs. The true average could only be obtained accurately from the analytical results from an hour long integrated sampling. For the present continuous method, six “snapshot” measurements were taken during each test run. The results rather described the NMOC concentration profile in the emission. It is





**Figure 6.5** Typical chromatogram generated by C-NMOC analyzer. The arrows represent the points in time when injections were made.

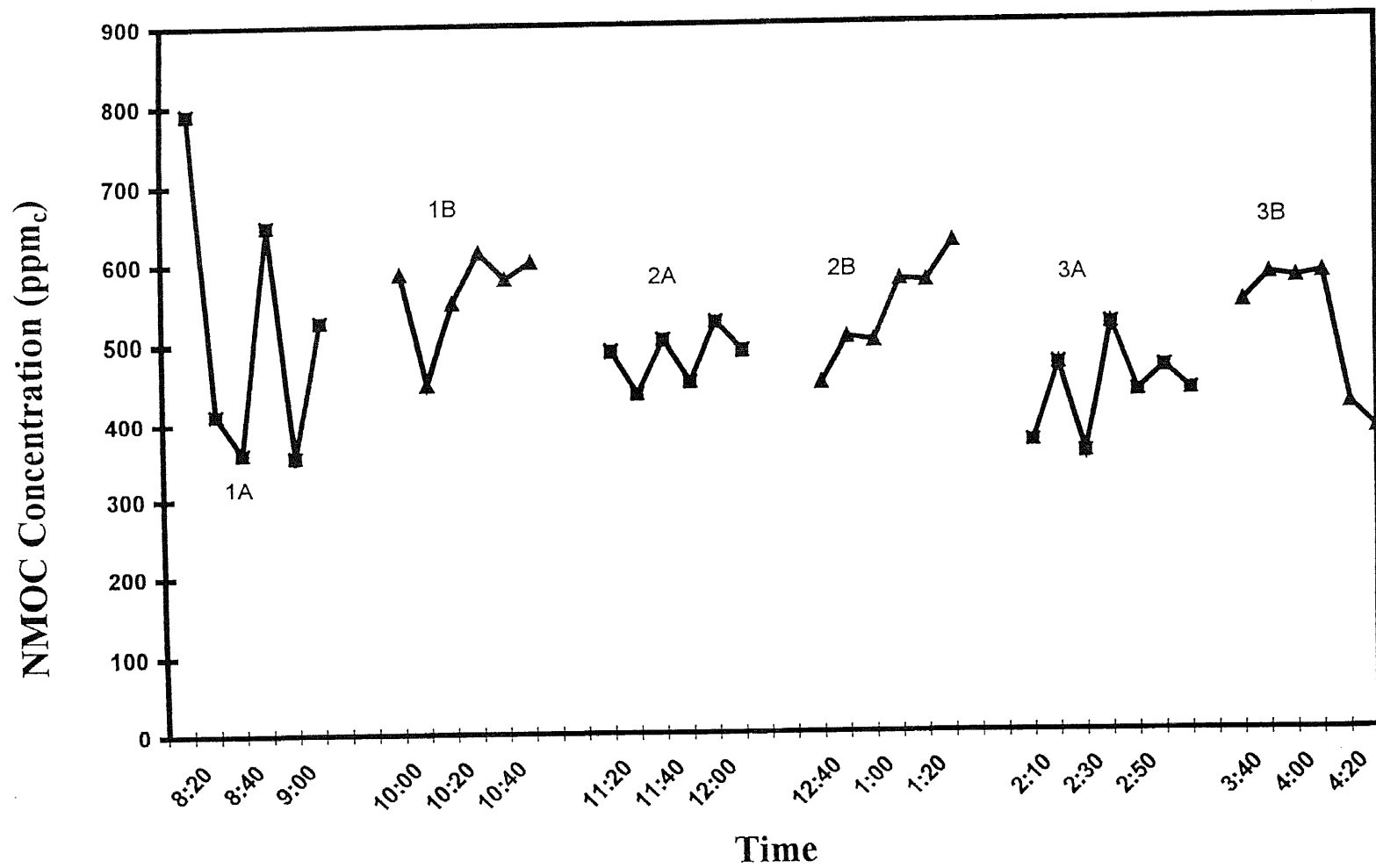


Figure 6.6 NMOc concentration profile on testing day one.

**Table 6.2** NMOC monitoring results on testing day one.

Run 1A start time 8:15, analysis every 10 min

							Average	R.S.D (%)
Estimated Concentration of CO <sub>2</sub> , CO, CH <sub>4</sub> (%)	1.8	1.6	1.4	2.0	2.0	2.1	1.8	15.9
Concentration of NMOC (ppm <sub>c</sub> )	790.7	412.4	361.1	648.6	356.9	526.3	515.9	33.9

Run 1B (Spiked) start time 9:45, analysis every 10 min

Estimated Concentration of CO <sub>2</sub> , CO, CH <sub>4</sub> (%)	3.3	3.3	3.2	3.1	3.1	3.0	3.2	3.2
Concentration of NMOC (ppm <sub>c</sub> )	585.5	450.2	549.9	614.0	580.0	601.1	563.5	10.6

Run 2A start time 11:05, analysis every 10 min

Estimated Concentration of CO <sub>2</sub> , CO, CH <sub>4</sub> (%)	1.6	1.5	1.4	1.5	1.4	1.4	1.5	6.3
Concentration of NMOC (ppm <sub>c</sub> )	487.6	436.6	502.1	451.0	542.4	487.5	484.5	7.8

Run 2B (Spiked) start time 12:25, analysis every 10 min

Estimated Concentration of CO <sub>2</sub> , CO, CH <sub>4</sub> (%)	3.0	3.1	3.0	3.0	3.0	3.0	3.0	1.6
Concentration of NMOC (ppm <sub>c</sub> )	448.6	502.7	499.2	576.4	574.0	624.4	537.6	12.1

Run 3A start time 2:00, analysis every 10 min

Estimated Concentration of CO <sub>2</sub> , CO, CH <sub>4</sub> (%)	1.2	1.3	1.5	1.4	1.4	1.3	1.3	6.3
Concentration of NMOC (ppm <sub>c</sub> )	371.7	469.7	356.7	518.2	435.8	465.4	436.3	14.2

Run 3B (Spiked) start time 3:25, analysis every 10 min

Estimated Concentration of CO <sub>2</sub> , CO, CH <sub>4</sub> (%)	2.8	2.8	2.8	2.7	2.7	2.7	2.8	2.7
Concentration of NMOC (ppm <sub>c</sub> )	543.0	577.7	573.3	579.3	415.5	383.6	512.1	17.3

clearly seen that the emission source fluctuated during this period. Considering all these issues, it was unreliable to estimate accuracy based on spike recovery alone.

**Table 6.3** Spike recovery results on the first day of testing.

Test ID	Background NMOC (ppm <sub>c</sub> )	Diluted Background NMOC (ppm <sub>c</sub> )	Spiked Sample NMOC (ppm <sub>c</sub> )	NMOC Added Spike (ppm <sub>c</sub> )	Percent Recovery
1	515.9	474.9	563.5	81.5	109
2	484.5	446.0	537.6	109.9	83
3	436.3	406.8	512.1	93.6	113

The method accuracy was also tested by measuring audit gases without having prior knowledge of their concentrations. The results of the audit are presented in Table 6.4. The percentage deviations for two measurements of 20.2 ppm ethanol (40.4 ppm<sub>c</sub>) with 17.9 % CO<sub>2</sub> were 13.1 and 3.6, respectively. Another 46 ppm hexane audit (276 ppm<sub>c</sub>) was determined to be 233.9 ppm<sub>c</sub>, a deviation of -15.3 %. They were less than the acceptable level (20 %) for field test. It demonstrated high accuracy of the C-NMOC analyzer even in presence of high CO<sub>2</sub> concentration.

The hydrophobic characteristics of the microtrap sorbent (Carbopack C) allowed the analysis of stack samples with very high moisture content. No ice formed inside the microtrap because it was maintained at room temperature. The drawback of EPA method 25 and others that use cryogenic cooling was overcome.

In general, the C-NMOC analyzer was able to monitor emissions with high moisture, as well as high CO<sub>2</sub> content.

**Table 6.4** Audit results.

Test ID	Test Results (ppmC)	% Error
Audit -1 40.4 ppmC as Ethanol	45.7	+13.1
Audit -2 40.4 ppmC as Ethanol	41.6	+3.6
Audit -3 276 ppmC as Hexane	233.9	-15.3

The NMOC concentration profile on the second day is shown in Figure 6.7. The NMOC concentration was 3069.9 ppmC when the monitoring was started in the morning. The high NMOC concentration on this day was due to changing of the coating material to polyester. The process of polyester coating seemed to produce much higher NMOC in the emission. In the next hour and a half, the NMOC concentration decreased sharply to very low levels. On later inquiry from plant personnel, it was found that around that time the coating process was stopped. This event was immediately detected by the decrease in NMOC concentrations in the stack emission. The last three injections in test run 4A showed NMOC concentrations of 58.0, 67.6, 68.3 ppm<sub>c</sub>, respectively. The average of NMOC concentration and the RSD of the monitoring results of each test run were listed in Table 6.5.

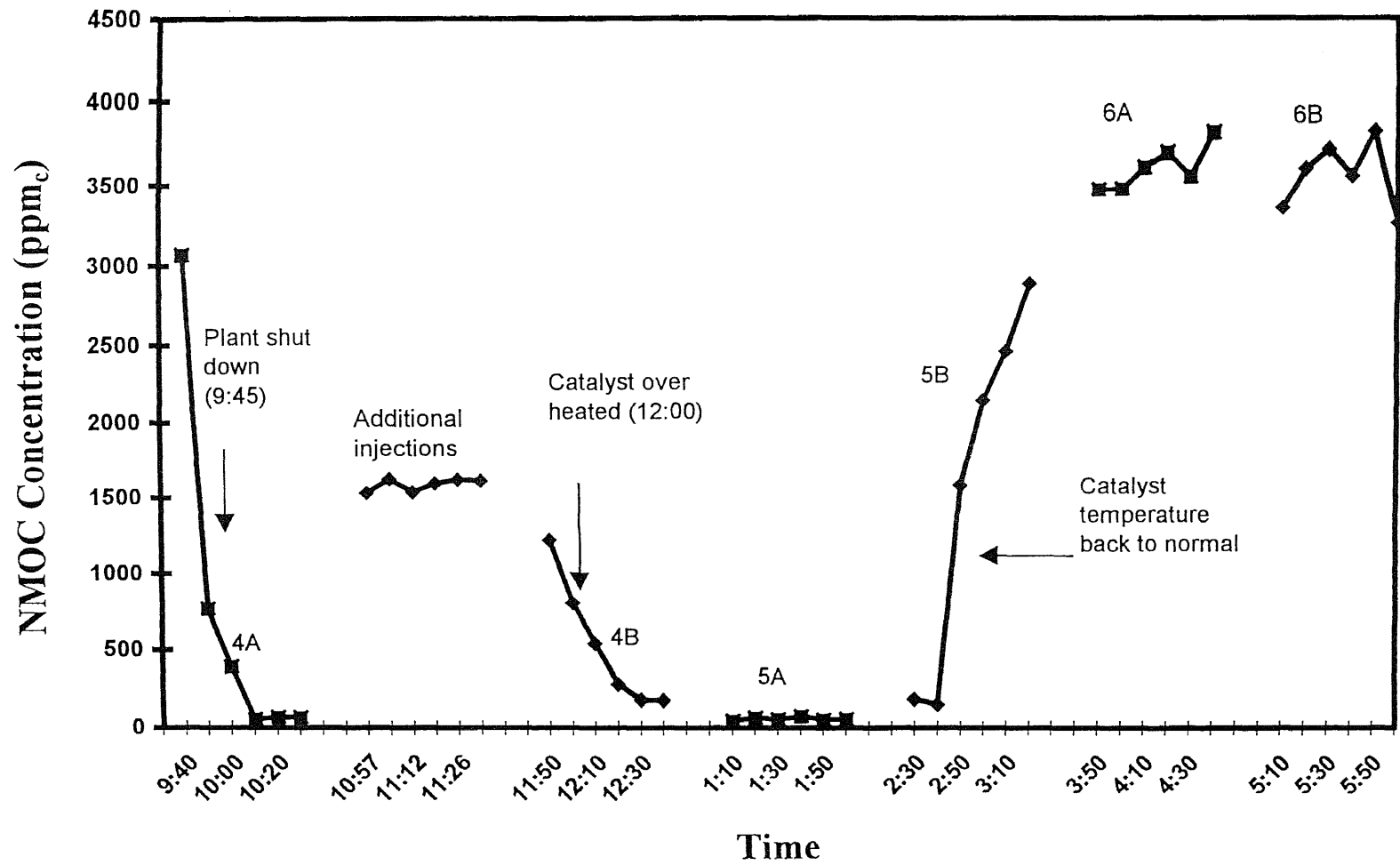


Figure 6.7 NMOc concentration profile on testing day two.

**Table 6.5** NMOC monitoring results on testing day two.

Run 4A start time 9:30, analysis every 10 min							Average	R.S.D (%)
Estimated Concentration of CO <sub>2</sub> , CO, CH <sub>4</sub> (%)	2.4	2.3	1.1	1.0	1.1	1.0	1.5	44
Concentration of NMOC (ppm <sub>c</sub> )	3069.9	768.5	391.8	58.0	67.6	68.3	737.4	159

(Spiked) start time 10:50, analysis every 7 min							Average	R.S.D (%)
Estimated Concentration of CO <sub>2</sub> , CO, CH <sub>4</sub> (%)	3.0	2.9	3.0	2.9	3.3	3.1	3.0	4.6
Concentration of NMOC (ppm <sub>c</sub> )	1533.4	1622.7	1537.7	1593.4	1620.1	1611.0	1586.4	2.57

Run 4B (Spiked) start time 11:45, analysis every 10 min							Average	R.S.D (%)
Estimated Concentration of CO <sub>2</sub> , CO, CH <sub>4</sub> (%)	3.3	3.3	3.4	3.3	3.4	3.4	3.3	1.2
Concentration of NMOC (ppm <sub>c</sub> )	1223.7	807.5	543.5	278.2	179.4	178.4	535.1	77.9

Run 5A start time 12:55, analysis every 10 min							Average	R.S.D (%)
Estimated Concentration of CO <sub>2</sub> , CO, CH <sub>4</sub> (%)	2.3	2.2	2.2	2.1	2.4	2.3	2.2	1.2
Concentration of NMOC (ppm <sub>c</sub> )	47.1	63.9	56.4	75.7	55.8	59.6	59.7	16.0

Run 5B (Spiked) start time 2:16, analysis every 10 min							Average	R.S.D (%)
Estimated Concentration of CO <sub>2</sub> , CO, CH <sub>4</sub> (%)	3.3	3.2	3.3	3.2	3.2	3.2	3.2	0.77
Concentration of NMOC (ppm <sub>c</sub> )	185.0	150.8	1579.4	2135.9	2452.3	2875.3	1563.5	74.3

Run 6A start time 3:34, analysis every 10 min							Average	R.S.D (%)
Estimated Concentration of CO <sub>2</sub> , CO, CH <sub>4</sub> (%)	1.5	1.6	1.6	1.6	1.5	1.5	1.5	3.7
Concentration of NMOC (ppm <sub>c</sub> )	3467.5	3470.5	3602.5	3688.8	3547.7	3803.1	3596.7	3.65

Run 6B (Spiked) start time 4:55, analysis every 10 min							Average	R.S.D (%)
Estimated Concentration of CO <sub>2</sub> , CO, CH <sub>4</sub> (%)	3.2	3.2	3.2	3.1	3.1	3.1	3.1	1.2
Concentration of NMOC (ppm <sub>c</sub> )	3346.2	3595.5	3706.5	3551.2	3812.0	3250.9	3543.7	6.00

Six measurements were made every 7 minutes between test run 4A and 4B for monitoring the activities of the coating process. The plant resumed operation at 10:30 AM and the output of C-NMOC detected this activity. The average NMOC concentration was found to be around 1586 ppm<sub>C</sub>. The sample stream was spiked for run 4B, the spike recovery could not be calculated since there was no information about the background NMOC concentration as it fluctuated during run 4A. Moreover, the NMOC concentration began to decrease after the initiation of run 4B and then it stabilized to around 200 ppm<sub>C</sub> which was the target spiking concentration. At this point cause of this decrease was unknown and the plant personnel were unable to give a plausible explanation. Malfunction of C-NMOC was suspected, and the 112 ppm<sub>C</sub> standard was injected to check its operation. No problems were detected.

The NMOC concentration dropped to around 50 ppm<sub>C</sub> during run 5A although the plant was still operating. At this point, based on the C-NMOC output, the plant personnel thoroughly checked all operating conditions in the coating process. They discovered that the air pollution control device catalyst had accidentally overheated to nearly 1200 °C (750 °C being normal operating temperature). The high temperature resulted in high catalytic activity and near complete oxidation of all organics. The catalyst temperature was reset to its normal value, and the corresponding NMOC concentration began to increase in run 5B and reached 2576.5 ppm<sub>C</sub> by the end of that run. Consequently, the spike recovery could not be estimated for run 5B also. The average monitoring results of run 6A and 6B, which were 3596.7 and 3543.7 ppm<sub>C</sub> respectively, showed the



NMOC emission from the coating process were back to the levels of early morning. For all six monitoring runs, the average combined concentration of CO, CO<sub>2</sub> and CH<sub>4</sub> were between 1.5 –3.3 %.

One of the best illustrations of the advantages of using a CEM for observing process events was obtained from the second test day. Using conventional methods based on field sampling followed by laboratory analysis, it may have taken several days to get these results. Consequently, no corrective action could have been taken based on the analytical results. For example, catalyst overheating over a long period of time could have ruined expensive catalysts. Often, air sampling involves collecting time integrated sample in a sorbent trap, or a canister. The emission transients as seen in run 4A or 5B would have been lost, and no information about the events would have been known.

#### **6.4 Conclusion**

The C-NMOC analyzer was validated in a field test as an effective continuous emission monitor for measurement of air emissions in stack gases. The instrument was able to monitor the transients of the process in real-time based on which corrective actions could be taken. The instrument demonstrated good accuracy based on audit sample analysis, and high precision. It was found to be stable over long periods of operation.

## REFERENCES

1. M. Trainer, E. J. Williams, D. D. Parrish, M. P. Buhr, E. J. Allwine, H. H. Westberg, F. C. Fehsenfeld and S. C. Liu, "Models and observations of the impact of natural hydrocarbons on rural ozone", *Nature*, vol. 329, pp. 705-707, 1987.
2. A. Cardelino and C.A. Chameides, "Natural hydrocarbons urbanization, and urban ozone", *J. Geophys. Res.*, vol. 95, pp. 13,971-13,979, 1990.
3. F. Fehsenfeld, J. Calvert, R. Fall, P. Goldan, A. B. Guenther, C. H. Nicholas, B. Lamb, S. C. Liu, M. Trainer, H. Westberg and P. Zimmerman, "Emissions of volatile organic compounds from vegetation and the implications for atmospheric chemistry", *Global Biogeochem Cycles*, vol. 6, pp. 389-430, 1992.
4. U. S. EPA, *Compendium of Methods for the Determination of Toxic Organic compounds in Ambient Air*, US EPA Document No.600/4-84-041, April 1984.
5. J. Moore, Jr., "Barriers to using field analytical technology instruments as an example adoption", *Environ. Sci. Technol.*, vol. 28, No. 4, pp. 193A-195A, 1994.
6. J. Poppiti, "The role of field testing in environmental measurements", *Environ. Sci. Technol.*, vol. 28, No. 12, pp. 538 A, 1994.
7. T. J. Kelly, P. J. Callahan, J. Pleil and G. F. Evans, "Method development and field measurements for polar volatile organic compounds in ambient air", *Environ. Sci. Technol.*, vol. 27, pp. 1146-1153, 1993.
8. K. C. Bayne, D. D. Schmoyer, R. A. Jenkins, "Practical reporting times for environmental samples", *Environ. Sci. Technol.*, vol. 28, pp. 1430-1436, 1994.
9. S. Shelley, "Real-time emissions monitors now detect smaller quantities of more compounds at breakneck speed," *Chemical Engineering*, pp. 30-37, November 1991.
10. C. R. Strang, S. P. Levine and W. F. Herget, *Am. Ind. Hyg. Assoc. J.*, vol. 50, No. 2, pp. 70-77, 1989.
11. C. R. Strang and S. P. Levine, *Am. Ind. Hyg. Assoc. J.*, vol. 50, No. 2, pp. 78-84, 1989.

12. L. Ying, S. P. Levine, C. R. Strang and R. Herget, *Am. Ind. Hyg. Assoc. J.*, vol. 50, No. 7, pp. 354-359, 1989.
13. P. W. Morrison, Jr., J. E. Cosgrove, R. M. Carangelo, M. D. Caravello, P. R. Solomon, P. Leroueil and P. A. Thorn, *Tappi Journal*, pp. 68-78, December 1991.
14. L. Ying and S. P. Levine, *Am. Ind. Hyg. Assoc. J.*, vol. 50, No. 7, pp. 360-365, 1989.
15. W. M. Doyle and N. A. Jennings, "The applications of on-line IR", *Spectroscopy*, vol. 5, No. 1, pp. 34-38, 1990.
16. B. F. Dudenbostel, Jr. and W. Priestly, *Ind. Eng. Chem.*, vol. 48, pp. 55A, 1956.
17. H. G. Eaton, M. E. Umstead and W. D. Smith, "Total hydrocarbon analyzer for use in nuclear submarines and other closed environments", *J. Chromatogr. Sci.*, vol. 11, pp. 275-278, 1973.
18. R. Annino and R. Villalobos, "Application of process GC instrumentation to environmental monitoring", *American Laboratory*, pp. 15-25, October 1991.
19. R. Annino, "Process gas chromatographic instrumentation", *Am. Lab.* vol. 21, No. 10, pp. 60-71, 1990.
20. S. Mitra and A. Lai, "A sequential valve-microtrap injection system for continuous, on-line gas chromatographic analysis at trace levels". *J. of Chromatogr. Sci.*, vol. 33, June 1995.
21. Z. Liu, M. Zhang and J. B. Phillips, "High-speed gas chromatographic analysis of a simulated process stream using on-column thermal desorption modulation for sample preconcentration and introduction", *J. Chromatogr. Sci.*, vol. 28, November 1990.
22. J. B. Phillips, D. Luu and J. B. Pawliszyn, "Multiplex gas chromatography by thermal modulation of a fused silica capillary column", *Anal. Chem.*, vol. 57, pp. 2779-2787, 1985.
23. Z. Liu and J. B. Phillips, "High-speed gas chromatography using an on-column thermal desorption modulator", *J. Microcolumn Separations*, vol. 1, No. 5, pp. 249-256, 1989.

24. S. Mitra and J. B. Phillips, "High-capacity thermal desorption modulators for gas chromatography", *J. Chromatogr. Sci.*, vol. 26, pp. 620, 1988.
25. S. Mitra and J. B. Phillips, "Automated on-line analysis using thermal desorption modulators", *Analytical Instrumentation*, vol. 18, No. 2, pp.127-145 1989.
26. F. R. Cropper and S. Kaminsky, "Determination of toxic organic compounds in admixture in the atmosphere by gas chromatography", *Anal. Chem.*, vol. 35, No. 6, pp. 735-743, 1963.
27. Y. H. Xu and S. Mitra, "Continuous monitoring of volatile organic compounds in water using on-line membrane extraction and microtrap gas chromatography system", *Journal of Chromatography A*, vol. 688, pp. 171-180, 1994.
28. B. V. Burger and Z. Munro, "Quantitative trapping and thermal desorption of volatiles using fused-silica open tubular capillary traps", *Journal of Chromatography*, vol. 370, pp. 449-464, 1986.
29. S. Mitra and C. Yun, "Continuous gas chromatographic monitoring of low concentration sample streams using an on-line microtrap", *Journal of Chromatography*, vol. 648, pp. 415-421, 1993.
30. V. M. Clair, M. F. Grnnord, B. Fatima and G. Guiochon, "Performances of various adsorbents for the trapping and analysis of organohalogenated air pollutants by gas chromatography", *J. Chromatogr. Sci.*, vol.16, pp. 190-196, 1978.
31. S. Mitra, N. Zhu, X. Zhang and B. Kebbekus, "Continuous monitoring of volatile organic compounds in air emission using on-line membrane extraction microtrap GC system", *J. Chromatogr. A*, vol. 736, pp. 165-173, 1996.
32. S. Mitra, L. Zhang, N. Zhu, and X. Guo, *J. Microcolumn Separations*, vol. 8, No. 1, pp. 21-27, 1996.
33. P. G. Simmonds, S. O'Doherty, G. Nickless and G. A. Sturrock, "Automated gas chromatography/mass spectrometer for routine atmospheric field measurements of the CFC replacement compounds, the hydrofluorocarbons and hydrochlorofluorocarbons", *Anal. Chem.*, vol. 67, pp. 717-723, 1995.
34. B. Gokhan and V. Annette, "Spray extraction of volatile organic compounds from aqueous systems into the gas phase for gas chromatography/mass spectrometry", *Anal. Chem.*, vol. 64, pp. 677-681, 1992.

35. A. Robbat, Jr., T. Liu and B. M. Abraham, "Evaluation of a thermal desorption gas chromatography/mass spectrometer: on-site detection of polychlorinated biphenyls at a hazardous waste site", *Anal. Chem.*, vol. 64, pp. 358-364, 1992.
36. G. Matz and P. Kesners, "Spray and trap method for water analysis by thermal desorption gas chromatography/mass spectrometry in field applications", *Anal. Chem.*, vol. 65, pp. 2366-2371, 1993.
37. J. W. Coburn and W. W. Harrioso, *Appl. Spectrosc. Rev.* vol. 17, pp. 95, 1981.
38. D. L. Ashley, M. A. Bonin, L. F. Gardinali, J. M. McGraw and J. S. Holler, "Determining volatile organic compounds in human blood from a large sample population by using purge and trap gas chromatography/mass spectrometry", *Anal. Chem.*, vol. 64, pp. 1021-1029, 1992.
39. F. Hartmut, D. Renschen, A. Klein and H. Scholl, "Trace analysis of airborne haloacetates", *J. High Resol. Chromatogr.*, vol. 18, pp. 83-88, 1995.
40. W. C. McDonald, M. D. Erickson, B. M. Abraham and A. Robbat, Jr., "Developments and applications of field mass spectrometers", *Environ. Sci. Technol.*, vol. 28, No. 7, pp. 336A-343A, 1994.
41. M. Soni, S. Bauer, J. W. Amy, P. Wong and R. G. Cooks, "Direct determination of organic compounds in water at parts-per-quadrillion levels by membrane introduction Mass spectrometry", *Anal. Chem.*, vol. 67, No. 8, pp. 1409-1412, 1995.
42. P. S. H. Wong, R. G. Cooks, M. E. Cisper and P. H. Hemberger, "On-line, in situ analysis with membrane introduction MS", *Environ. Sci. Technol.*, vol. 29, No. 5, pp. 215A-218A, 1995.
43. M. E. Bier and R. G. Cooks, *Anal. Chem.*, vol. 59, pp. 597, 1987.
44. P. S. H. Wong and R. G. Cooks, *Anal. Chem.*, vol. 66, pp. 4422, 1994.
45. L. E. Dejarne, S. J. Bauer, R. G. Cooks, F. R. Lauritsen, T. Kotiaho and T. Graf, *Rapid Commun. Mass Spectrom.*, vol. 7, pp. 935, 1993.
46. F. R. Lauritsen and S. Gylling, *Anal. Chem.*, vol. 67, pp. 1418, 1995.
47. V. T. Virkki, R. A. Ketola, M. Ojala, T. Katiaho, V. Komppa, A. Grove and S. Facchetti, *Anal. Chem.*, vol. 67, pp. 1421, 1995.

48. S. A. McLuckey, G. L. Glish, K. G. Asano and B. C. Grant, "Atmospheric sampling glow discharge ionization source for trace organic compounds in ambient air", *Anal. Chem.*, vol. 60, pp. 2220-2227, 1988.
49. E. C. Horning, M. G. Horning, D. I. Carroll, I. Dzidic and R. N. Stillwell, *Anal. Chem.*, vol. 45, pp. 936, 1973.
50. M. E. Cisper, C. G. Gill, L. E. Townsend and P. H. Hemberger, *Anal. Chem.*, vol. 67, pp. 1413, 1995.
51. D. I. Carroll, I. Dzidic, R. N. Stillwell, M. G. Horning and E. C. Horning, *Anal. Chem.*, vol. 46, pp. 706, 1974.
52. D. A. Lane, B. A. Thomson, A. M. Lovett and N. M. Reid, *Adv. Mass Spectrom.*, vol. 8, pp. 1480, 1980.
53. H. Kambara, *Anal. Chem.*, vol. 54, pp. 143, 1982.
54. J. B. French, B. A. Thomson, W. R. Davidson, N. M. Reid and J. A. Buckley, *Mass Spectrometry in the Environmental Sciences*, edited by F. W. Karasek, Pergamon, Oxford, U.K., 1982.
55. W. W. Harrison, K. R. Hess, R. K. Marcus and F. L. King, *Anal. Chem.*, vol. 58, pp. 341A, 1986.
56. S. N. Ketkar, S. M. Penn and W. L. Fite, "Real-time detection of parts per trillion levels of chemical warfare agents in ambient air using atmospheric pressure ionization tandem quadrupole mass spectrometry", *Anal. Chem.*, vol. 63, pp. 457-459, 1991.
57. M. E. Cisper, W. L. Earl, N. S. Nogar and P. H. Hemberger, "Silica-fiber microextraction for laser desorption ion trap mass spectrometry", *Anal. Chem.*, vol. 66, pp. 1897-1901, 1994.
58. F. St-Germain, O. Mamer, J. Brunet, B. Vachon, R. Tardif, T. Abribat and C. D. Rosiers, J. Montgomery, "Volatile organic compound analysis by an inertial spray extraction interface coupled to an ion trap mass spectrometer", *Anal. Chem.*, vol. 67, pp. 4536-4541, 1995.
59. M. B. Wise, R. H. Ilgner and M. V. Buchanan, *Proceedings of the 38<sup>th</sup> ASMS Conference on Mass Spectrometry*, Tuscon, AZ, pp. 1481, 1990.
60. C. Y. Ma, J. T. Skeen, A. B. Dindl, C. E. Higgins and R. A. Jenkins, "Proceedings of the 1994 USEPA/A&WMA International Symposium,

- Measurement of Toxic and Related Air Pollutants”, *Air & Waste Management Association*, Pittsburgh, PA, pp. 30, 1994.
61. B. Dindal, C. Y. Ma, R.A. Jenkins, C. E. Higgins, J. T. Skeen and C. K. Bayne, “Proceedings of the 1995 USEPA/A& WMA international symposium, measurement of toxic and related air pollutants”, *Air & Waste Management Association*, Pittsburgh, PA, 1995.
  62. J. R. Conder and C. L. Young, *Physicochemical Measurement by Gas Chromatography*, John Wiley & Sons, Inc., New York, 1979.
  63. O. L. Hollis and W. V. Hayes, *J. Gas Chromatogr.*, vol. 4, pp. 235, 1966.
  64. A. V. Kiselev and Y. I. Yashin. *Gas Adsorption Chromatography*, Plenum Press, New York, 1969.
  65. L. D. Butler and M. F. Burke, *J. Chromatogr. Sci.*, vol. 14, pp. 117 –121, 1976.
  66. J. M. H. Daeman and M. E. Hendriks, *J. Chromatogr. Sci.*, vol. 13, pp. 79-83, 1975.
  67. U. S. EPA, *Process Design Manual for Carbon Adsorption*, pp.1-2, 1973.
  68. W. R. Betz, S. G. Margoldo, G. D. Wachob, and M. C. Firth, “Characterization of carbon molecular sieves and activated charcoal for use in airborne contaminant sampling”, *Am. Ind. Hyg. Assoc. J.*, vol. 50, No. 4, pp. 181-187, 1989.
  69. W. R. Betz, K. S. Ho, S. A. Hazard and S. J. Lambiase, *Sampling and analysis of airborne pollutants*, Lewis Publishers, New York, 1993.
  70. R. J. B. Peters and H. A. Bakkeren, *Analyst*, vol. 119, pp. 71, 1994.
  71. P. Comes, N. Gonzalez-Flesca and T. Menard, *Anal. Chem.*, vol. 65, pp.1048, 1993.
  72. W. T. Sturges and J. W. Elkins, *J. Chromatogr.*, vol. 642, pp. 123, 1993.
  73. S. Seshadri and J. W. Bozzelli, *Chemosphere*, vol.12, pp. 809, 1983.
  74. H. Hori, I. Tanaka and T. Akiyama, *J. Air Pollut. Control Assoc.*, vol. 38, pp. 269, 1988.
  75. S. P. Patil and S. T. Lonkar, *J. Chromatogr.*, vol. 600, pp. 344, 1992.

76. A. Przyjazny, *J. Chromatogr.*, vol. 346, pp. 61, 1985.
77. S. Coppi, A. Betti, G. Blo and C. Bigli, *J. Chromatogr.*, vol. 267, pp. 91, 1983.
78. K. A. Persson and S. Berg, *Chromatographia*, vol. 27, pp. 55, 1989.
79. J. Janak, J. Ruzickova and J. Novak, *J. Chromatogr.*, vol. 99, pp. 689-696, 1974.
80. M. Harper; L. S. Conyne and D. L. Florito, "Validation of sorbent sampling methods for methylene chloride", *Appl. Occup. Environ. Hyg.*, vol. 9, No. 3, pp. 198-205, 1994.
81. Y. H. Yoon and J. H. Nelson, "Effects of humidity and contaminant concentration on respirator cartridge breakthrough", *Am. Ind. Hyg. Assoc. J.*, vol. 51, No. 4, pp. 202-209, 1990.
82. X. L. Cao, *J. Chromatogr.*, vol. 586, pp. 161, 1991.
83. K. Ventura, M. Dostal and J. Churacek, *J. Chromatogr.*, vol. 642, pp. 379, 1993.
84. I. Maier and M. Fieber, *J. High Resolut. Chromatogr. Chromatogr. Commun.*, vol. 11, pp. 566, 1998.
85. P. Lovkvist and J. A. Jonsson, *Anal. Chem.*, vol. 59, pp. 818, 1987.
86. R. H. Brown and C. J. Purnell, *J. Chromatogr. Sci.*, vol. 79, pp. 178, 1979.
87. G. O. Nelson and C. A. Harder, "Respirator cartridge efficiency studies: VI. effect of concentration", *Am. Ind. Hyg. Assoc. J.*, vol. 37, pp. 205-216, 1976.
88. M. M. Dubinin, "Physical adsorption of gases and vapors in micropores", *Prog. Surf. Membr. Sci.*, vol. 9, pp. 1-70, 1975.
89. J. J. Hacskeylo, and M. D. LeVan, "Correlation of adsorption equilibrium data using a modified Antonie equation: a new approach for pore-filling models", *Langmuir*, vol. 1, pp. 97-100, 1985.
90. V. Simon, M. Riba, A. Waldhart and L. Torres, "Breakthrough volume of monoterpenes on Tenax TA: influence of temperature and concentration



- for  $\alpha$ -pinene”, *Journal of Chromatography A*, vol. 704, pp. 465-471, 1995.
91. W. R. Betz and W.R. Supina, “Use of thermally modified carbon black and carbon molecular sieve adsorbents in sampling air contaminants”, *Pure Appl. Chem.*, vol. 61, No. 11, pp. 105-112, 1989.
  92. G. Bertoni, F. Bruner, A. Liberti and C. Perrino, “Some critical parameters in collection, recovery and gas chromatographic analysis of organic pollutants in ambient air using light adsorbents”, *J. Chromatogr.*, vol. 203, pp. 263-270, 1981.
  93. W. K. Lewis, E. R. Gilliland, B. Chertow and W. P. Cadagon, “Adsorption equilibrium: hydrocarbon gas mixtures”, *Ind. Eng. Chem.*, vol. 42, pp. 1319-1326, 1950.
  94. L. A. Jonas, E. B. Sansone and T. S. Ferris, “The effect of moisture on the adsorption of chloroform by activated carbon”, *Am. Ind. Hyg. Assoc. J.*, vol. 46, pp. 20-23, 1985.
  95. J. M. Schork and J. R. Fair, *Ind. Eng. Chem. Res.*, vol. 27, pp. 4576, 1986.
  96. R. T. Yang, *Gas Separation by Adsorption Process*, Butterworths, Boston, 1987.
  97. R. M. Conforti and T. A. Barbari, “A thermodynamic analysis of gas sorption desorption hysteresis in glassy polymers”, *Macromolecules*, vol. 26, pp. 5209-5212, 1993.
  98. C. Huang and J. R. Fair, “Study of the adsorption and desorption of multiple adsorbates in a fixed bed”, *ALChE Journal*, vol. 34, No. 11, pp. 1861-1877, 1988.
  99. J. N. J. Wilson, *Am. Chem. Soc.* vol. 63, pp. 1583, 1940.
  100. R. Aris and N. R. Amundson, *Mathematical Methods in Chemical Engineering*, Prentice Hall: Englewood Cliffs, NJ. 1973.
  101. S. Golshan-Shirazi, A. Jaulmes, *Anal. Chem.*, vol. 66, pp. 506, 1988.
  102. M. Czok and G. Guiochon, *G. Comput. Chem. Eng.*, vol. 14, pp. 1435, 1990.
  103. J. C. Giddings, *Dynamics of Chromatography*, Marcel Dekker: New York, 1965.

104. S. Golshan-Shirazi and G. Guiochon, "Combined effects of finite axial dispersion and slow adsorption /desorption kinetics on band profiles in nonlinear chromatography", *J. Phys. Chem.*, vol. 95, pp. 6390-6395, 1991.
105. R. D. Whitley, K. E. Van Cott and N. H. Wang, *Ind. Eng. Chem. Res.*, vol. 32, pp. 149-159, 1993.
106. L. A. Jonas and J. A. Rehrmann, "Predictive equations in gas adsorption kinetics", *Carbon*, vol. 11, pp. 59-64, 1973.
107. S. Hazard and J. L. Brown, "Desorption efficiencies of air samples collected on thermal desorption tubes", *Pittsburgh Conference*, Chicago, Illinois, Supelco Inc. 1994.
108. J. F. Rowell, A. Fletcher and C. Packham, *Analyst*, vol. 122, pp. 793 – 796, 1997.
109. X. Cao and C. N. Hewitt, *Chemosphere*, vol. 27, No. 5, pp. 695-705, 1993.
110. W. R. Betz and W. R. Supina, *Pure & Appl. Chem.*, vol. 61, No. 11, pp. 2047-2050, 1989.
111. Supelco GC Bulletin 849C, Division of ROHM and HAAS, *Supelco, Inc.*, 1988.
112. J. E. Peterson, H. R. Hoyle and E. J. Schneider, *Am. Ind. Hyg. Assoc. Q.*, vol.17, pp. 429, 1956.
113. R. G. Melcher, R. R. Langer and R. O. Kagel, *Am. Ind. Hyg. Assoc. Q.*, vol. 39, pp. 349, 1978.
114. M. Harper, M. L. Kimberland, R. J. Orr and L. V. Guild, "An evaluation of sorbents for sampling ketones in workplace air", *Appl. Occup. Environ. Hyg.*, vol. 8, No. 4, pp. 293-304, 1993.
115. M. Harper and D. L. Fiorito, *Appl. Occup. Environ. Hyg.*, vol. 11, No. 10, pp. 1239-1246, 1996.
116. M. Harper, *Analyst*, vol. 119, pp. 65-69, 1994.
117. G. O. Wood and E. S. Moyer, *Am. Ind. Hyg. Assoc. J.*, vol. 52, No. 6, pp. 235-242. 1991.

118. H. J. Cohen, D. E. Briggs and R. P. Garrison, *Am. Ind. Hyg. Assoc. J.*, vol. 52, No. 1, pp. 34-43, 1991.
119. P. Lovkvist and J. A. Jonsson, "Description of sample introduction in chromatography as a separate term in the mass-balance equation", *J. Chromatogr.*, vol. 365, pp. 1-8, 1986.
120. H. Freundlich, *Colloid and Capillary Chemistry*, Methuen, London, 1926.
121. A. W. Adamson and A. P. Gast, *Physical Chemistry of Surfaces*, John Wiley & Sons, New York, 1997.
122. E. B. Overton, *J. of Hazardous Materials*, vol. 22, pp. 187, 1989.
123. M. A. Lapack and J. C. You, *Anal. Chem.* vol. 63, pp. 1631, 1991.
124. J. Erb, E. Ortiz and G. Woodside, *Chemical Engineering Proceeding*, vol. 4, pp. 40, 1990.
125. S. Bauer and D. Solyom, *Anal. Chem.*, vol. 66, pp. 4422, 1994.
126. K. J. Hart, A. B. Dindal and R. R. Smith; *Rapid Communications in Mass Spectrometry*, vol. 10, pp. 352-360, 1996.
127. S. Mitra, Y. H. Xu, W. Chen and A. Lai, *J. of Chromatogr. A*, vol. 727, pp. 111, 1996.
128. R. R. Arnts and S. B. Tejada, *Environ. Sci. Technol.*, vol. 23, pp. 1428, 1989.
129. L. J. Macgregor, *Air & Waste Manage. Assoc.*, vol. 43, pp. 1576-1584, 1993.
130. F. W. Lurnamm, A. C. Lloyd and B. Nitta, *Atmos. Environ.*, vol. 17, pp. 1951-1963, 1983.
131. M. Jackson, "Final report EPA method 25 nonmethane organic analyzer evaluation. July 1986", *Research Triangle Institute, Center for Environmental Measurements*, Research Triangle Park, NC 27709, 1986.
132. G. B. Howe, S. T. Sherrill and R. K. M. Jayanty, *Method 25 - Varian Instrument Evaluation*, RTI/5960/195-01D, U. S. Environmental Protection Agency, September, 1993.
133. J. B. Callis, D. L. Illman and A. B. R. Kowalki, *Anal. Chem.*, vol. 59, No. 9, pp. 624A-637A, 1986.

134. J. A. Jahnke, *Continuous Emission Monitoring*, Van Nostrand Reinhold, New York, 1993.
135. Y. Fukui and P. V. Doskey, "An enclosure technique for measuring nonmethane organic compound emissions from grasslands", *J. Environ. Qual.*, vol. 25, pp. 601-610, 1996.
136. L. Cone, T. Logan and R. Rollins, "Carbon monoxide and total hydrocarbon continuous monitoring at hazardous waste incineration facilities", *The AWMA Specialty Conference on Continuous Emission Monitoring - Present and Future Application*, Chicago, IL, Nov. 12-15, 1989.
137. Z. Mao, J. C. Demirgian and E. Hwang, *Proceedings of the International Incineration Conference*, pp. 115, Bellevue, Washington, 1995.
138. T. Yu and S. Mitra, "Application of microtrap based non methane organic carbon (NOMC) analyzer for continuous monitoring of NMOC emissions", *Research Report*, New Jersey Institute of Technology, Newark, NJ, 1998.
139. T. Yu, G. McAllister and S. Mitra, "Monitoring effluents from an air toxic control device using continuous non-methane organic carbon (C-NMOC) analyzer", *Research Report*, New Jersey Institute of Technology, Newark, NJ, 1998.
140. Z. Huang, "Flame dynamics in unsteady strained flows," *Ph.D. dissertation*, New Jersey Institute of Technology, Newark, NJ, 1999.